

# New Trends and Techniques in Nuclear Structure Studies with High-Resolution In-Beam $\gamma$ -Spectroscopy

A.Gadea IFIC-CSIC Valencia

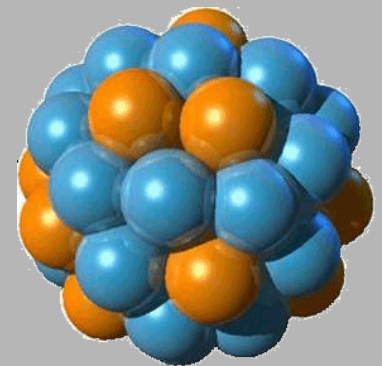
Counts

## 1. High Resolution Spectroscopy techniques

- Introduction
- $\gamma$ -tracking arrays

## 2. Nuclear Structure & Complementary instrumentation

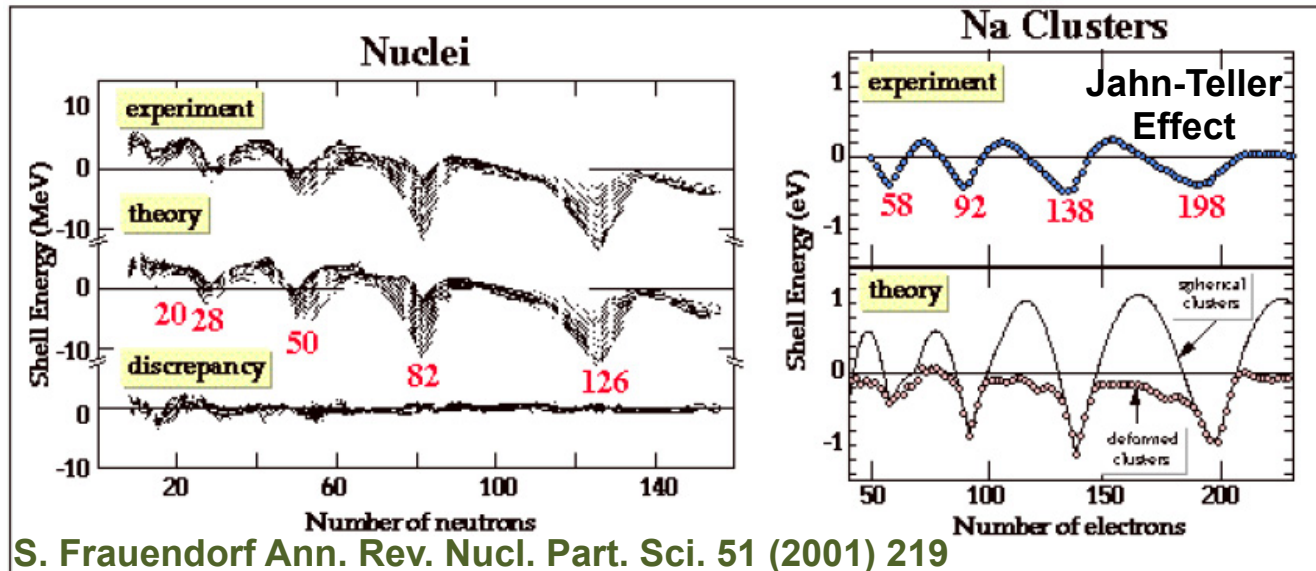
- Proton-Rich & N=Z Nuclei
- Neutron-rich  $\rightarrow$  Large Isospin Values
- Collective & Transitional Phenomena



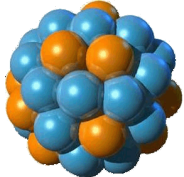
Energy [keV]

# Structure of the atomic nucleus

- The atomic nucleus is a complex fermionic system, based on two different particles, interacting via an effective force strongly influenced by in-medium effects.
- Nuclei are small enough that the quantum nature of its constituents determines its properties but large enough that macroscopic features begin to evolve.
- Nuclei have been the traditional objects for studying mesoscopic (many body) phenomena, as well as Open Quantum Systems in the limits of stability.



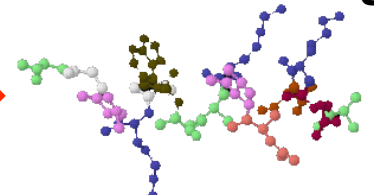
Nuclei



Many-body systems: phase transitions  
piloted by few quantal states

R.A.Brogia JoP Conf. Ser. 41 (2006) 1

Protein Folding



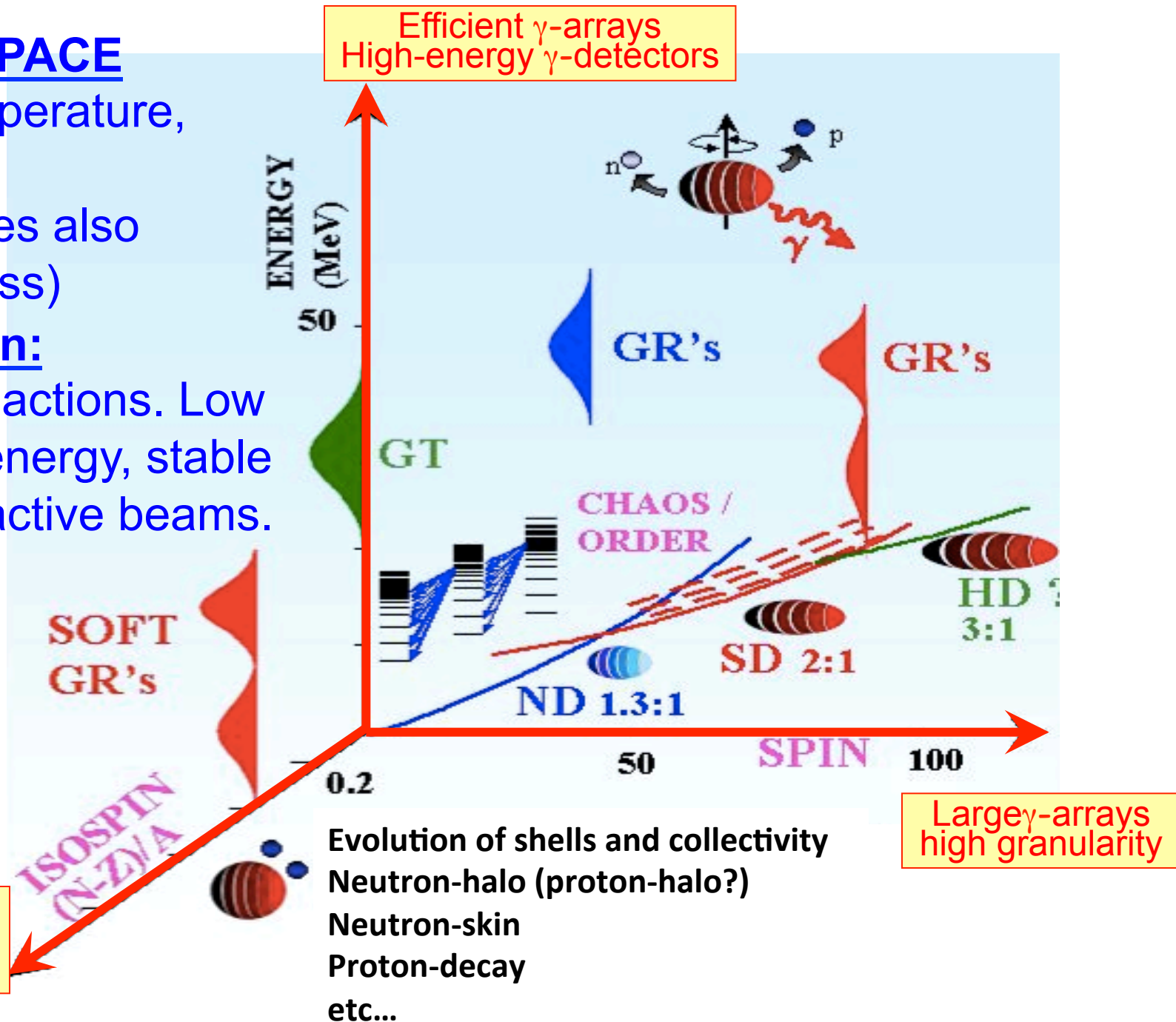
# PHASE SPACE

Spin, Temperature, Isospin.

(Sometimes also strangeness)

## Population:

Nuclear reactions. Low and high energy, stable and radioactive beams.



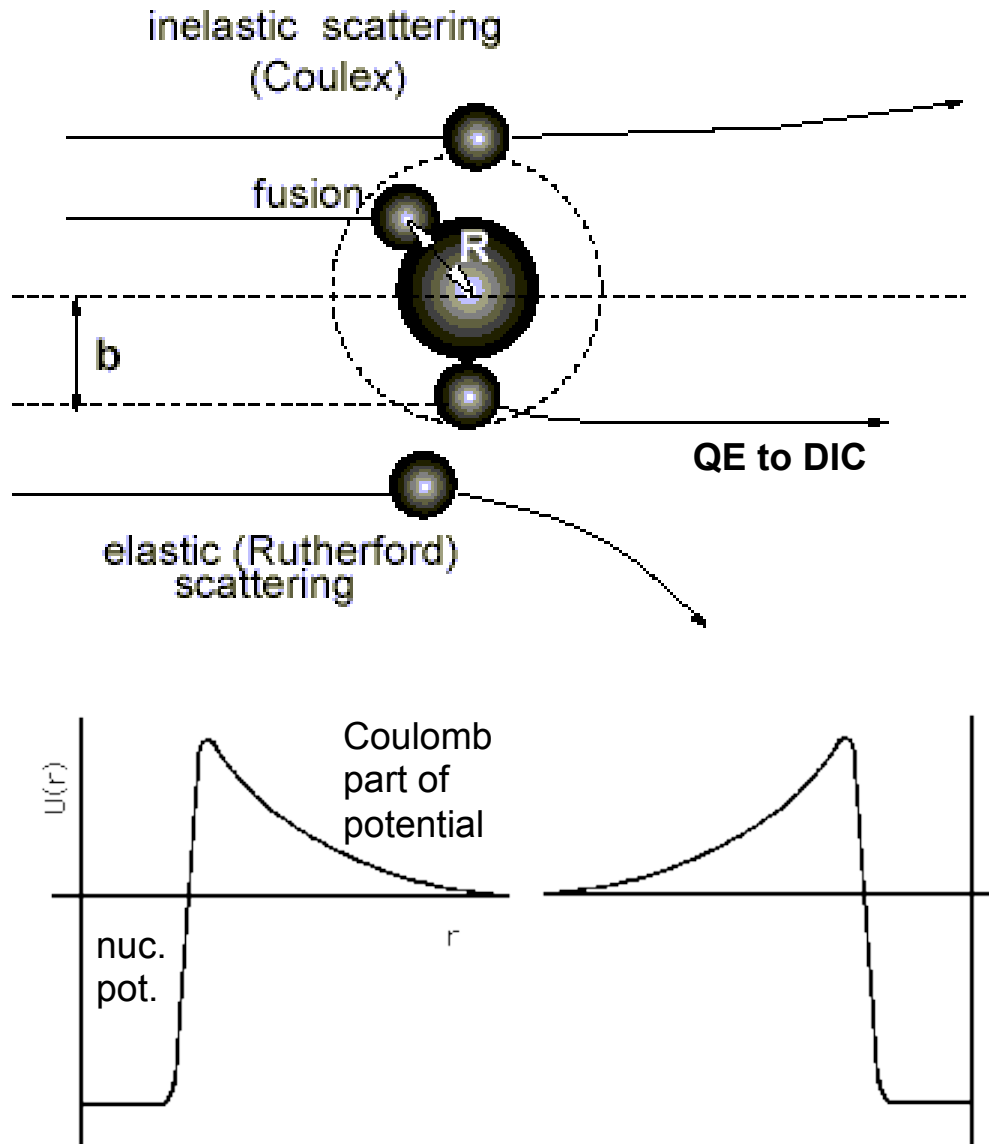
# **In-Beam Spectroscopy**

## **Key-Issues**

- **Direct detection of the “prompt” de-excitation  $\gamma$ -rays emitted by the nucleus of interest**
- **The nucleus to be studied “must” be in a excited state:**
  - **The nucleus can be created in a excited state or**
  - **The nucleus must be excited during the reaction process**
- **The detection system are installed around the reaction point**
- **Key factors are Efficiency, Peak-to-Total and Selectivity.**
- **Reaction rates could by limited by the detector counting rates**



# Low Energy reaction mechanisms used for $\gamma$ -Spectroscopy (up to $\sim 10$ MeV.A)



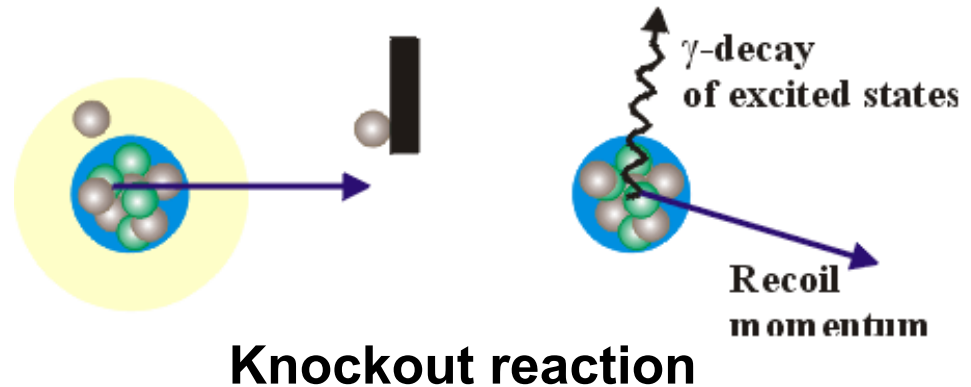
Smaller impact parameter "b"

- Coulomb excitation and Inelastic scattering.
- Transfer and quasi-elastic processes (p,n capture...).
- Multi-nucleon transfer.
- Deep Inelastic Collisions.
- Quasi-fusion reactions.
- Fusion with light particles evaporation .
- Fusion with evaporation of Massive Fragments (IMF)
- Fusion-fission

# High energy reaction mechanisms used for $\gamma$ -Spectroscopy (above $\sim 40$ MeV.A)

Generally used with exotic ion beams produced by fragmentation or fission at relativistic energies

- ➔ Relativistic (single step) Coulomb excitation
- ➔ Inverse proton scattering
- ➔ Knockout reactions
- ➔ Fragmentation reactions

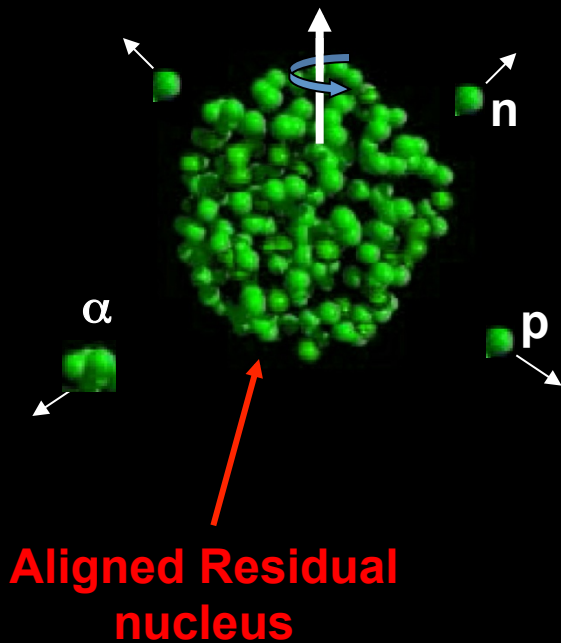
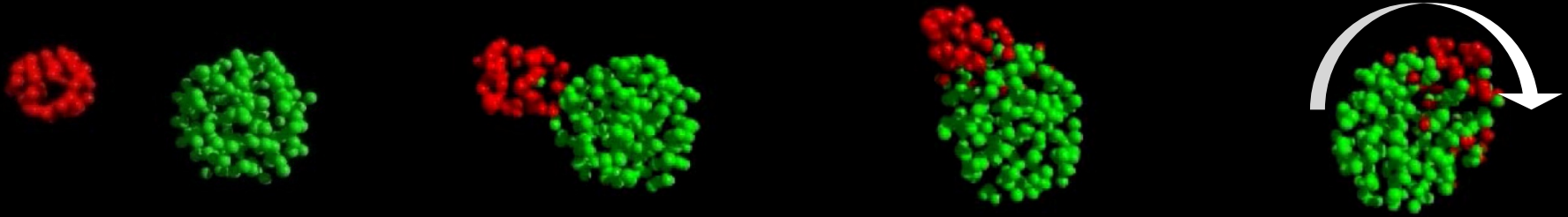


Cross sections :

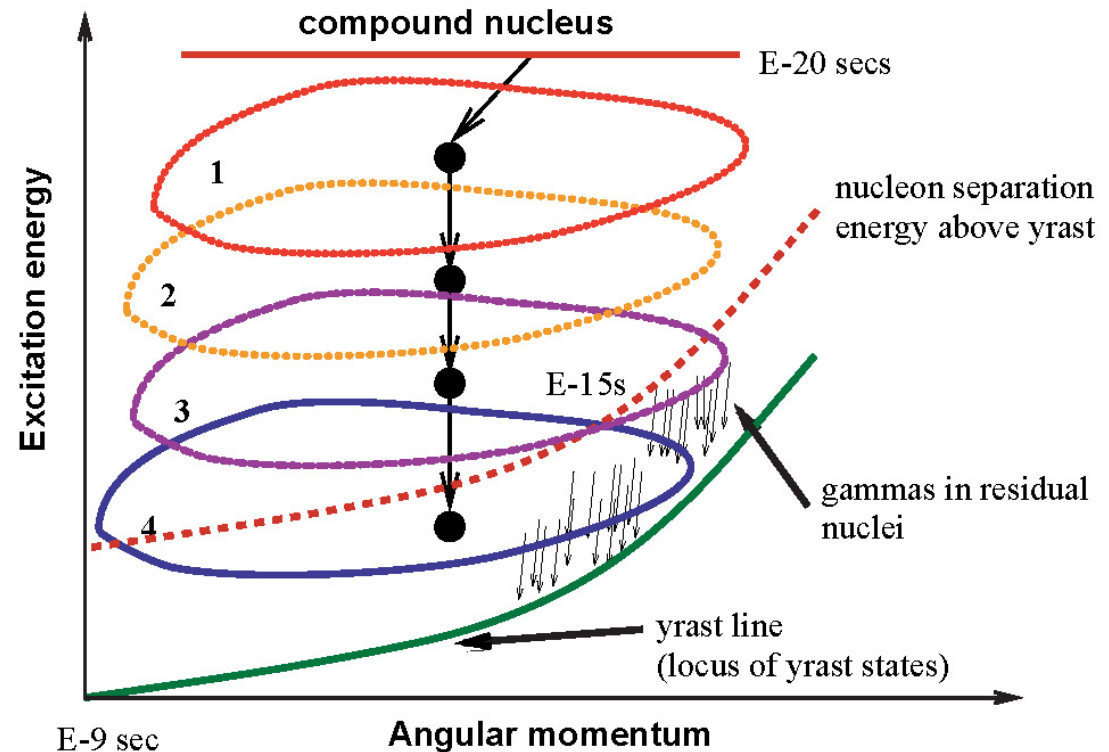
- up to 1 barn for Coulex (large Z nuclei)
- tens of mbarn for proton scattering and 1 nucleon knockout,
- down to few mb for 2 nucleons knockout.
- smaller cross sections for fragmentation



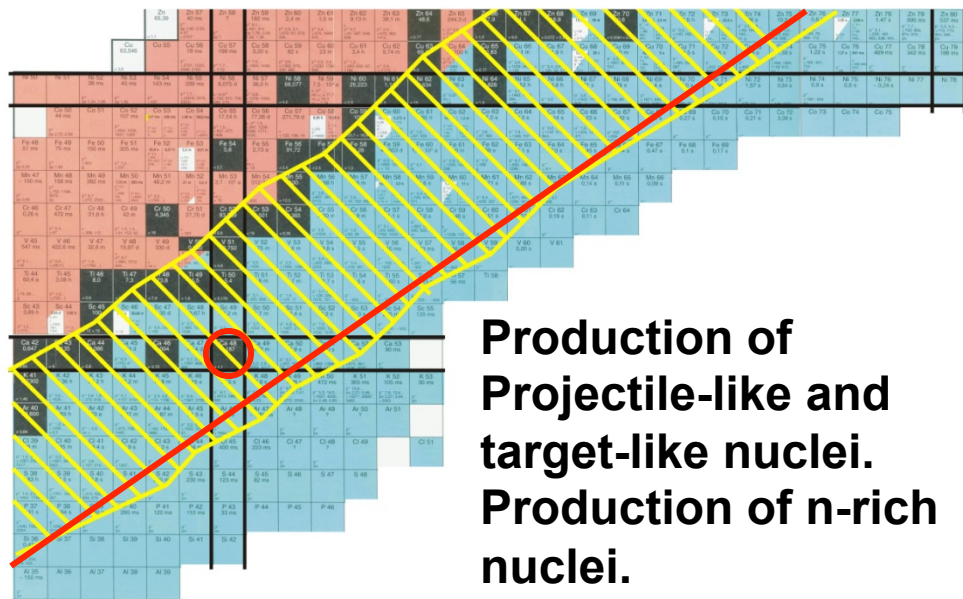
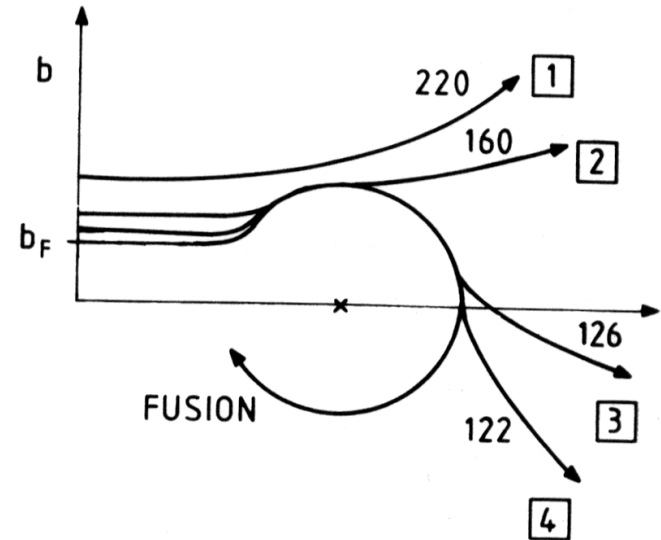
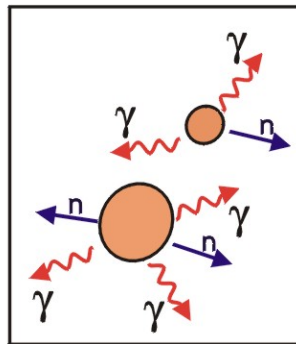
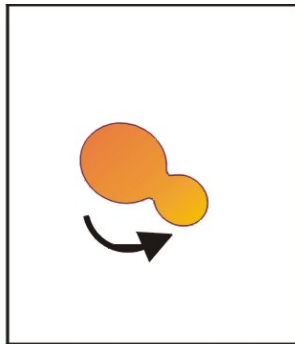
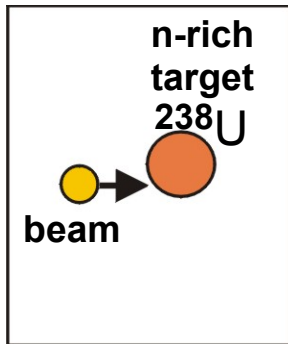
# Example: FUSION-EVAPORATION REACTIONS



## Hauser-Feshbach Theory

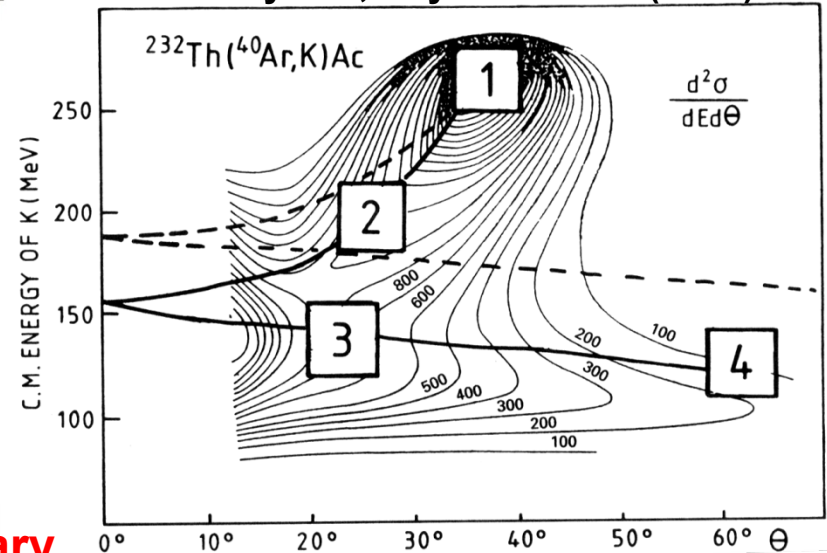


# Example: GRAZING REACTIONS

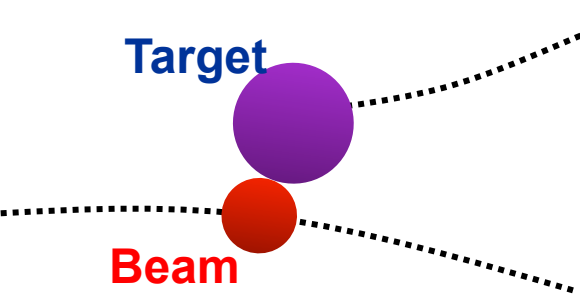


Production of Projectile-like and target-like nuclei. Production of n-rich nuclei.

J. Wilczynski, Phys. Lett. 47B(1973) 484



Identification of products with complementary detectors or by  $\gamma$ -spectroscopy of the partner s is required

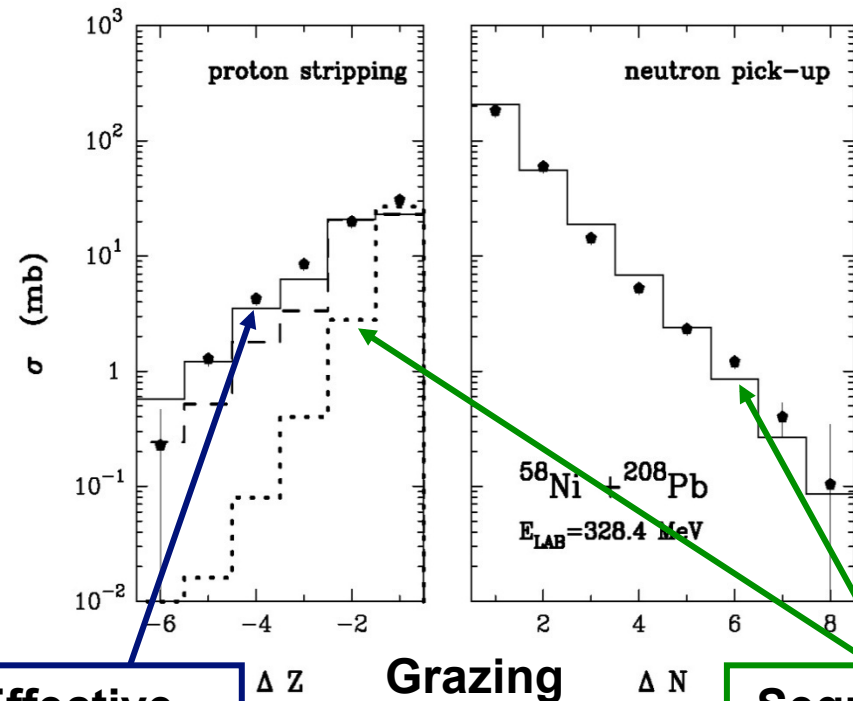
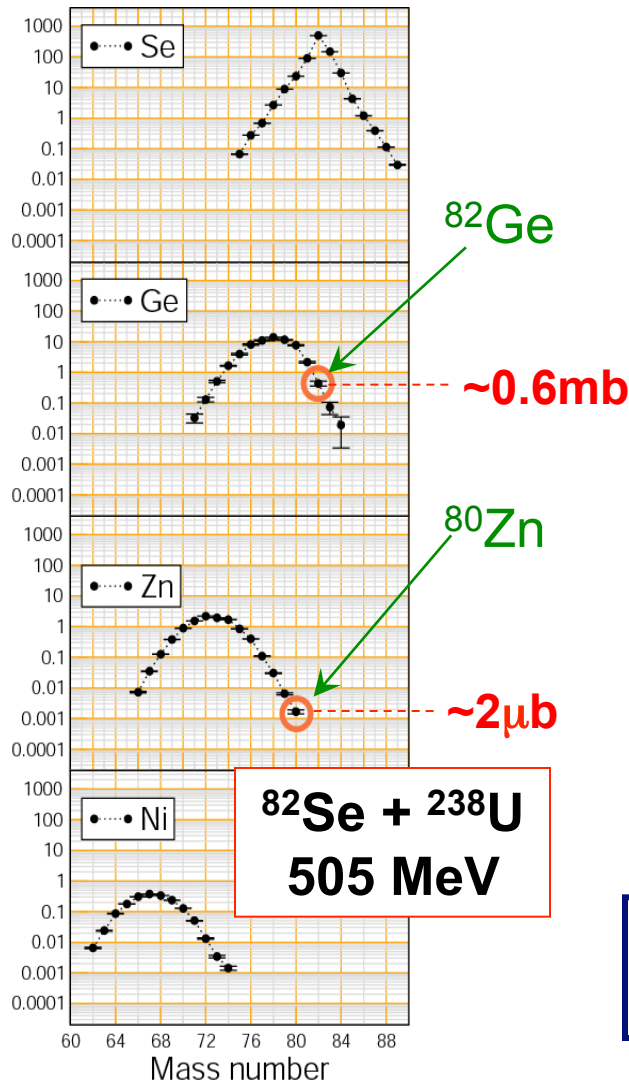


# Grazing reactions transferring several nucleons, a tool to study neutron-rich nuclei

Deep-inelastic reactions used since thick target pioneering work of R.Broda et al. (PLB 251 (90) 245)

Use of Multinucleon-transfer at the grazing angle triggered by the LNL reaction mechanism group.

Approximate cross sections [mb]



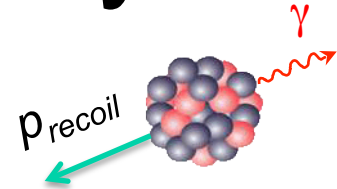
Effective  
Pairing Term

Grazing  
calculations

Sequential  
Transfer

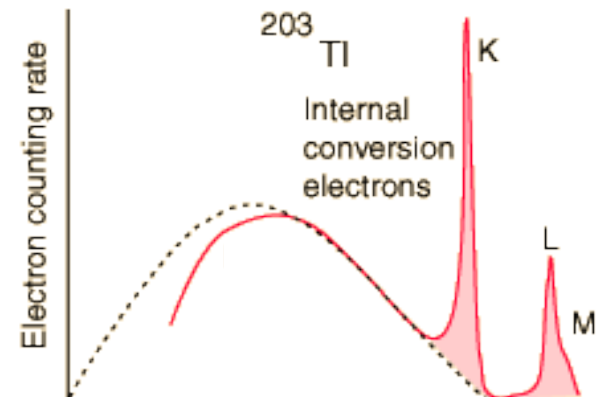
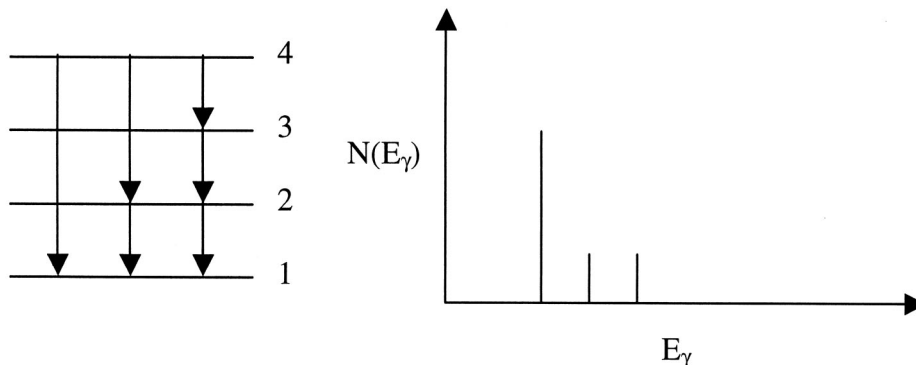
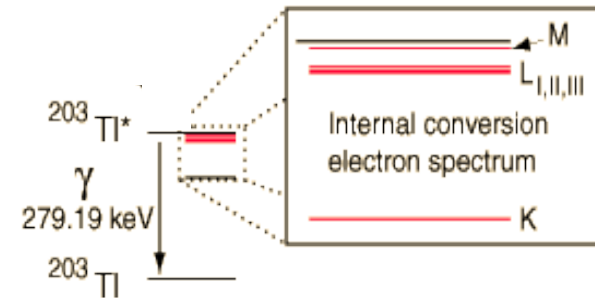
# Electromagnetic decay

- There are three types of electromagnetic decay,  $\gamma$ -ray emission, internal conversion (IC) and pair production ( $E > 1.02 \text{ MeV}$ ).
- In electromagnetic decays  $\Delta N = \Delta Z = \Delta A = 0$ , with just a lowering of the excitation energy of the nucleus.
- In  $\gamma$ -ray emission, the emitted photons are mono-energetic and have an energy corresponding to almost all of the energy difference between the final and initial state of the system.



$$p_{\gamma} = p_{\text{recoil}}$$

$$T_{\text{recoil}} = \frac{p_{\text{recoil}}^2}{2m_{\text{recoil}}} = \frac{p_{\gamma}^2}{2m_{\text{recoil}}} = \frac{E_{\gamma}^2}{2m_{\text{recoil}}c^2}$$





# Electromagnetic Decay

- The initial and final states have a definite angular momentum and parity. The photon carries away a definite amount of angular momentum. Angular momentum and parity must be conserved.
- Multipolarity is a measure of the angular momentum carried away by the photon.
- Transitions are classified as electric or magnetic based on whether the radiation is due to a shift in the charge distribution or a shift in the current distribution.
- Based upon the type of operator involved in the transition, there are restrictions on the parity change in the transition.

$$\left| (I_i - I_f) \right| \leq \ell \leq (I_i + I_f) \hbar$$

*A photon with  $\ell$  units of angular momentum*

*is called a  $2^\ell$ -pole photon.*

$\ell = 1 \Rightarrow$  dipole

$\ell = 2 \Rightarrow$  quadrupole

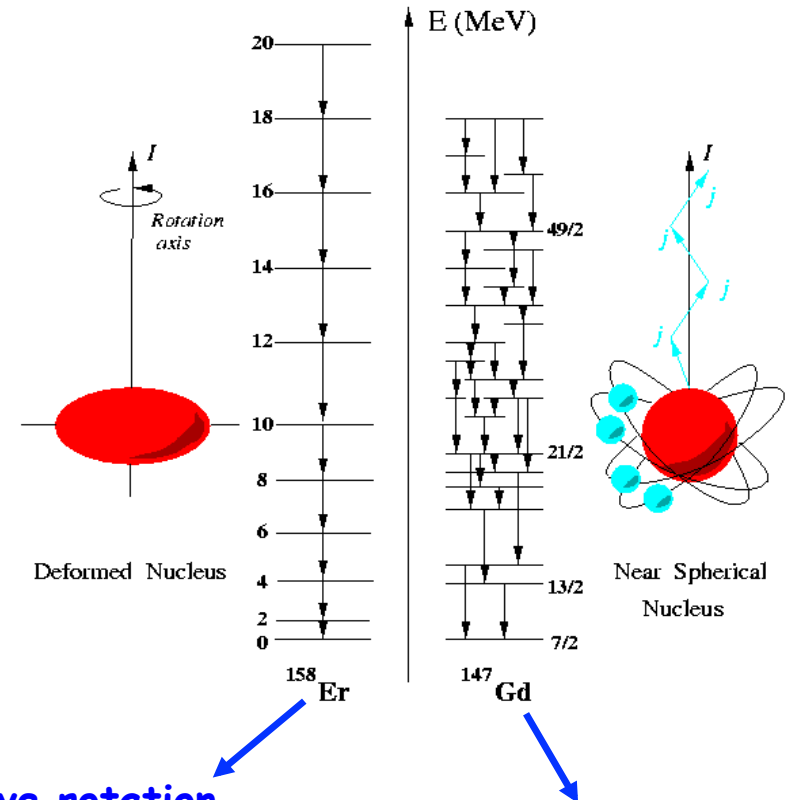
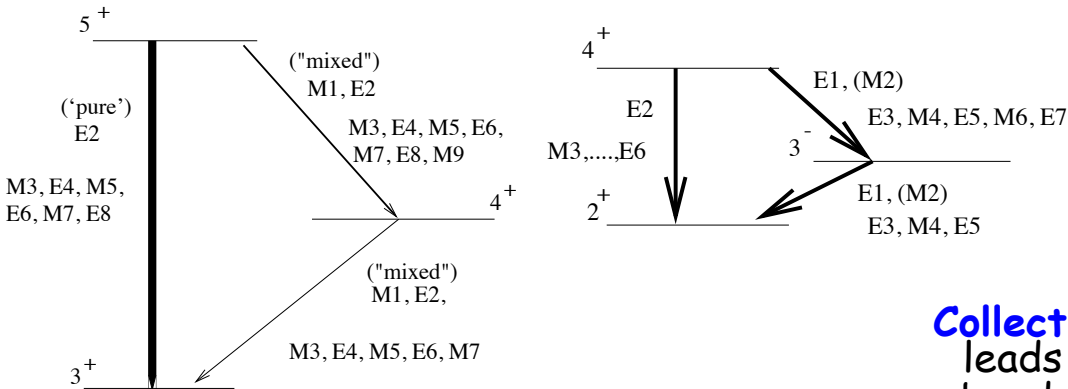
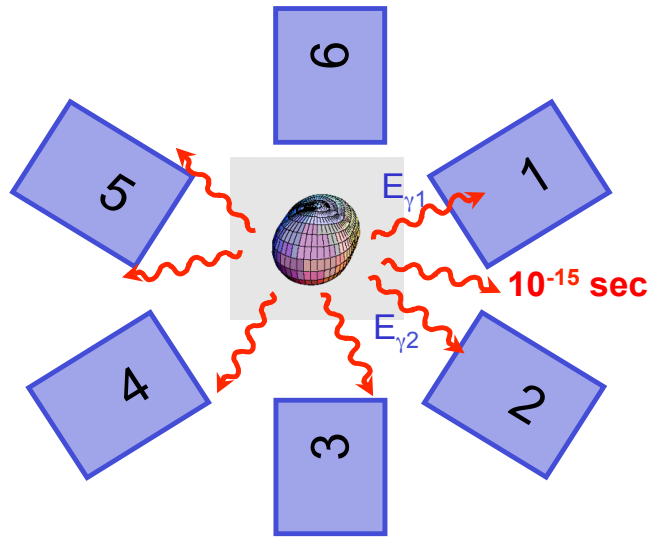
$\ell = 3 \Rightarrow$  octupole

**TABLE 9.1  $\gamma$ -Ray Selection Rules and Multipolarities**

Radiation Type	Name	$l = \Delta I$	$\Delta\pi$
E1	Electric dipole	1	Yes
M1	Magnetic dipole	1	No
E2	Electric quadrupole	2	No
M2	Magnetic quadrupole	2	Yes
E3	Electric octupole	3	Yes
M3	Magnetic octupole	3	No
E4	Electric hexadecapole	4	No
M4	Magnetic hexadecapole	4	Yes



# In-beam Experiments and Nuclear Structure



Collective rotation  
leads to **regular**  
band structures

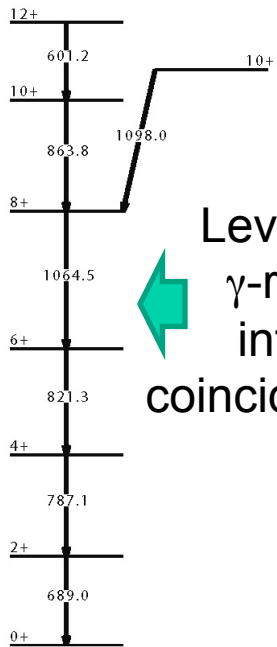
Single-particle generation  
of spin leads to an  
**irregular** level structure

$B(E/M\lambda)$

The decay probability is governed by the matrix element of the multipole operator

$$m_{fi}(\sigma L) = \int \Psi_f^* m(\sigma L) \Psi_i dv$$

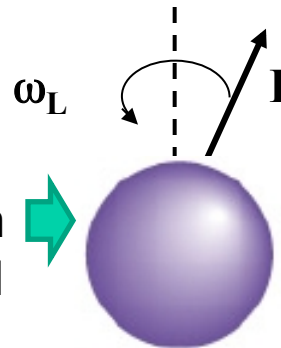
# Measurements with HR $\gamma$ -ray spectroscopy



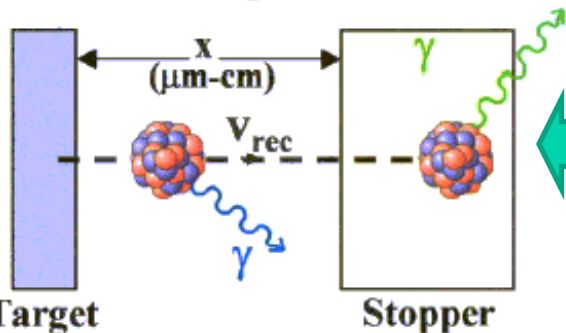
Level Energies:  
 $\gamma$ -ray Energy,  
intensity and  
coincidence analysis

Level  $J^\pi$ :  
 $\gamma$ -ray angular distribution,  
correlations and linear  
polarization

g-factors by  
precession on  
magnetic field

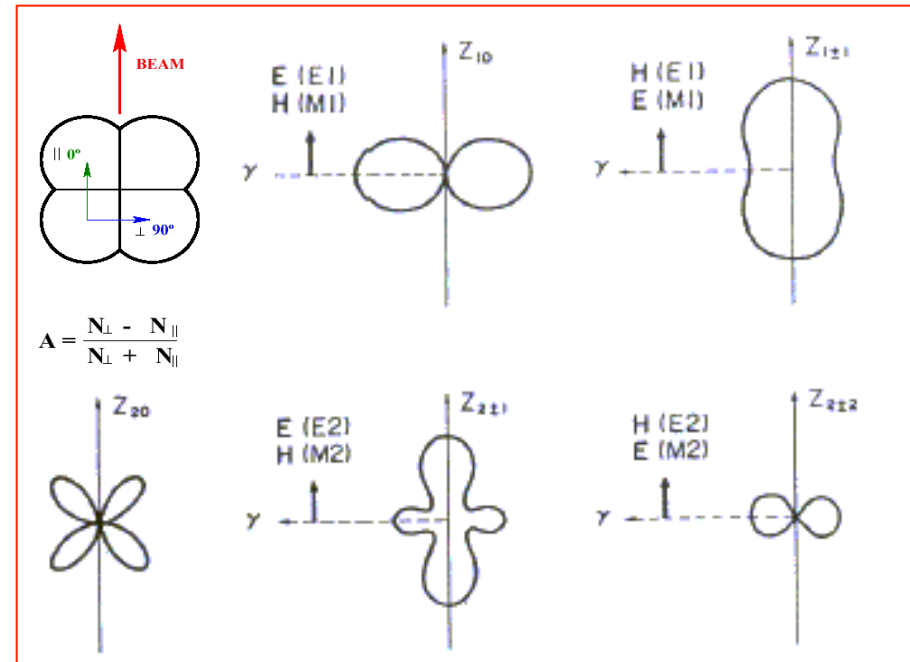
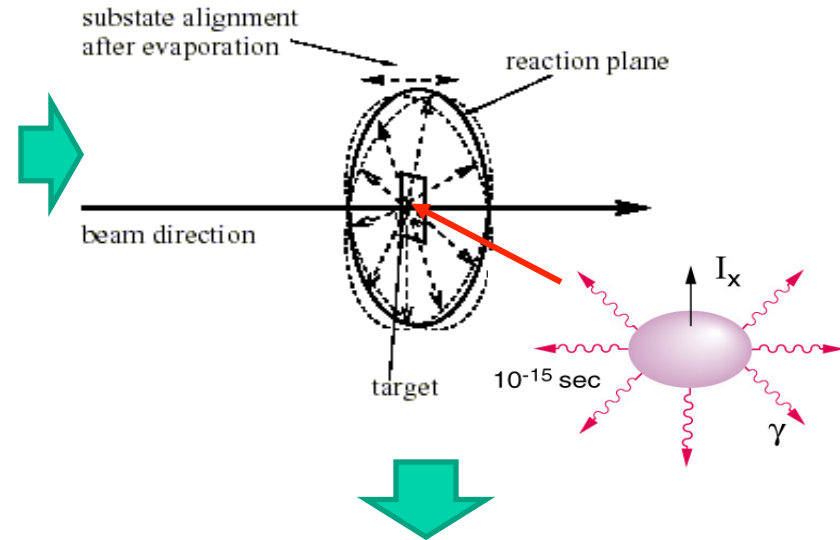


$\tau = 1\text{ps} - 3\text{ns}$



Lifetimes by  
Doppler or  
indirect methods

Example RDDS Method



# Electromagnetic emission from Oriented Nuclei: Angular distributions

$$Z_{1\pm 1}(\theta) = 1/4\pi \{1 + 1/2 P_2(\cos \theta)\}$$

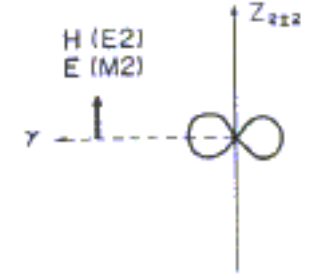
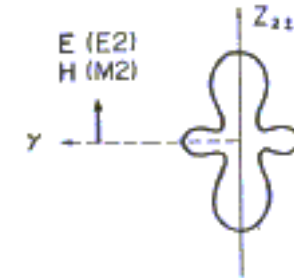
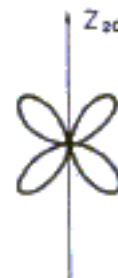
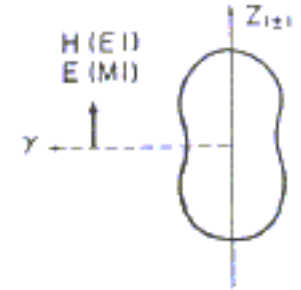
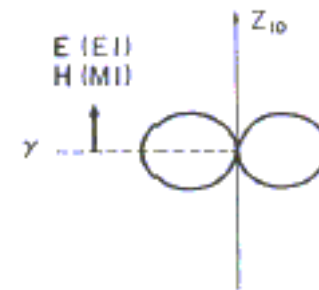
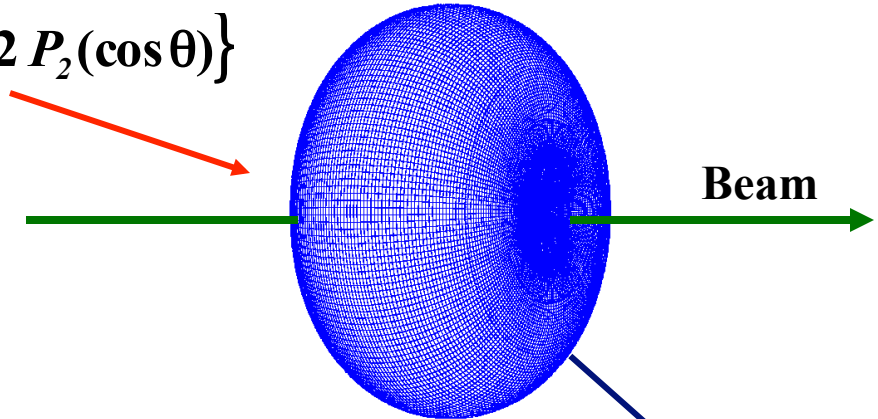
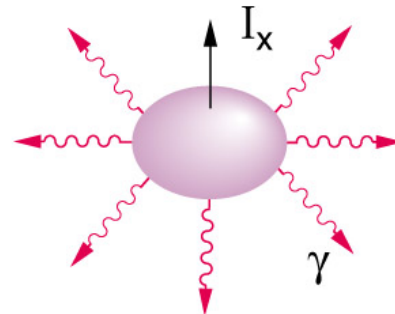
substate alignment  
after evaporation

$\sigma/J$

reaction plane

beam direction

target



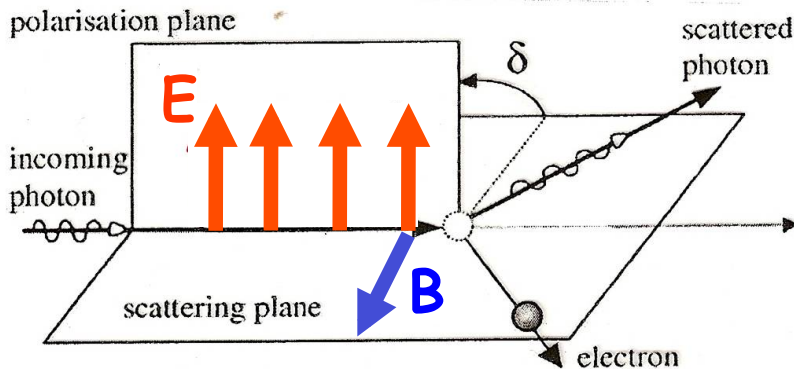
Angular distributions and correlations are only sensitive to the multipolarity  $L$   
Polarization measurements are more sensitive to Character

# Measurement of the linear polarization

- $\gamma$ -rays emitted by oriented nuclei are partially polarized. The polarization vector is different for E and M transitions (character)
- Compton scattering can be used to measure the degree of polarization through the dependency with the polarization vector

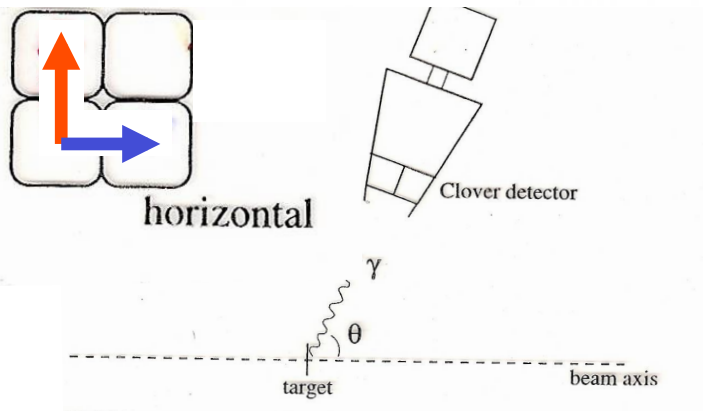
$$\frac{d\sigma_{KN}}{d\Omega} = \frac{r_0^2}{4} \left( \frac{E'}{E} \right)^2 \left[ \frac{E'}{E} + \frac{E}{E'} - 2 \sin^2 \theta \cos^2 \varphi \right]$$

$\varphi$  : angle between the scattering plane and the initial polarization plane



**Stretched  $E\lambda$  transitions will have positive asymmetry**

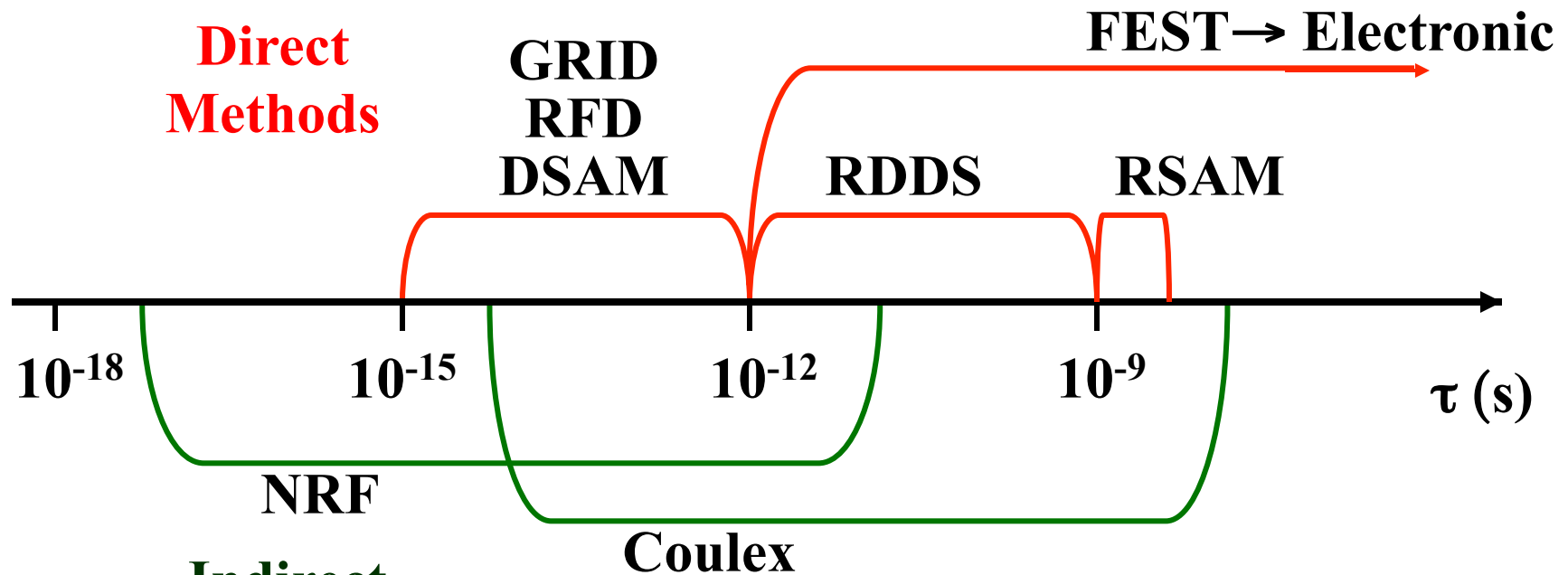
**Stretched  $M\lambda$  transitions will have negative asymmetry**



$$P_E(\theta) = \frac{1}{Q} \cdot \frac{N_{\perp} - N_{\parallel}}{N_{\perp} + N_{\parallel}}$$

Experiments measure the asymmetry.  
 $Q$  is the sensibility of the polarimeter

# Techniques for lifetime measurements



**Indirect  
Methods**

**GRID:** Gamma ray induced Doppler broadening

**DSAM:** Doppler shift attenuation method

**RFD:** Recoil straggling method

**RDDS:** Recoil distance Doppler shift method

**RSAM:** Recoil shadow anisotropy method

**FEST:** Fast electronic scintillation method

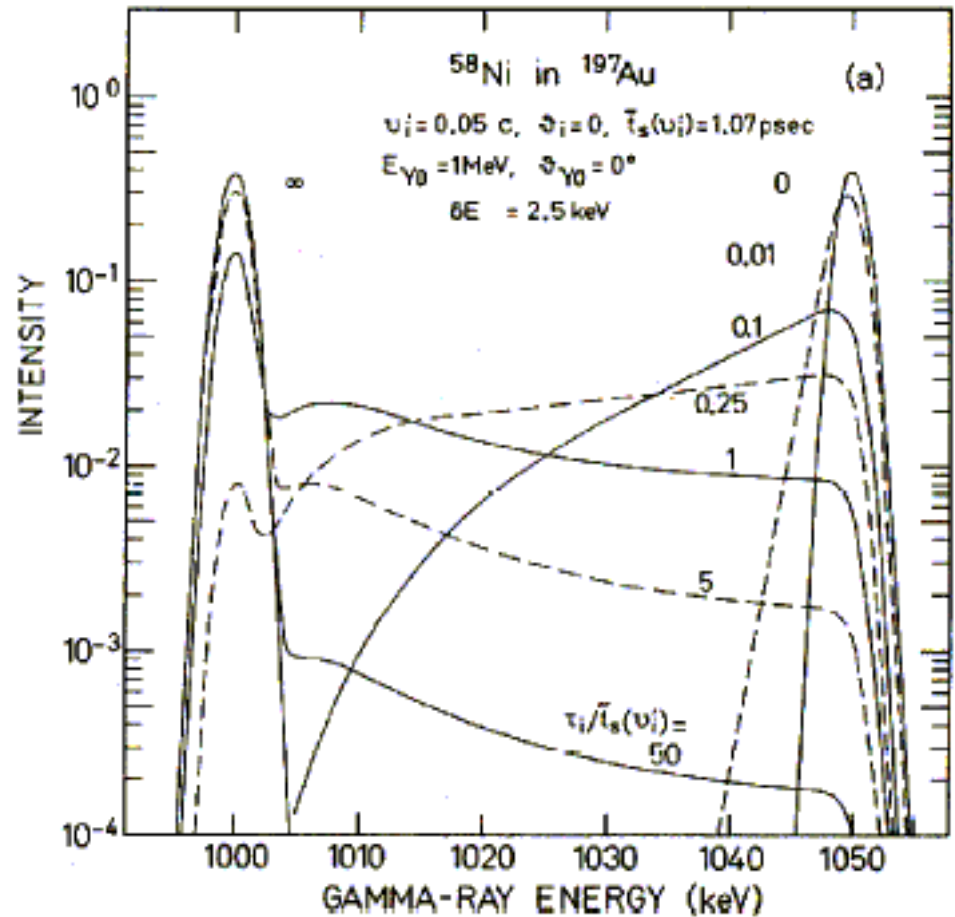
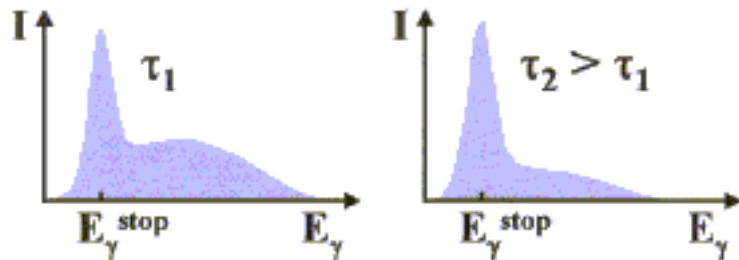
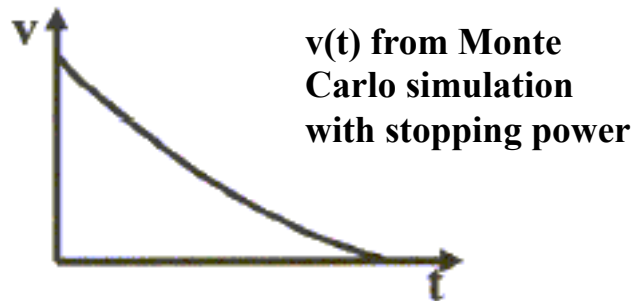
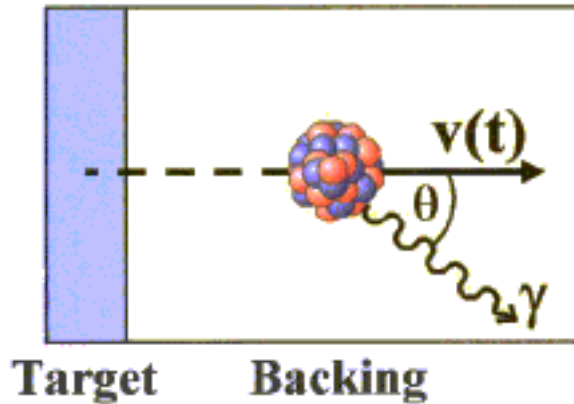
**NRF:** Nuclear resonance fluorescence

**Coulex:**

Coulomb excitation cross section

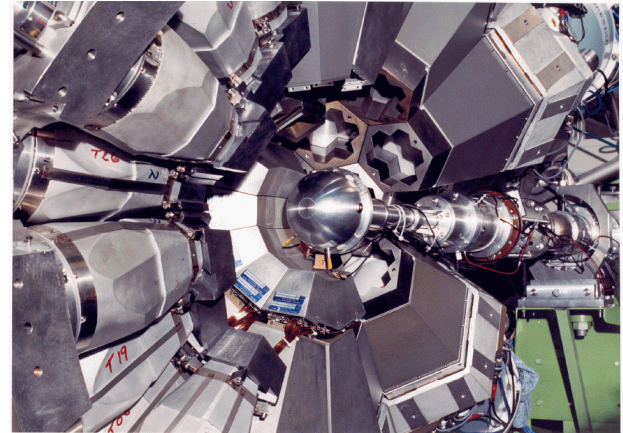
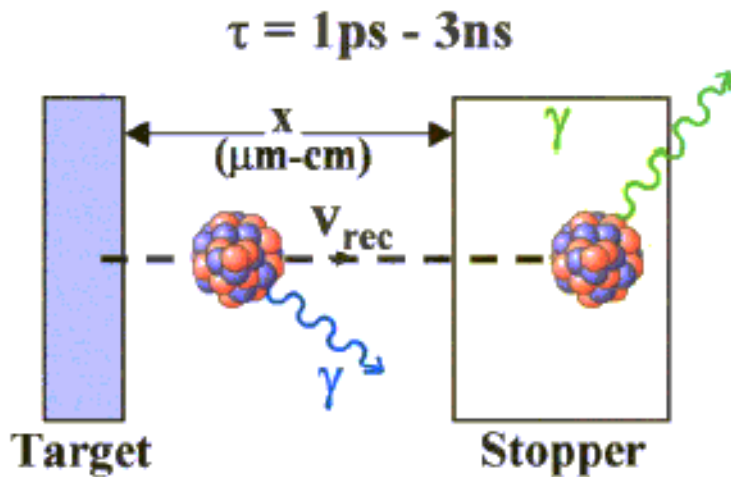
# Doppler Shift Attenuation Method

$$\tau = 0.1 - 1.5 \text{ ps}$$

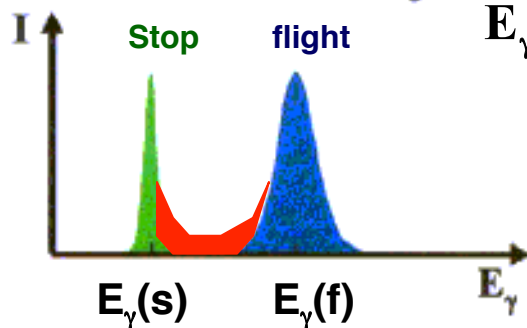
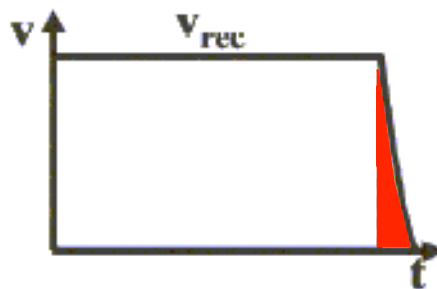


Line shapes for  $^{58}\text{Ni}$  stopped in  $^{197}\text{Au}$  with a beam velocity of  $v/c=0.05$  and measured at  $\theta=0^\circ$

# Recoil Distance Doppler Shift Method



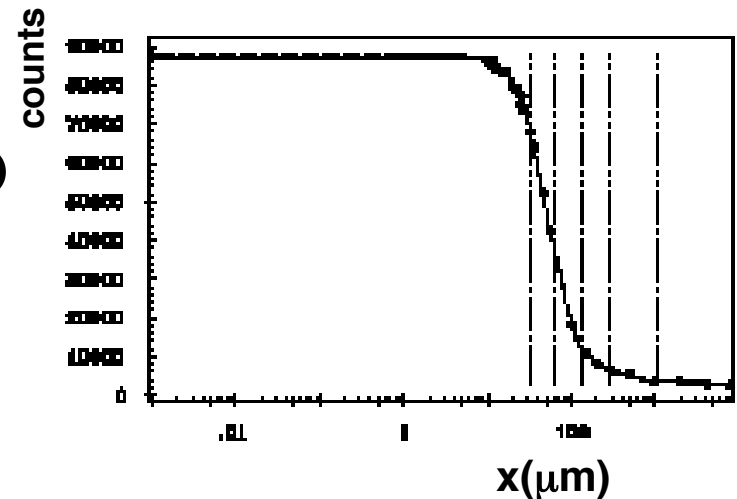
Koeln University plunger



$$E_{\gamma}(f) \approx E_{\gamma}(s) \left( 1 + \frac{v_{\text{rec}}}{c} \cos \theta \right)$$

$$I(f) = N_0 (1 - e^{-(x/v_{\text{rec}}\tau)})$$

Decay Curve





# Interaction of the $\gamma$ -rays with matter

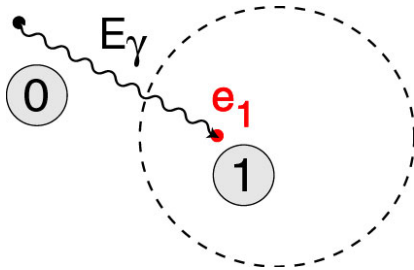
$\sim 100 \text{ keV}$

$\sim 1 \text{ MeV}$

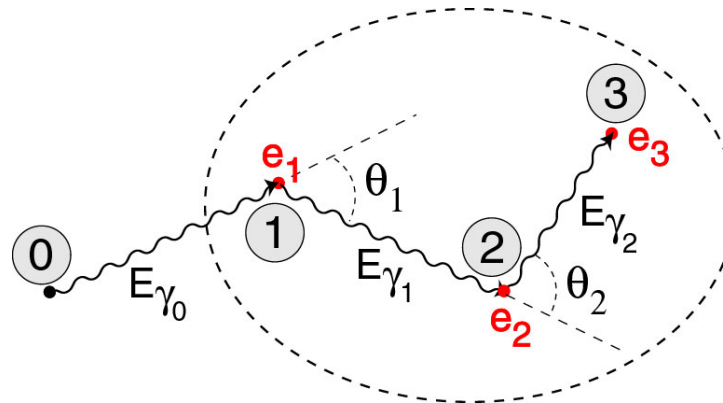
$\sim 10 \text{ MeV}$

$\gamma$ -ray energy

## Photoelectric

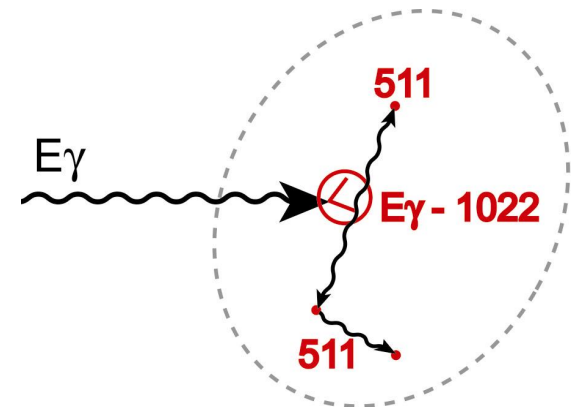


## Compton Scattering



$$E_{\gamma'} = \frac{E_\gamma}{1 + \frac{E_\gamma}{m_0 c^2} (1 - \cos\theta)}$$

## Pair Production

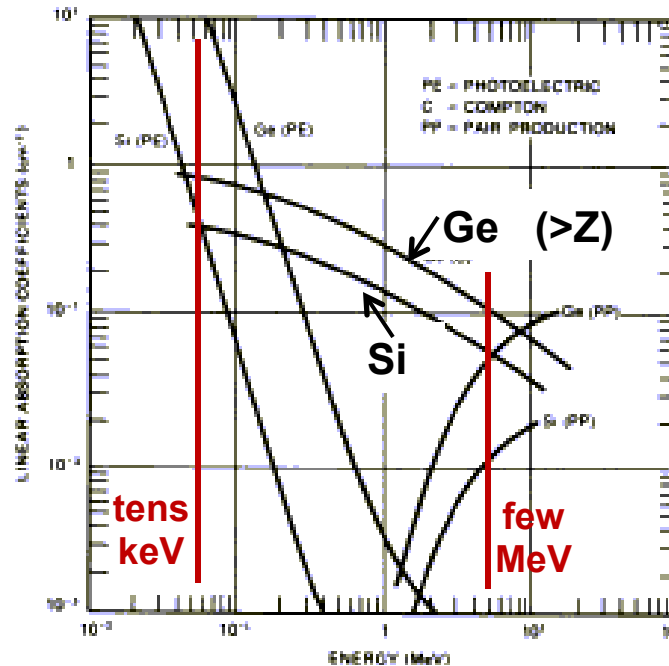
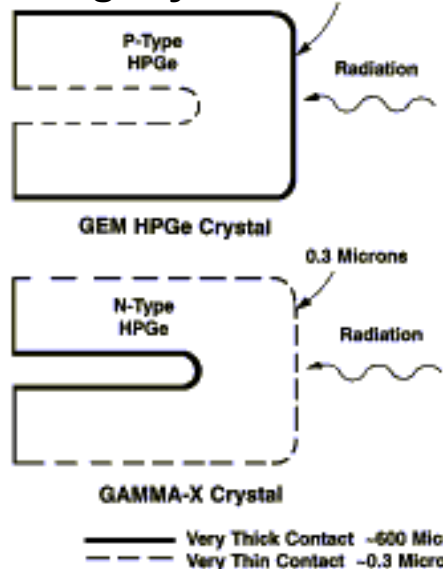


# Instrumentation for HR $\gamma$ -ray spectroscopy

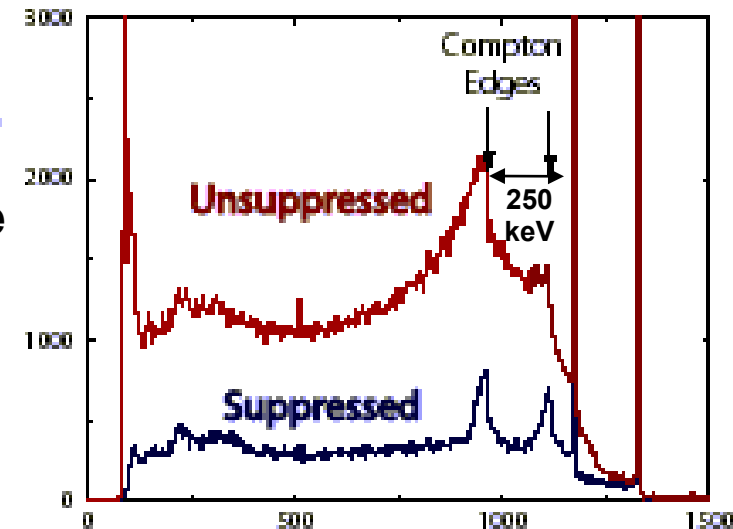
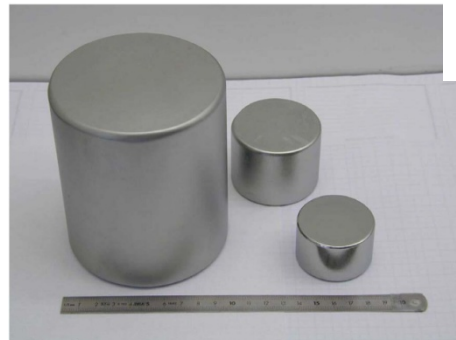
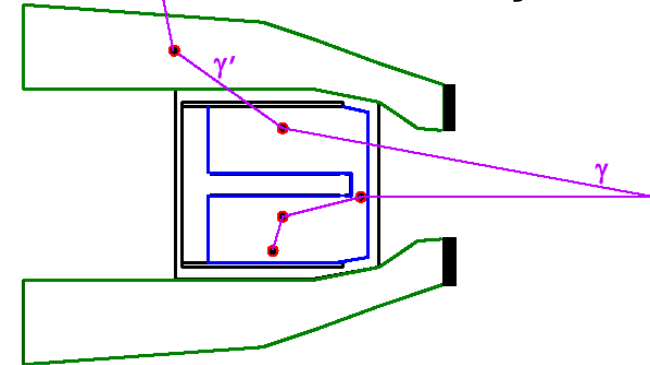
High resolution  $\gamma$ -ray spectroscopy  $\rightarrow$  large volume semiconductor detectors  
in particular detectors based on HP-Ge (impurities  $\sim 10^{-12}$ )

## Present Ge

>2 kg/crystal ~600 Microns

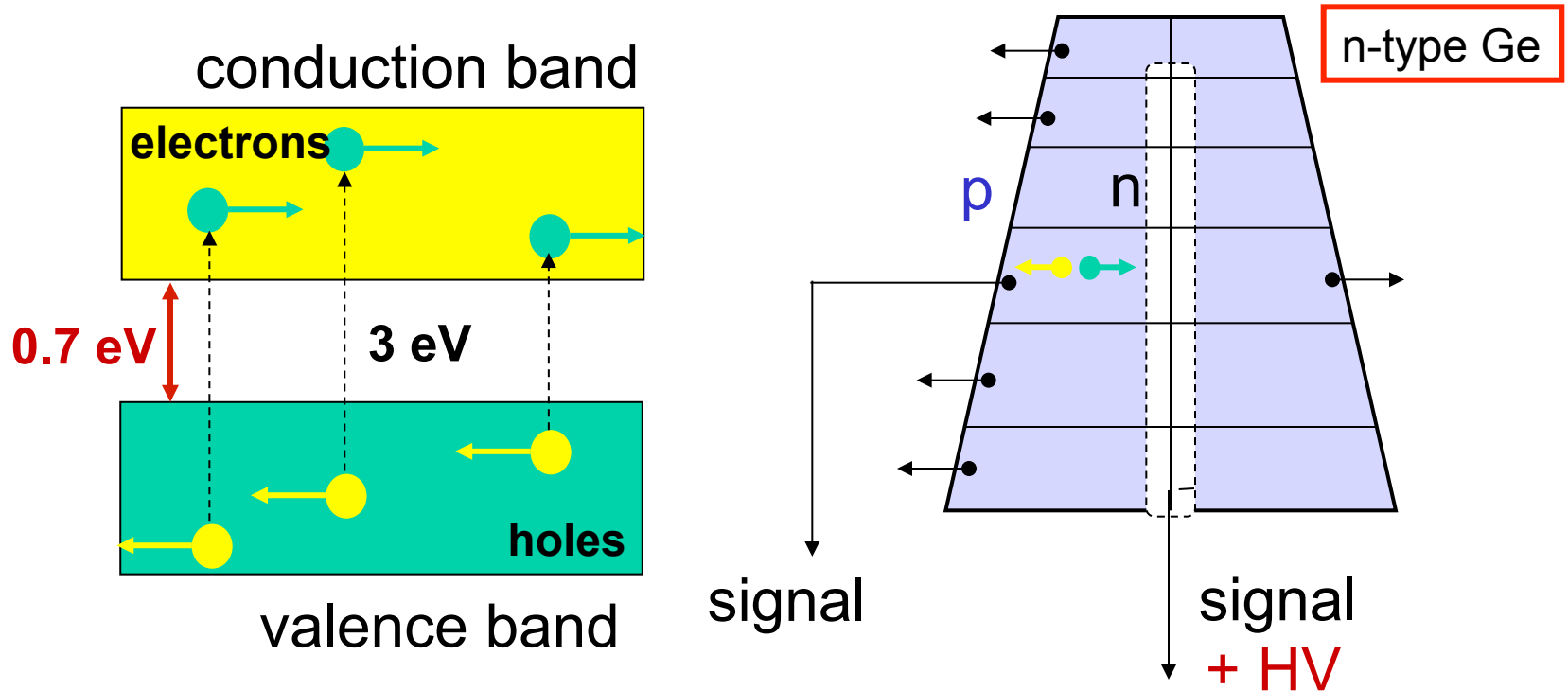


## Compton suppressed Ge-detectors $\rightarrow$ arrays



# Germanium detector

Sensitivity factors: Energy Resolution, Peak to Total Ratio



Number of e-h pairs for 1 MeV,  $N = 10^6 / 3 = 3 \times 10^5$

**Energy resolution (Fano Factor)**  $\sqrt{N}/N = 0.0018 \rightarrow 1.8 \text{ keV } (E_\gamma = 1 \text{ MeV})$

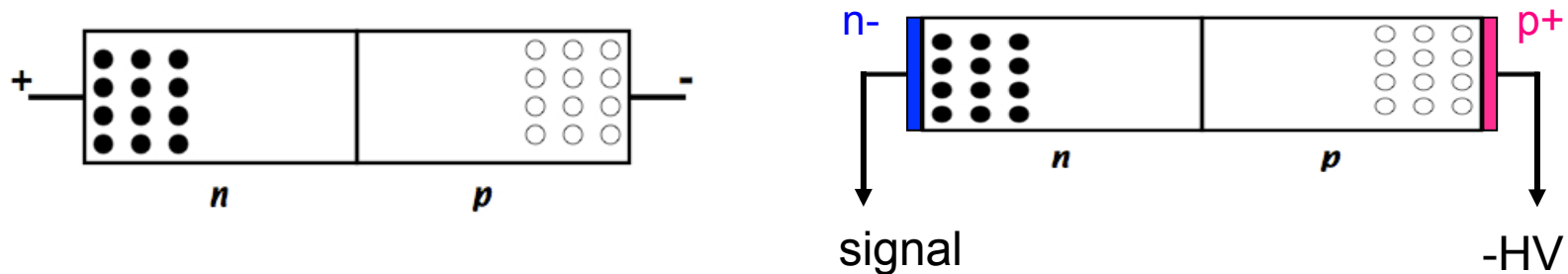
Thermally activated charge carriers in the conduction band density at room temperature  $\sim 2.5 \cdot 10^{13} \text{ cm}^{-3}$  for Ge ( $\sim 1.5 \cdot 10^{10} \text{ cm}^{-3}$  for Si)

To reduce the number of free charge carriers :

=> deplete material: np junction

=> increase depletion by applying a reverse bias

=> for Ge, cool detector with  $\text{LN}_2$  - 77K



$$\text{FWHM}^2 = W_D^2 + W_X^2 + W_E^2 + W_{\text{Doppler}}^2$$

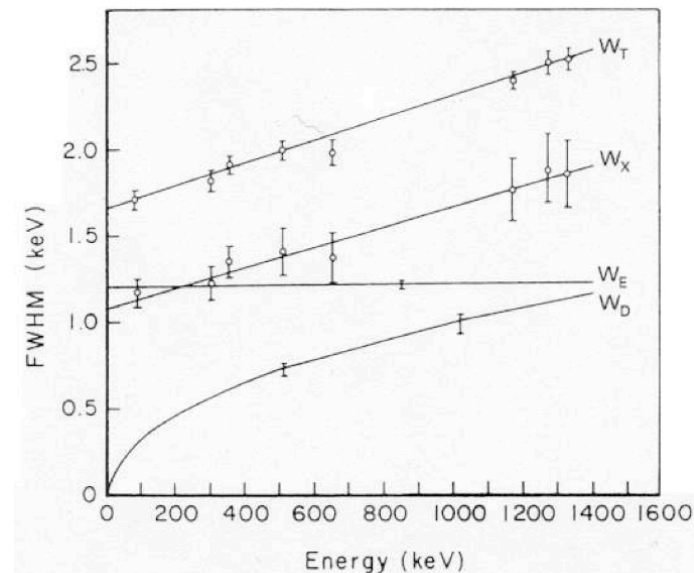
$$W_D = 2.35 \sqrt{F \epsilon E_\gamma} \text{ Statistical fluctuations of carriers}$$

$\epsilon = 2.96 \text{ eV @ 77 K}$  Fano factor  $F \sim 0.1$   
(not all the deposited energy goes to create e-h pairs)

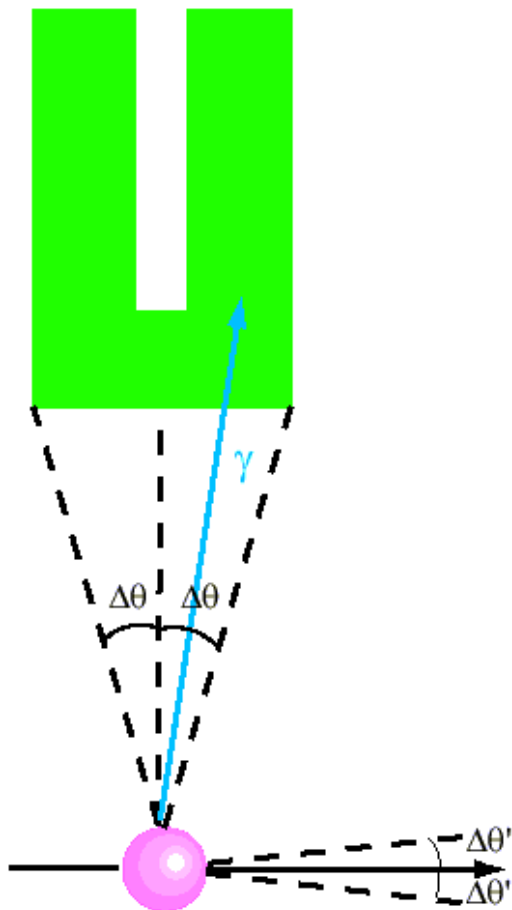
$W_X$  incomplete charge collection

$W_E$  electronic noise

$W_{\text{doppler}}$  Doppler broadening

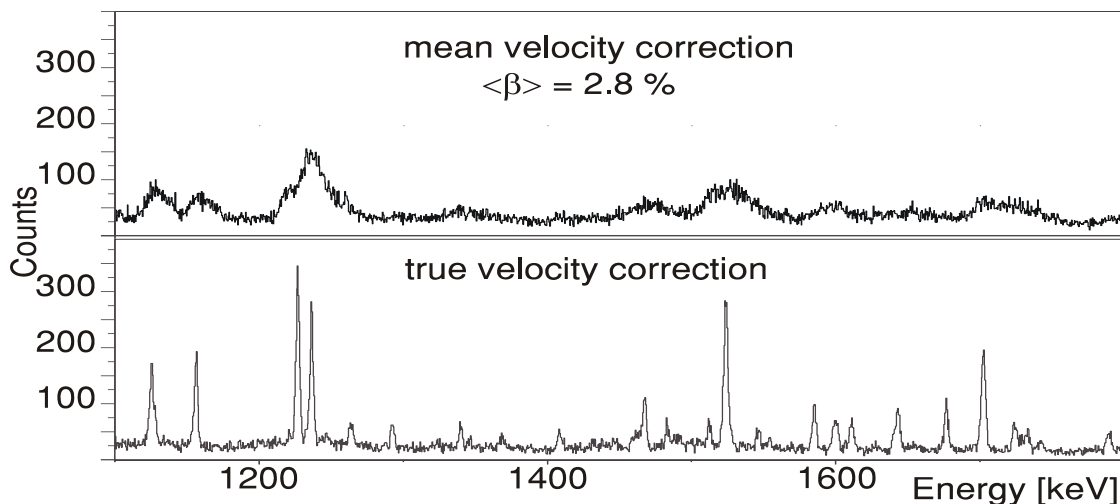


# Doppler Broadening

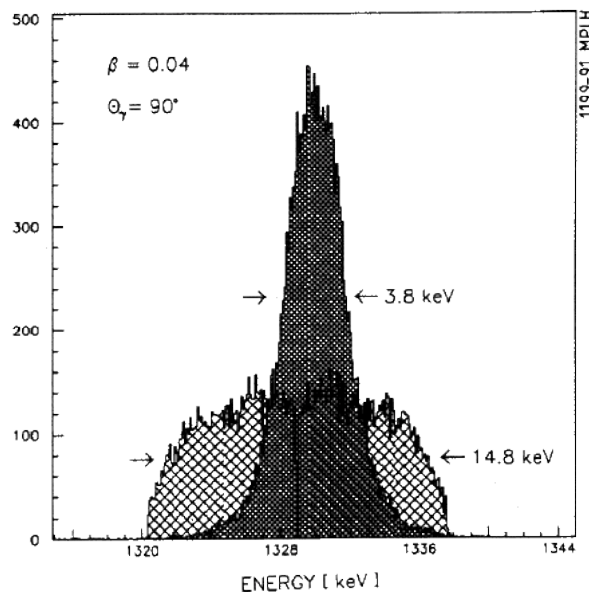


$$E_s = E_0 \left( 1 + v/c \cos \theta \right)$$

$$\Delta E_s = E_0 v/c \sin \theta \Delta \theta$$



Dedicated ancillary detectors for the determination of the recoil trajectory

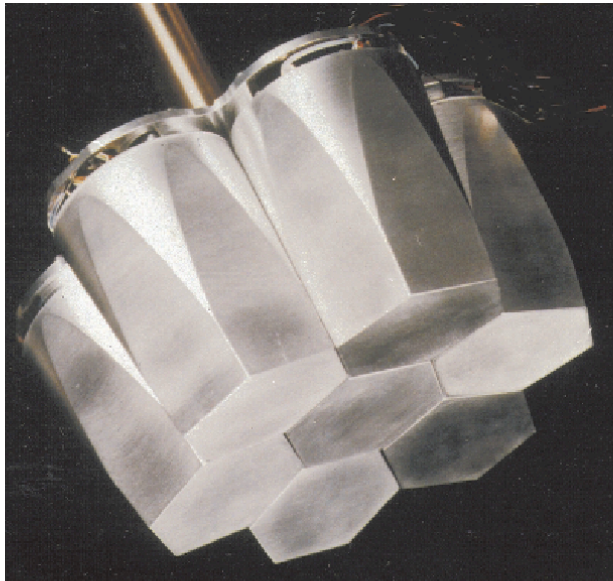
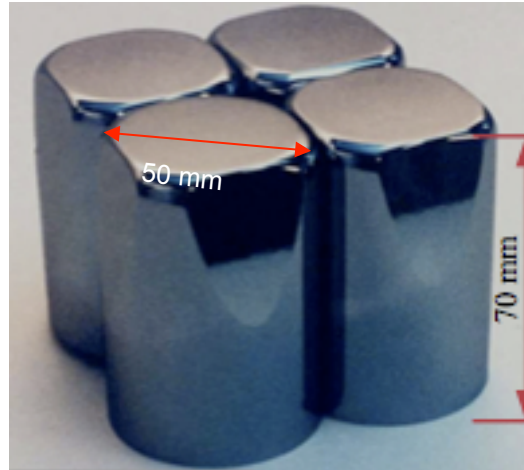


Development of segmented Ge detectors and Pulse Shape Analysis techniques for position determination

# Composite detectors

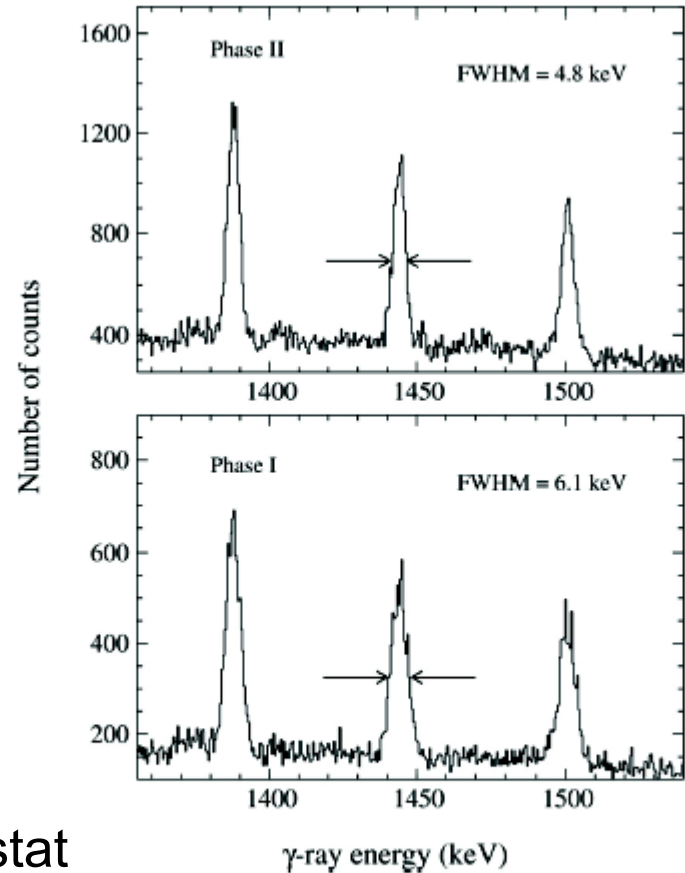
=> Reduction of  $\Delta\theta_D$

- Eurogam II
- Clovers:
  - 4 crystals in 1 cryostat



- Euroball
- Clusters:
  - 7 crystals in 1 cryostat

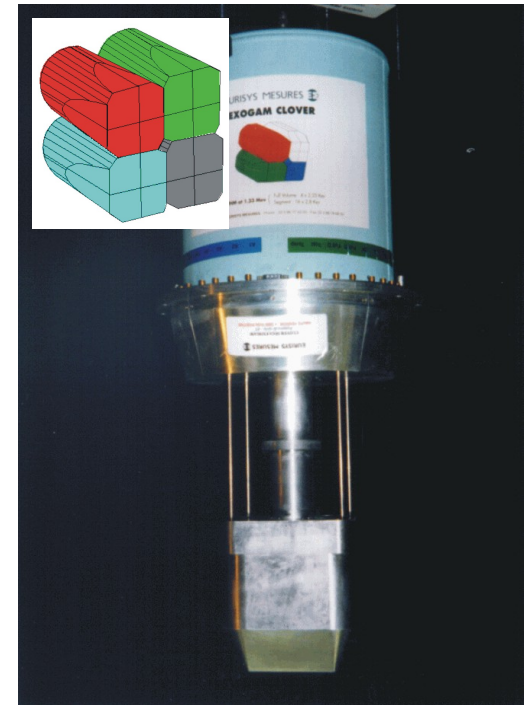
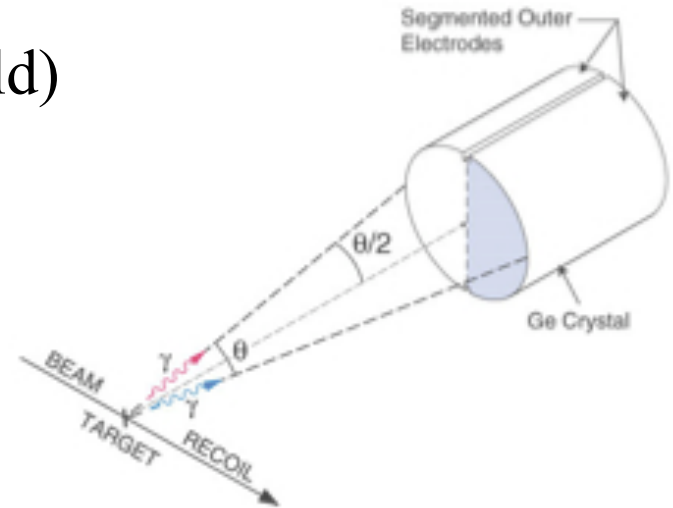
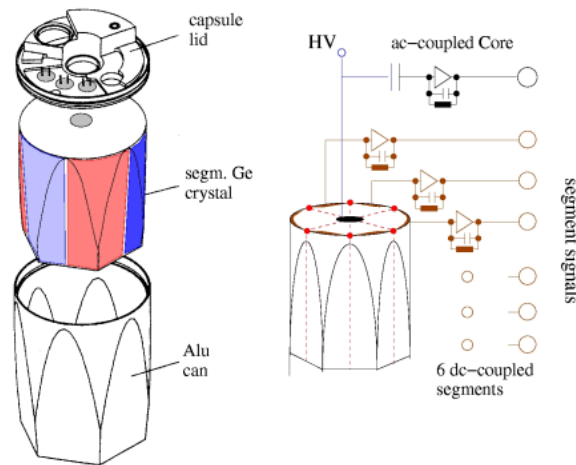
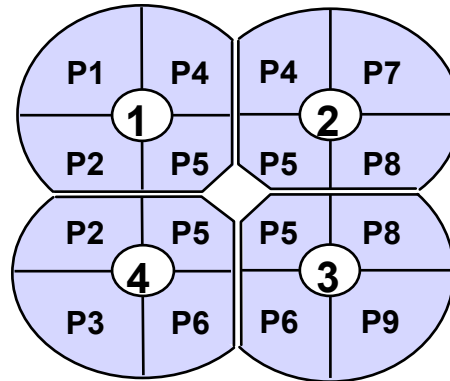
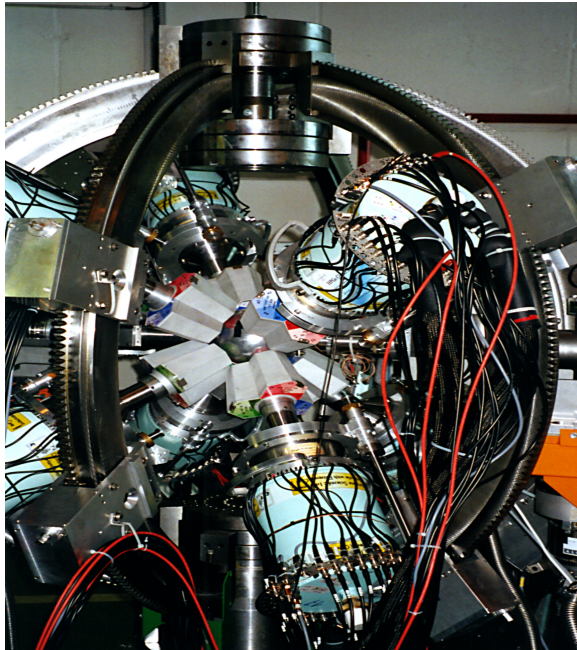
$^{30}\text{Si}(158 \text{ MeV}) + ^{124}\text{Sn} \rightarrow ^{149}\text{Gd}$   
 $v/c = 2.1\%$





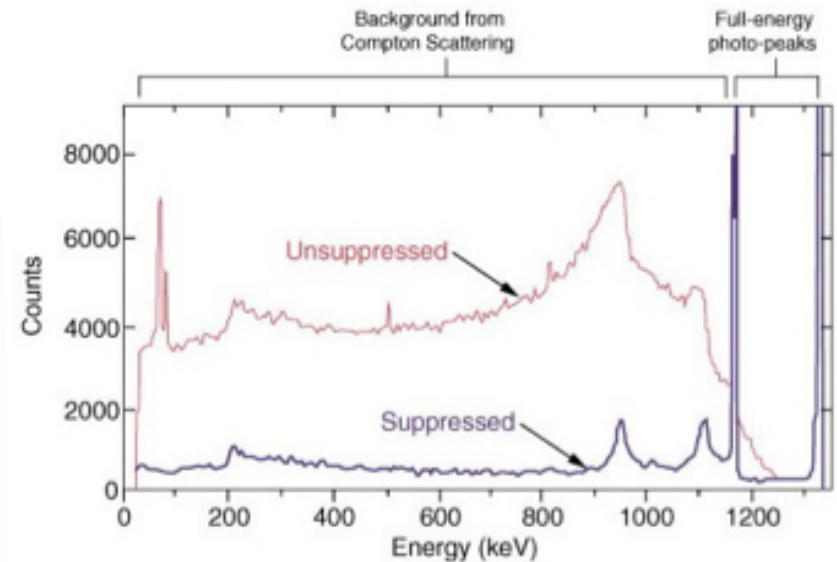
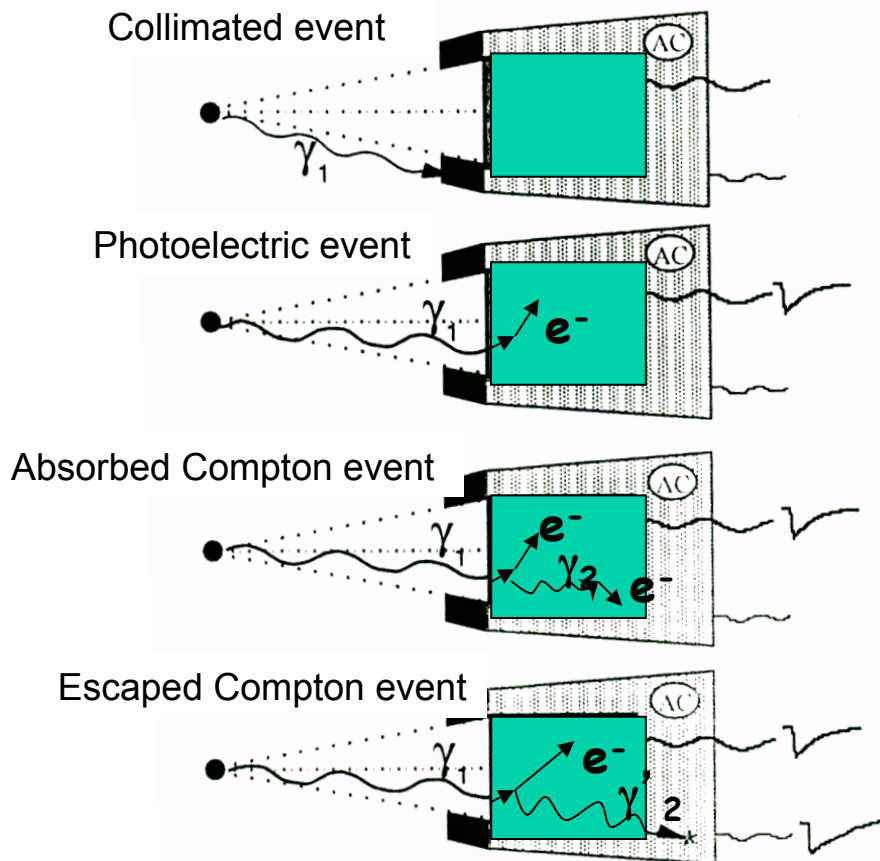
# Electrical Segmentation of detectors

- Gammasphere segmented detector (2 Fold)
- Exogam at Ganil (Segmented Clover)
- Miniball at Isolde (Segmented

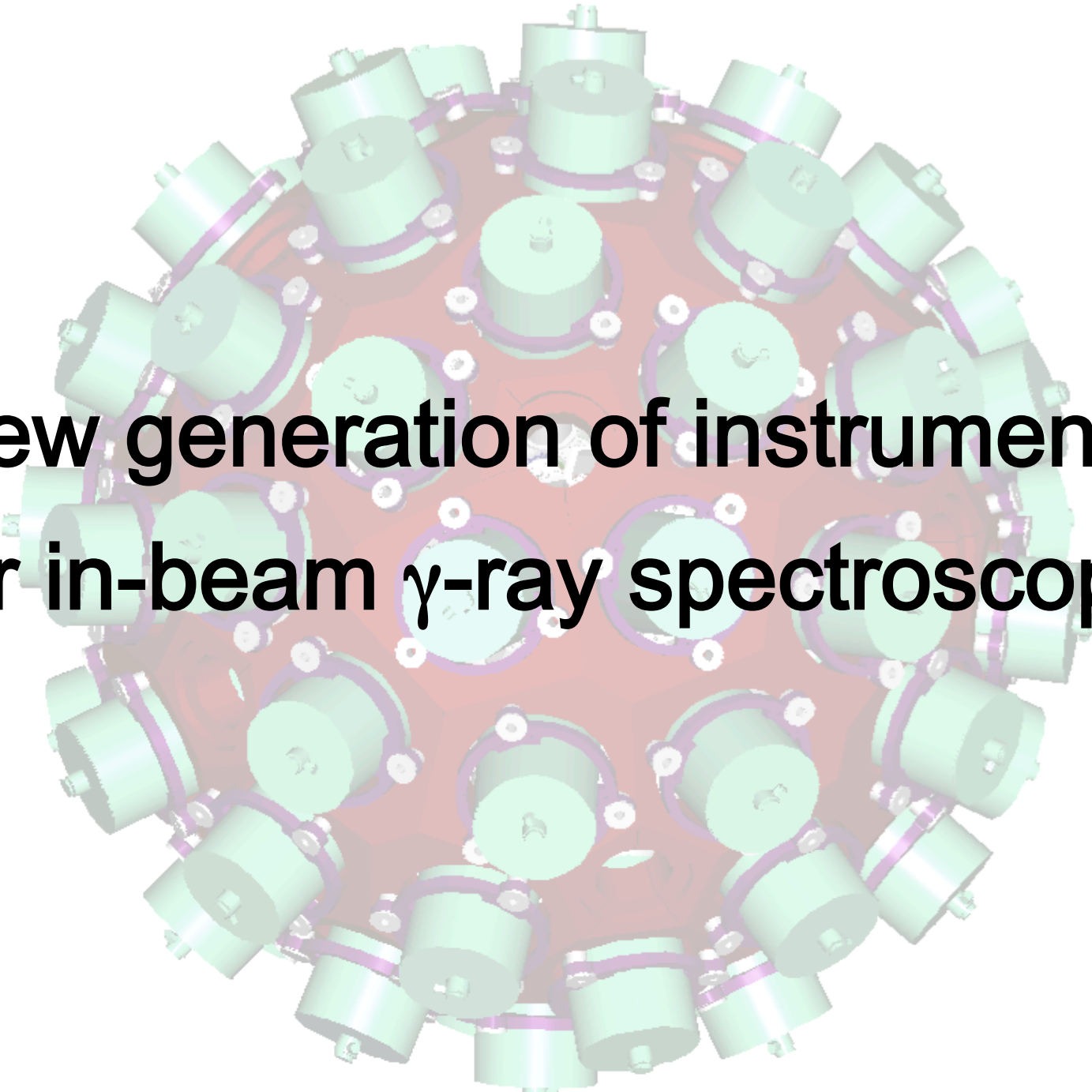




# Signal-to-noise ratio and Compton suppression



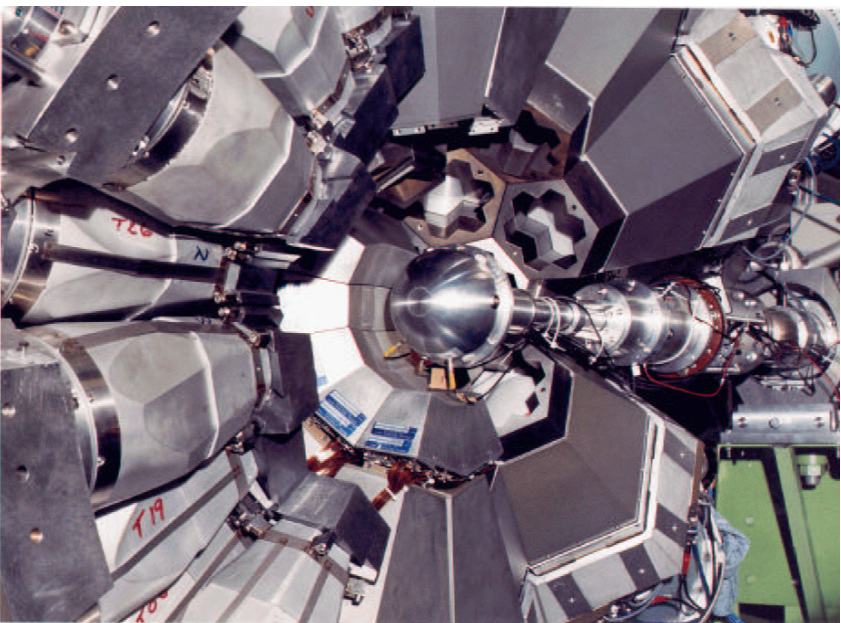
$$P/T \sim 0.2-0.3 \Rightarrow 0.5-0.6$$

A 3D CAD rendering of a circular detector array. The array consists of 24 green cylindrical detector modules arranged in a circular pattern. Each module is mounted on a purple ring. The entire assembly is mounted on a red circular base. The text "New generation of instruments for in-beam  $\gamma$ -ray spectroscopy" is overlaid in the center.

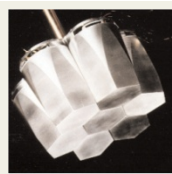
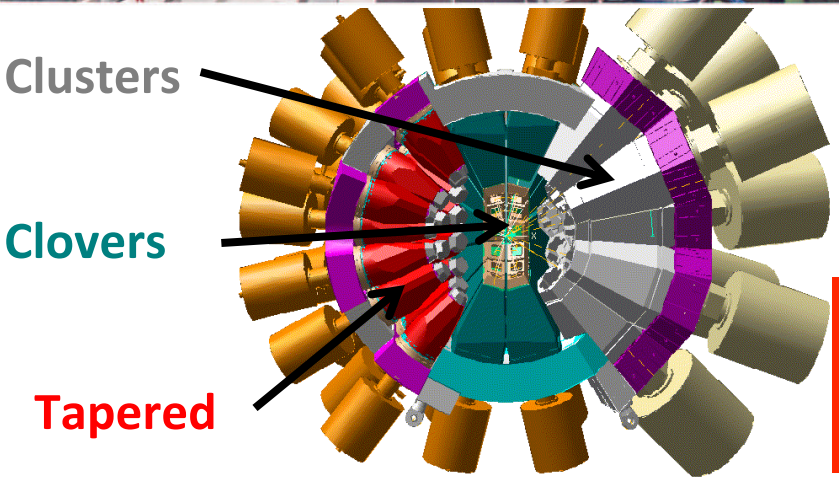
**New generation of instruments  
for in-beam  $\gamma$ -ray spectroscopy**



# EUROBALL: First Large Ge-Array build by a broad European collaboration

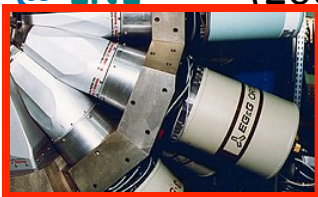
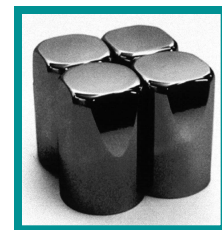


- EUROBALL collaboration started in early 90's. First campaigns at LNL in 1996-1998 and IReS 1999-2003.
- More than 150 publications in refereed journals. More than 60 from the sub-array campaigns
- Technological developments on composite and latter on encapsulated detectors



Cluster Composite Detectors 105 Ge  
(~60%) 15 Cluster → **RISING Campaigns**  
@FRS-GSI

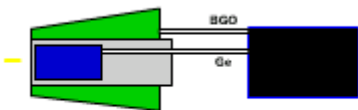
**Clover Composite Detectors:** 104 Ge  
(~20%) (26 Clover) → **CLARA Campaign**  
@ LNL (2008 → JUROGAM II)



**Tapered Detectors:** ~30 Ge (70%)  
→ **JUROGAM I Campaign @JYFL**  
(2008 → ORGAM )



## Large $\gamma$ -Arrays based on Compton Suppressed Spectrometers



$\epsilon \sim 10 - 5 \%$   
( $M_\gamma=1 - M_\gamma=30$ )

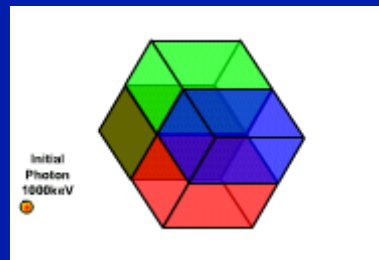


Compact  $\gamma$ -Arrays optimized  
Doppler correction, low  $M_\gamma$

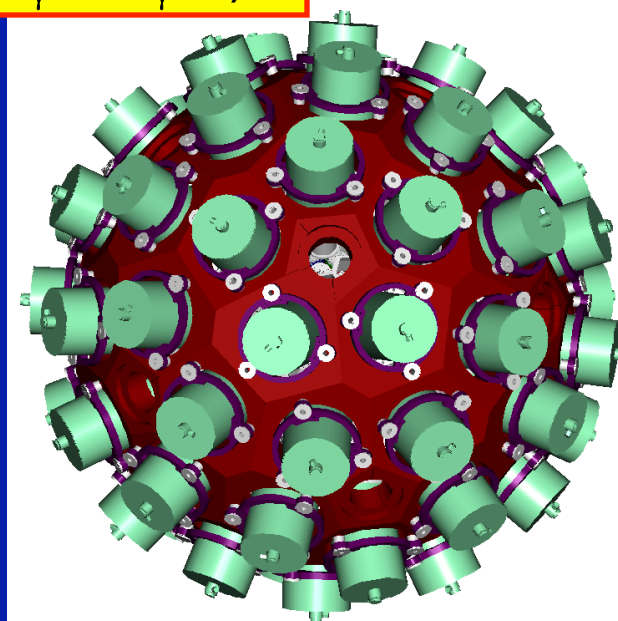
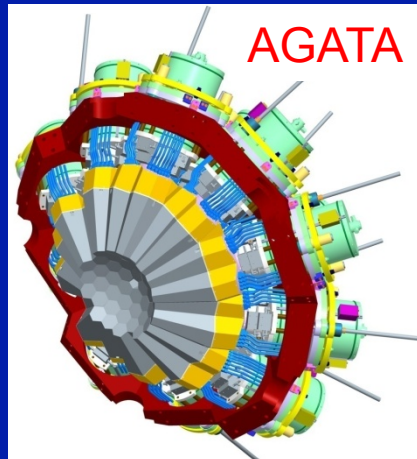


$\epsilon \sim 20 \%$   $M_\gamma=1$

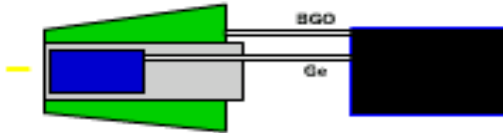
## Tracking Arrays based on Position Sensitive Ge Detectors



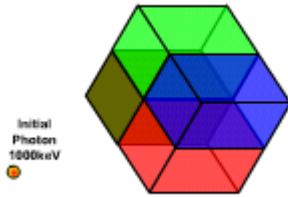
$\epsilon \sim 40 - 20 \%$   
( $M_\gamma=1 - M_\gamma=30$ )



# Advantages of $\gamma$ -ray tracking



**Compton Suppression**

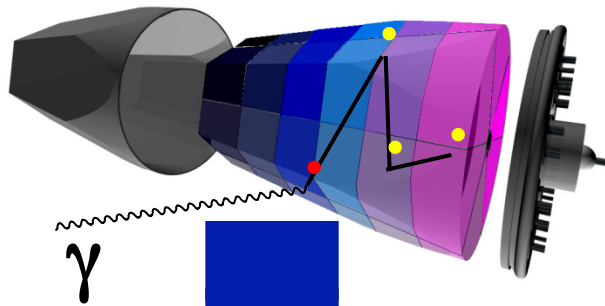


**Gamma Tracking**

- **Efficiency** – Proper reconstruction of scattered gamma rays, no solid angle used for Anti-Compton shield
- **Peak-to-background** – Reject Partially absorbed events
- **Doppler correction** - Position of first interaction determined
- **Polarization** – Angular distribution of the scattering sequence
- **Counting rate** – high segmentation and digital pile-up treatment

# Concept of $\gamma$ -Tracking

Highly segmented  
HPGe detectors  
NOVEL PRE-AMPS

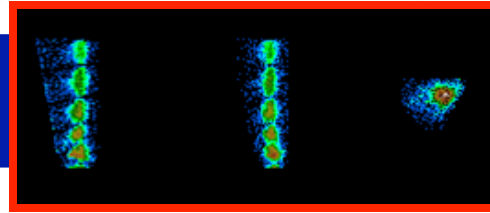
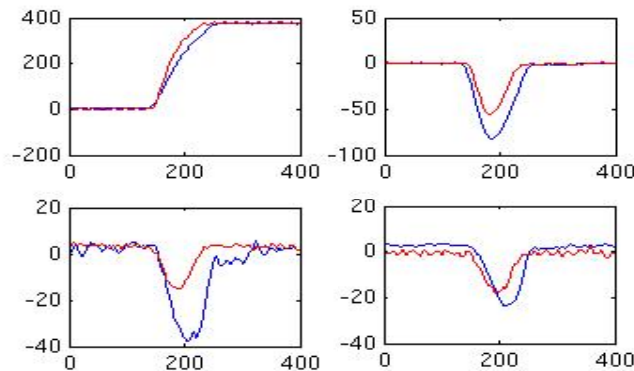


Synchronized digital  
electronics  
record and process  
the segment signals  
**DIGITIZERS +  
PRE-PROCESSING**

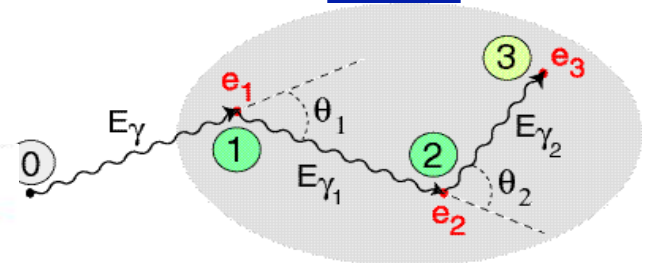
Identified  
interaction points

$$(x, y, z, E, t)_i$$

Pulse Shape Analysis  
to de-convolute the  
recorded waves  
**DAQ PSA - FARM**



Reconstruction of  
interaction tracks  
(tracking algorithms  
on interaction points)  
**DAQ TRACKING-FARM**

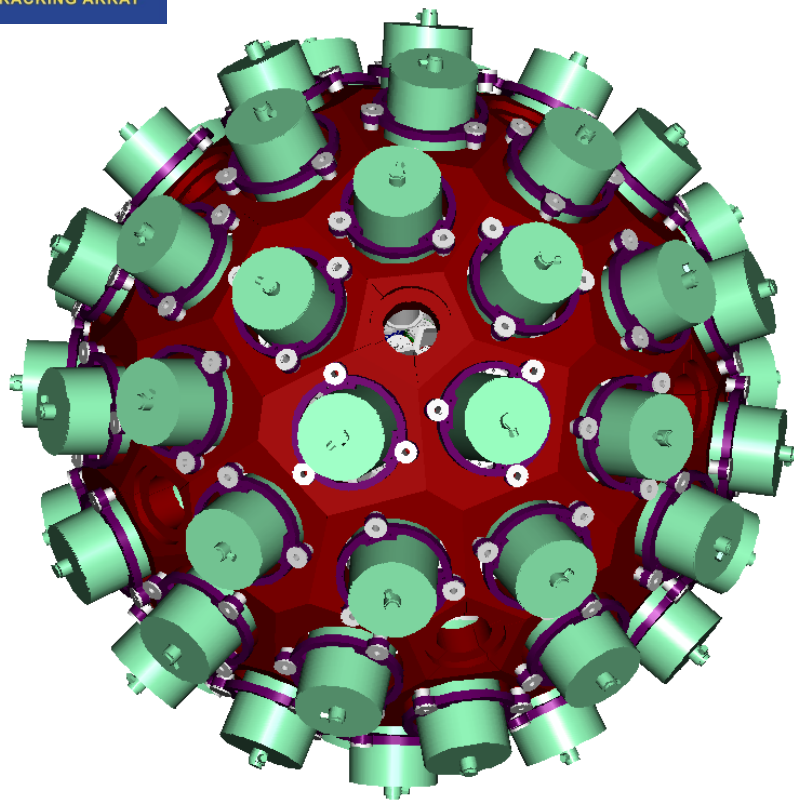
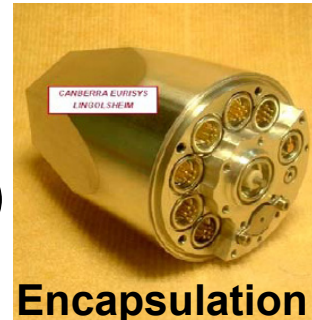


**On-line reconstruction  
of  $\gamma$ -rays**



# AGATA

(Advanced GAMMA Tracking Array)



180 hexagonal crystals	3 shapes
60 triple-clusters	all equal
Inner radius (Ge)	23.5 cm
Amount of germanium	362 kg
Solid angle coverage	82 %
36-fold segmentation	6480 segments
Singles rate	~50 kHz
Efficiency:	43% ( $M_\gamma=1$ )    28% ( $M_\gamma=30$ )
Peak/Total:	58% ( $M_\gamma=1$ )    49% ( $M_\gamma=30$ )

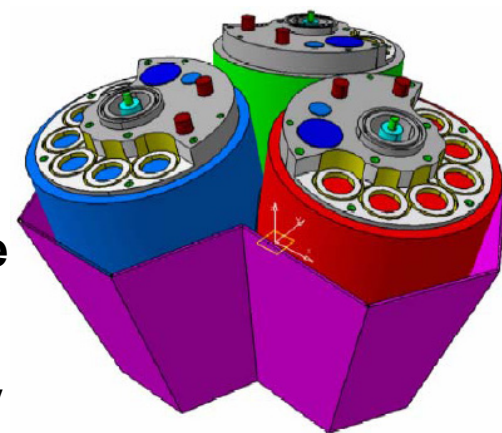
6660 high-resolution digital electronics channels

**High throughput DAQ**

Pulse Shape Analysis → position sensitive operation mode

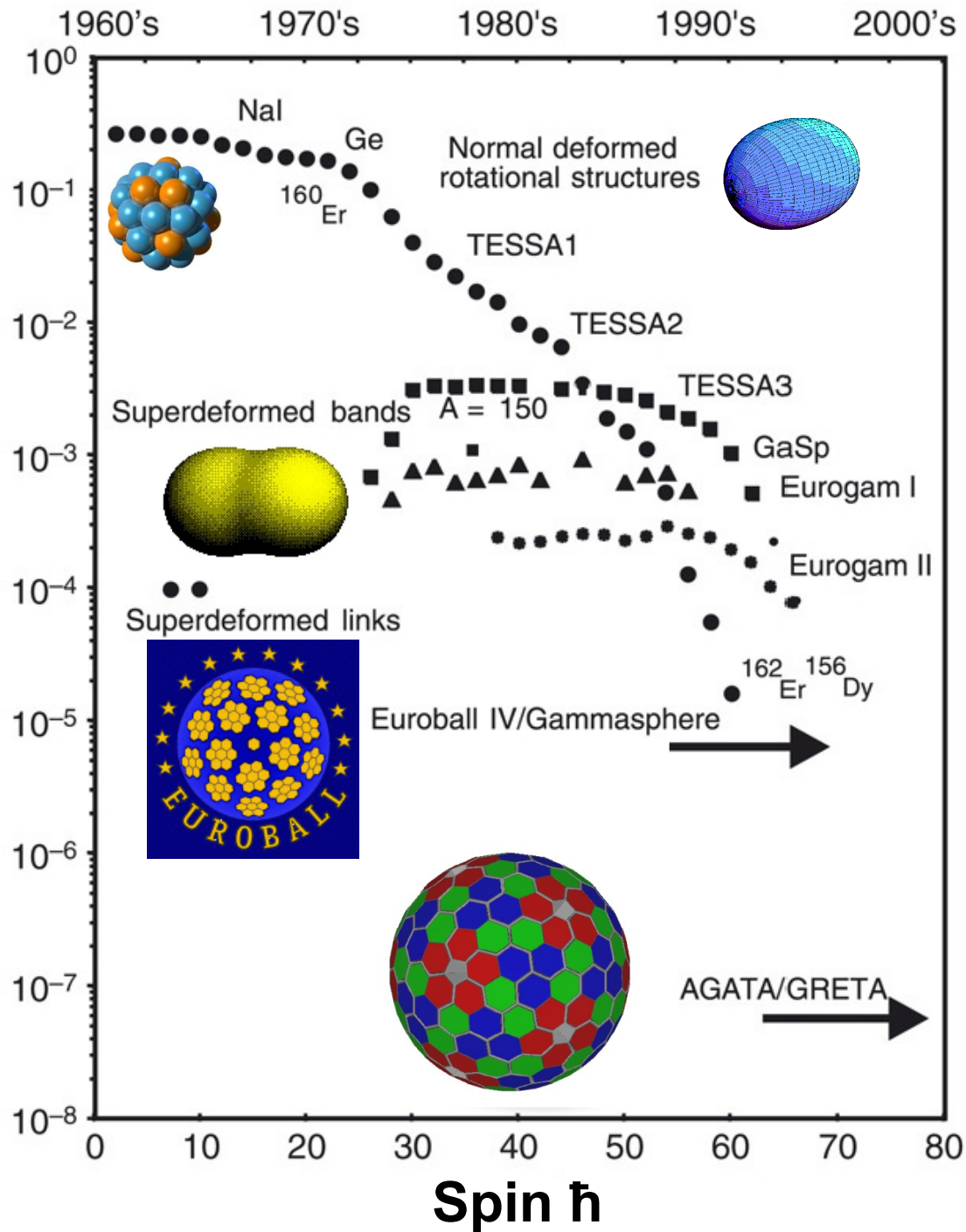
$\gamma$ -ray tracking algorithms to achieve maximum efficiency

Coupling to complementary detectors for added selectivity

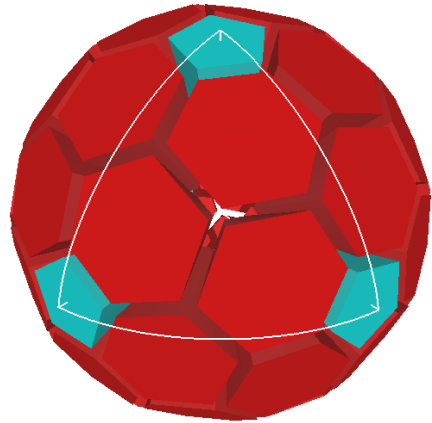




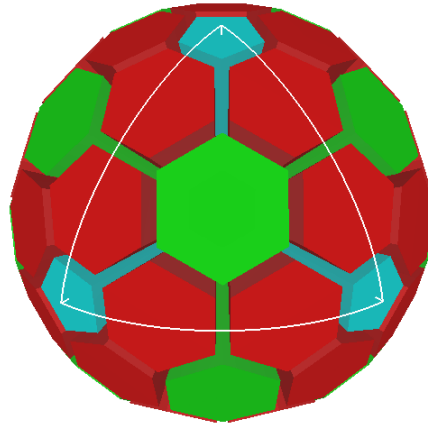
**Sensitivity as fraction of reaction channel**



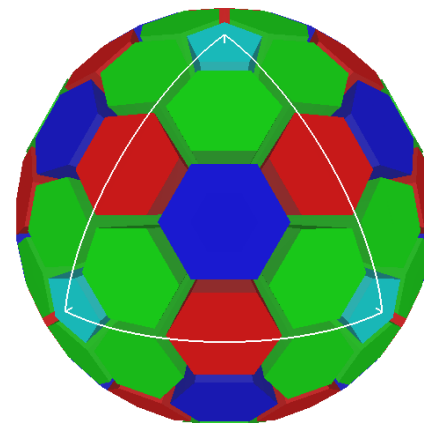
# Geodesic Tiling of Sphere using 60–240 hexagons and 12 pentagons



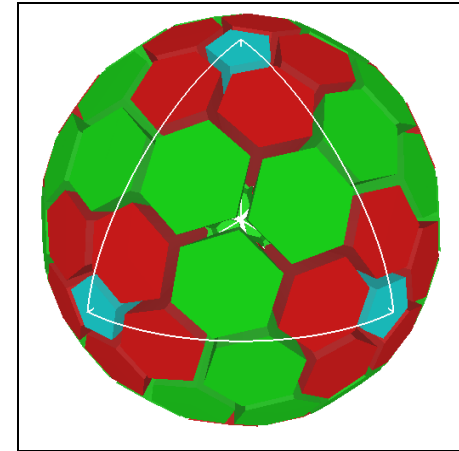
60



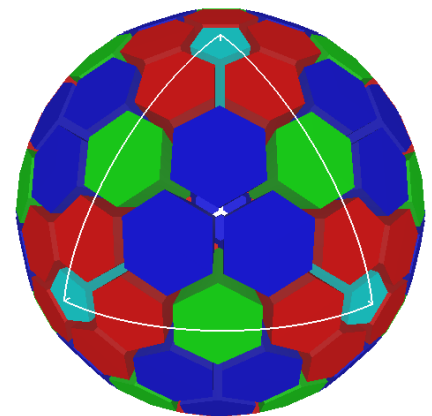
80



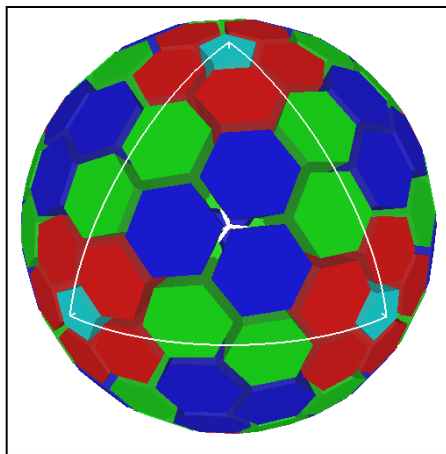
110



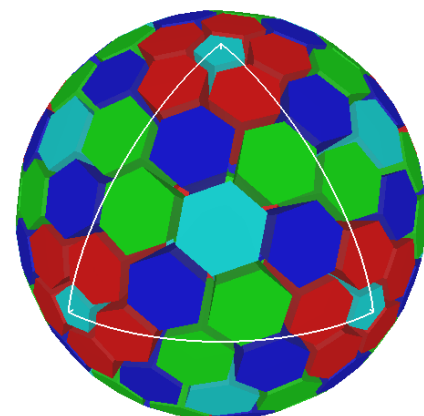
120



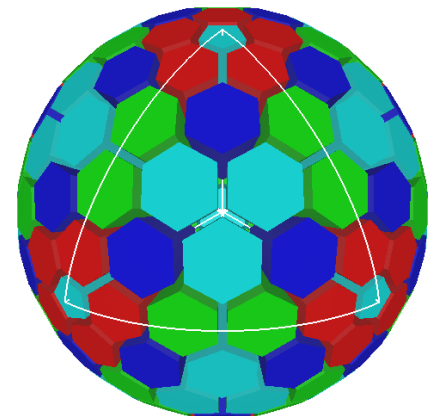
150



180

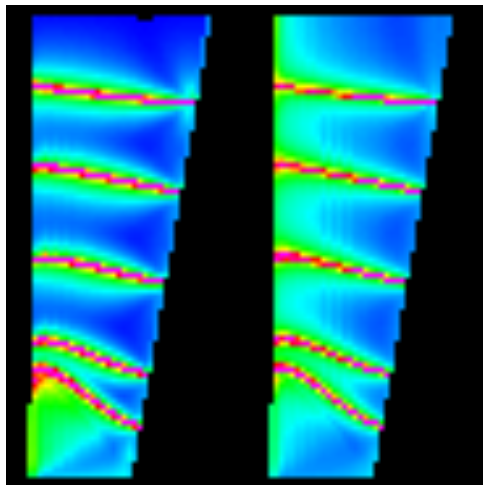
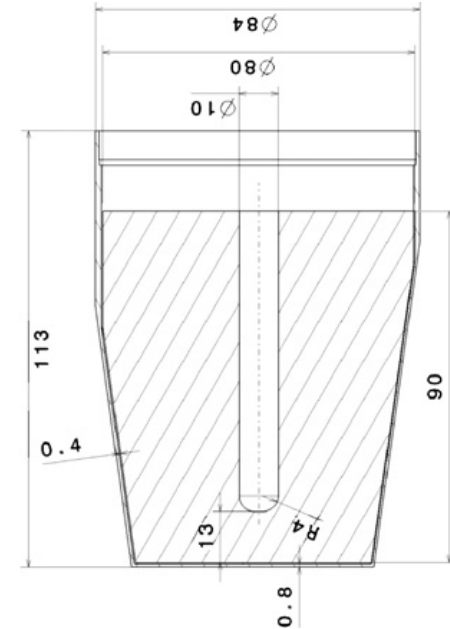
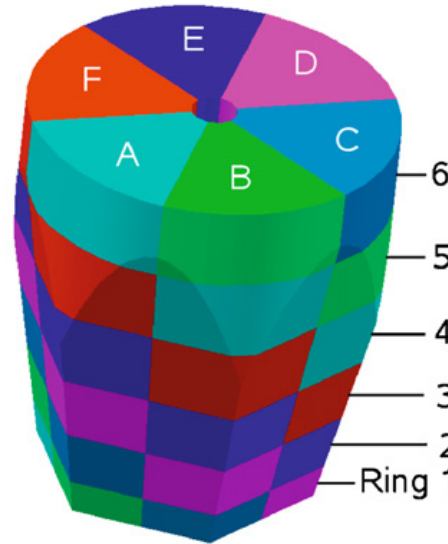
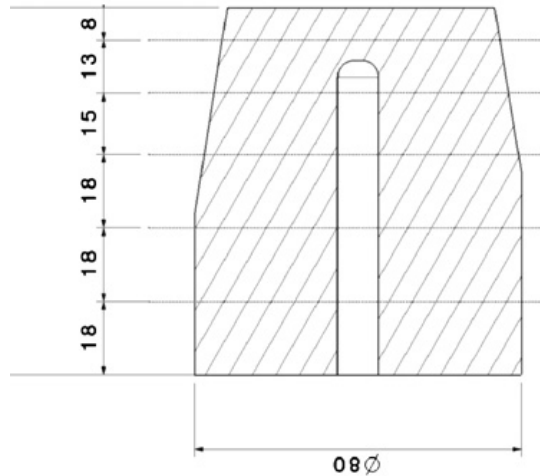


200



240

# Segmentation of the AGATA detector



Pulse Shape Simulations  
Th. Kröll, A. Görgen



Implementation in GEANT4

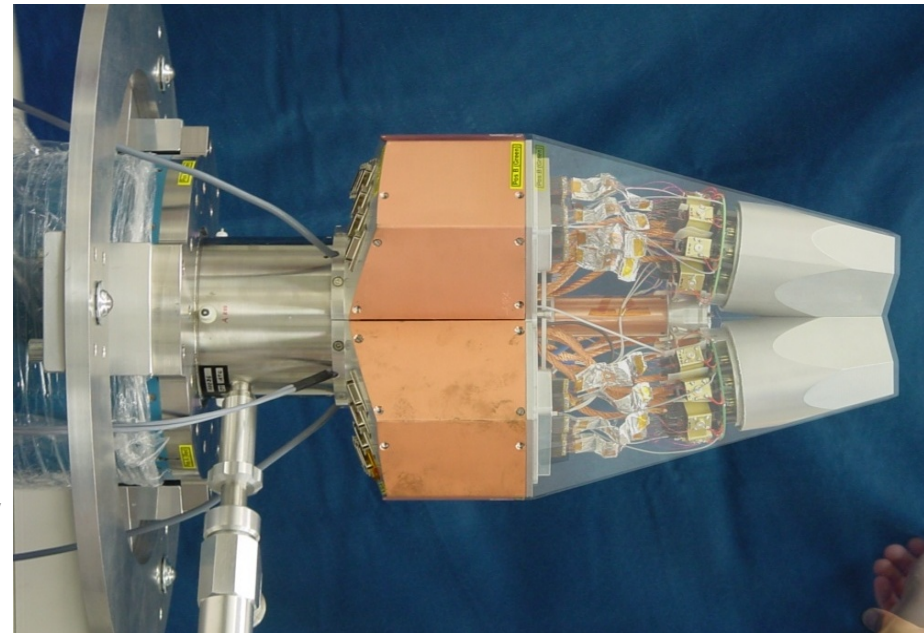
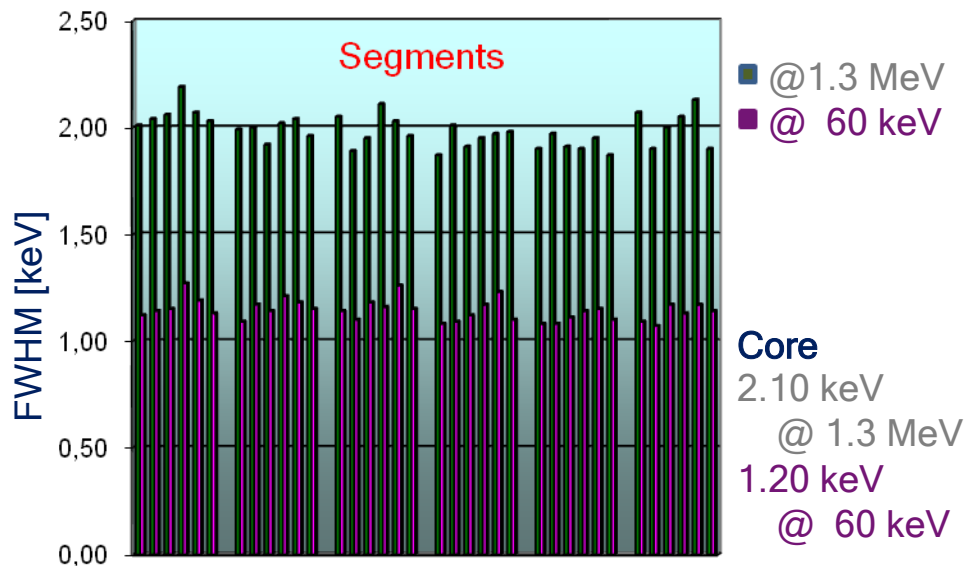
A.Wiens et al. NIMA 618 (2010) 223  
E.Farnea et al. NIMA 621 (2010)331

# AGATA Triple Cryostat

- integration of 111 high resolution spectroscopy channels
- cold FET technology for all signals

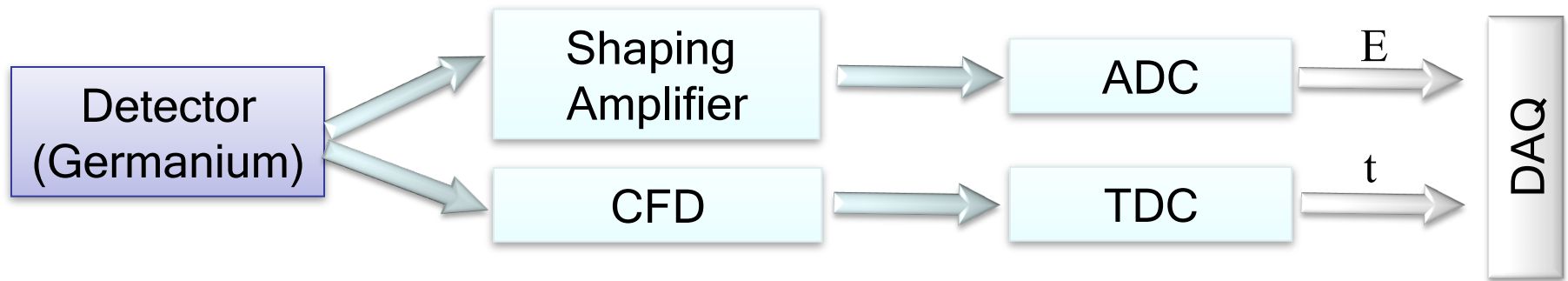
## Challenges:

- mechanical precision
- optimal LN2 consumption
- microphonics
- noise, high frequencies

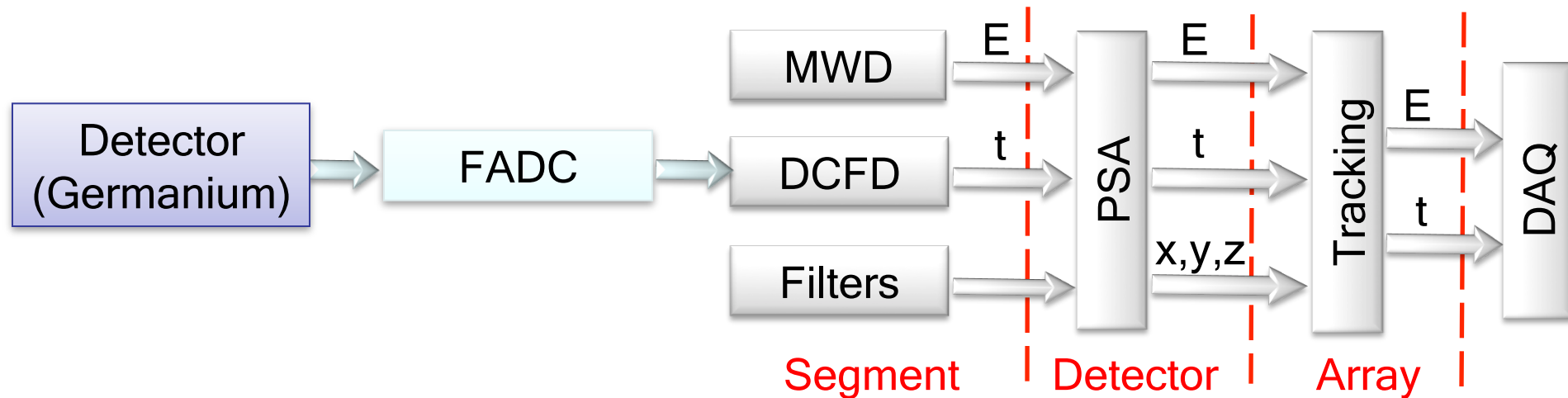


# Analogue vs Digital Electronics

## Standard Arrays



## AGATA



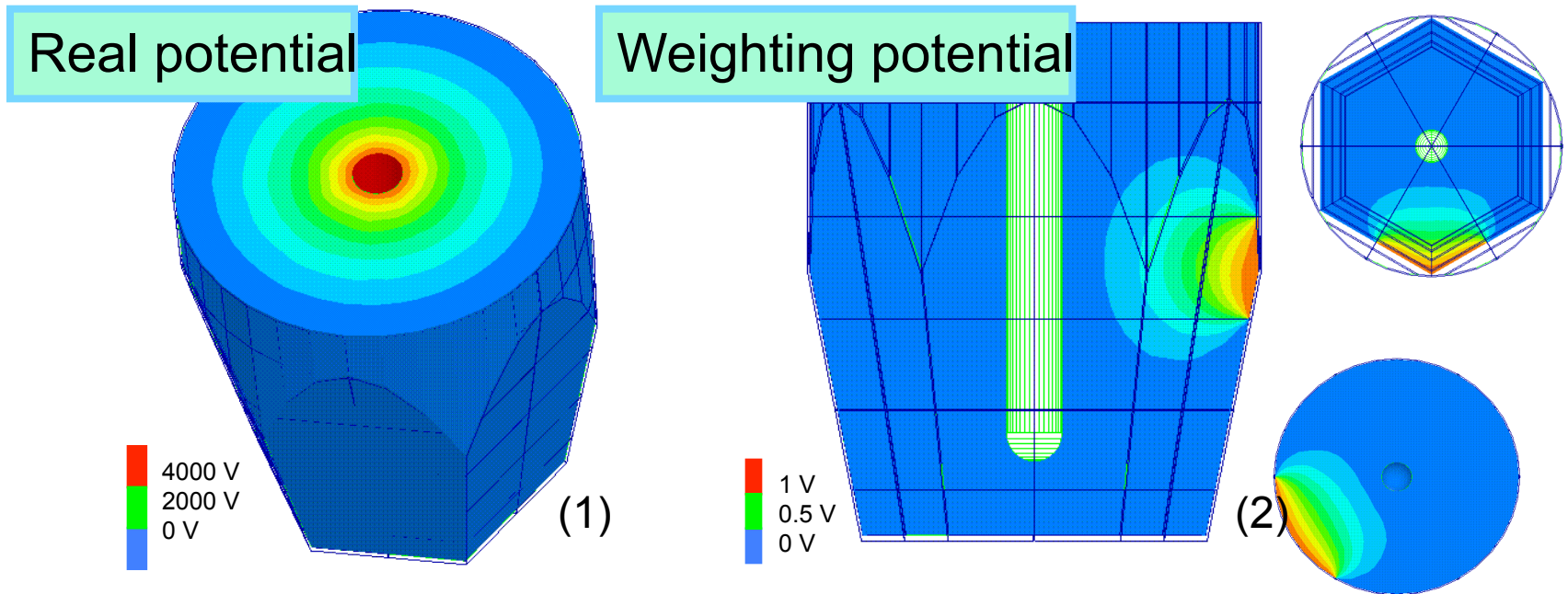


# Digital Pulse Processing for typical functions

- *Leading Edge Discrimination:*
  - $y[n] = x[n] - x[n-k]$  (*differentiation*)
  - $y[n] = (x[n] + x[n-2]) + x[n-1] \ll 1$  (*Gaussian filtering*)
  - Threshold comparison  $\rightarrow$  LED time
- *Constant Fraction Discrimination:*
  - $y[n] = x[n] - x[n-k]$  (*differentiation*)
  - $y[n] = (x[n] + x[n-2]) + x[n-1] \ll 1$  (*Gaussian filtering*)
  - $y[n] = x[n-k] \ll a - x[n]$  (*constant fraction*)
  - Zero crossing comparison  $\rightarrow$  CFD time



# Calculation of pulse shapes

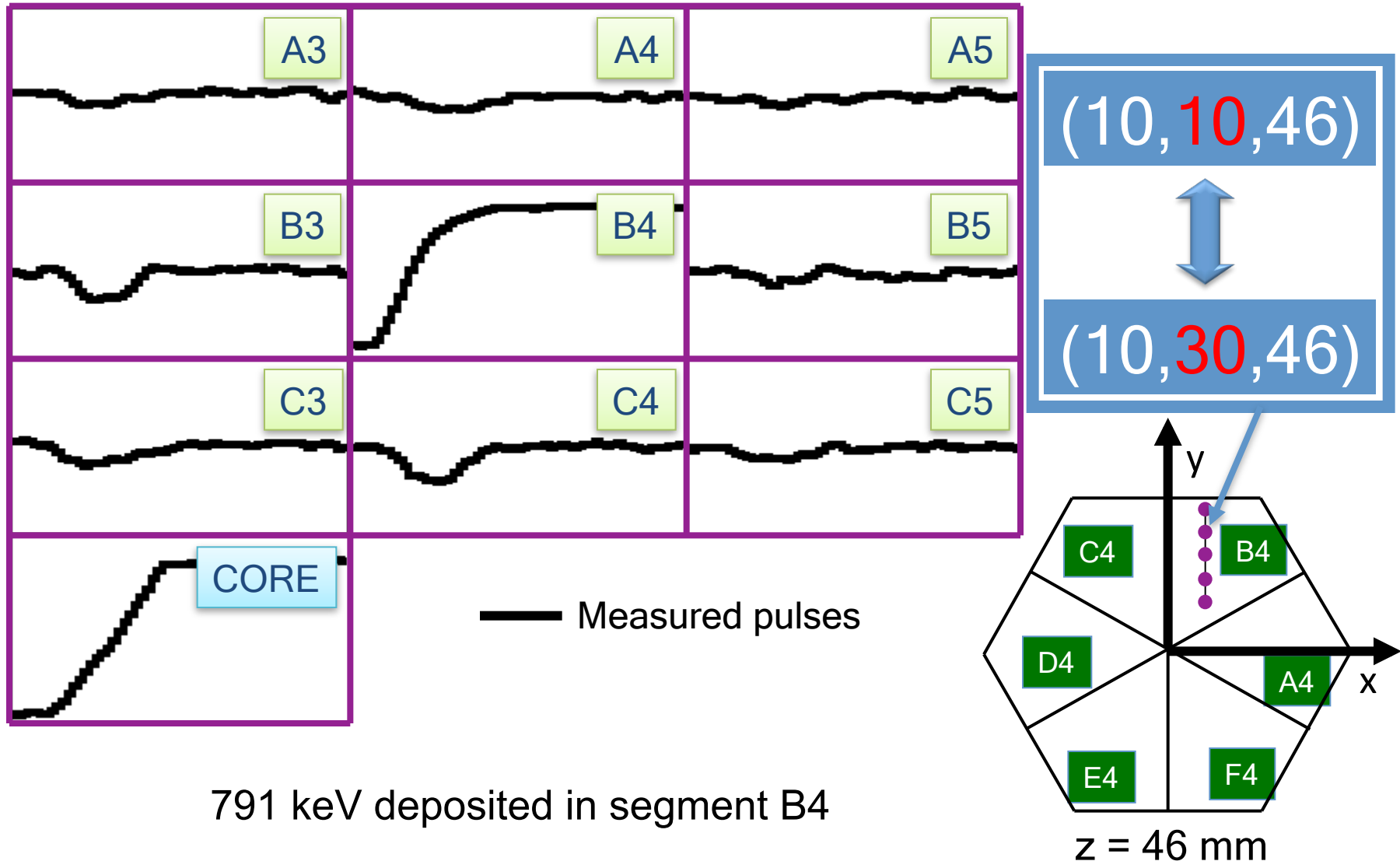


$$i_k = -q\vec{v} \cdot \vec{\nabla} \underbrace{\phi_k(r_q)}_{\text{Weighting potential}}$$

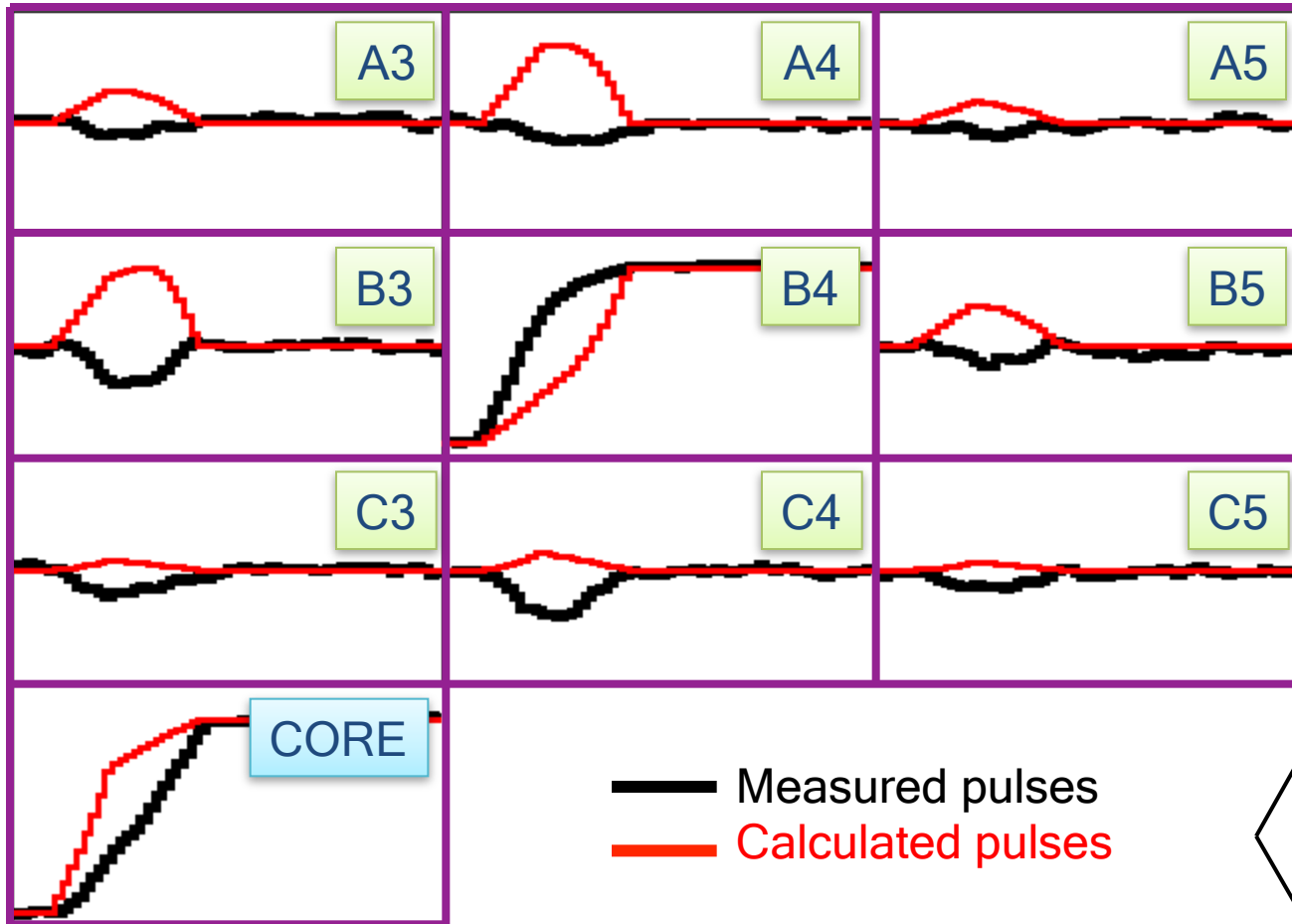
Current of electrode  $k$

- Weighting potential is calculated by applying 1 V on the segment collecting the charge and 0 V to all the others (Ramo's Theorem).
- It measures the electrostatic coupling (induced charge) between the moving charge and the sensing contact.

# Pulse Shape Analysis Concept

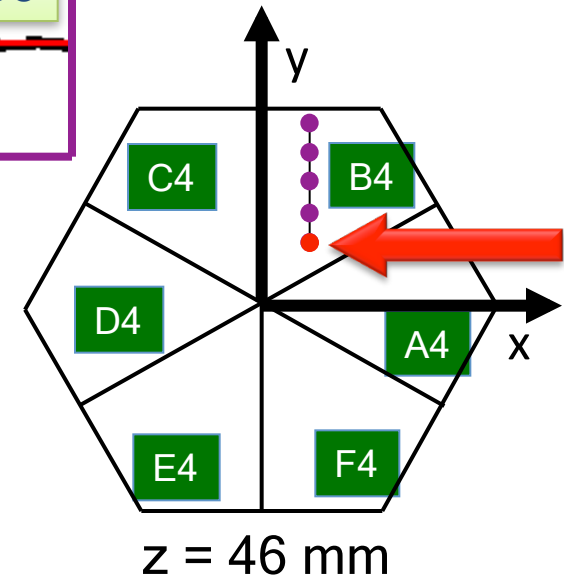


# Pulse Shape Analysis Concept

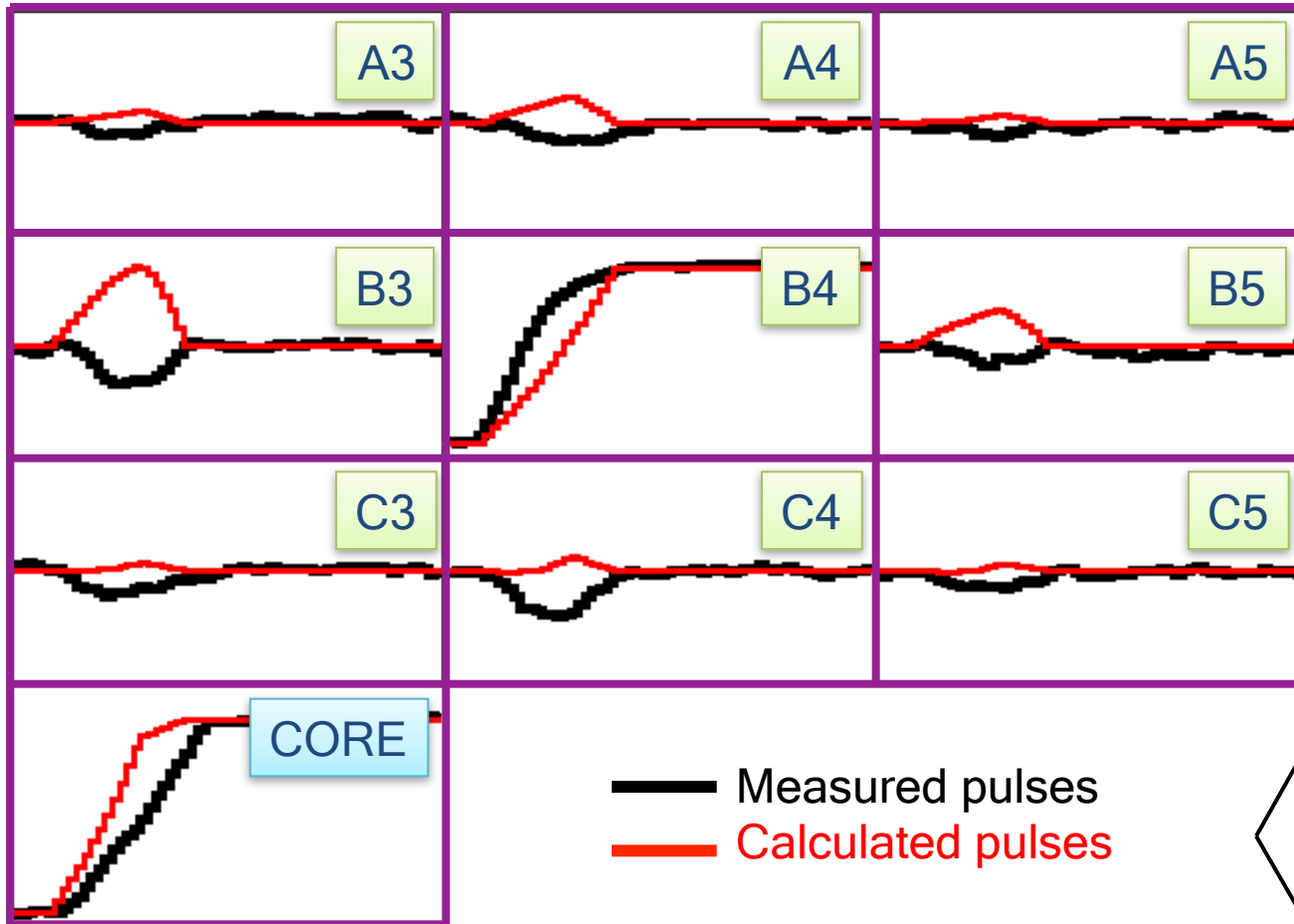


791 keV deposited in segment B4

(10, 10, 46)

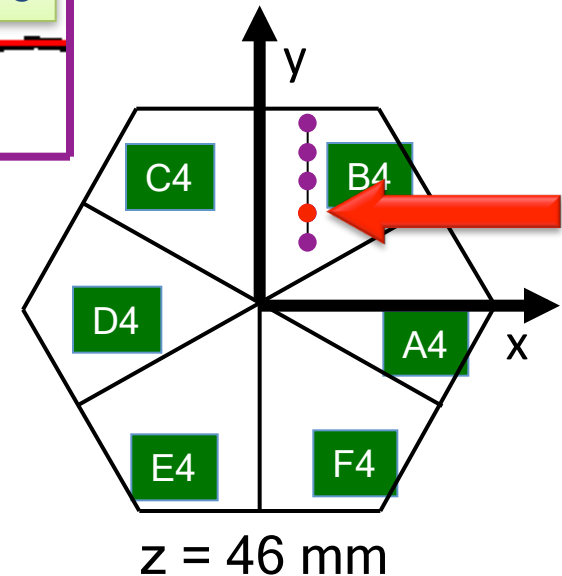


# Pulse Shape Analysis Concept

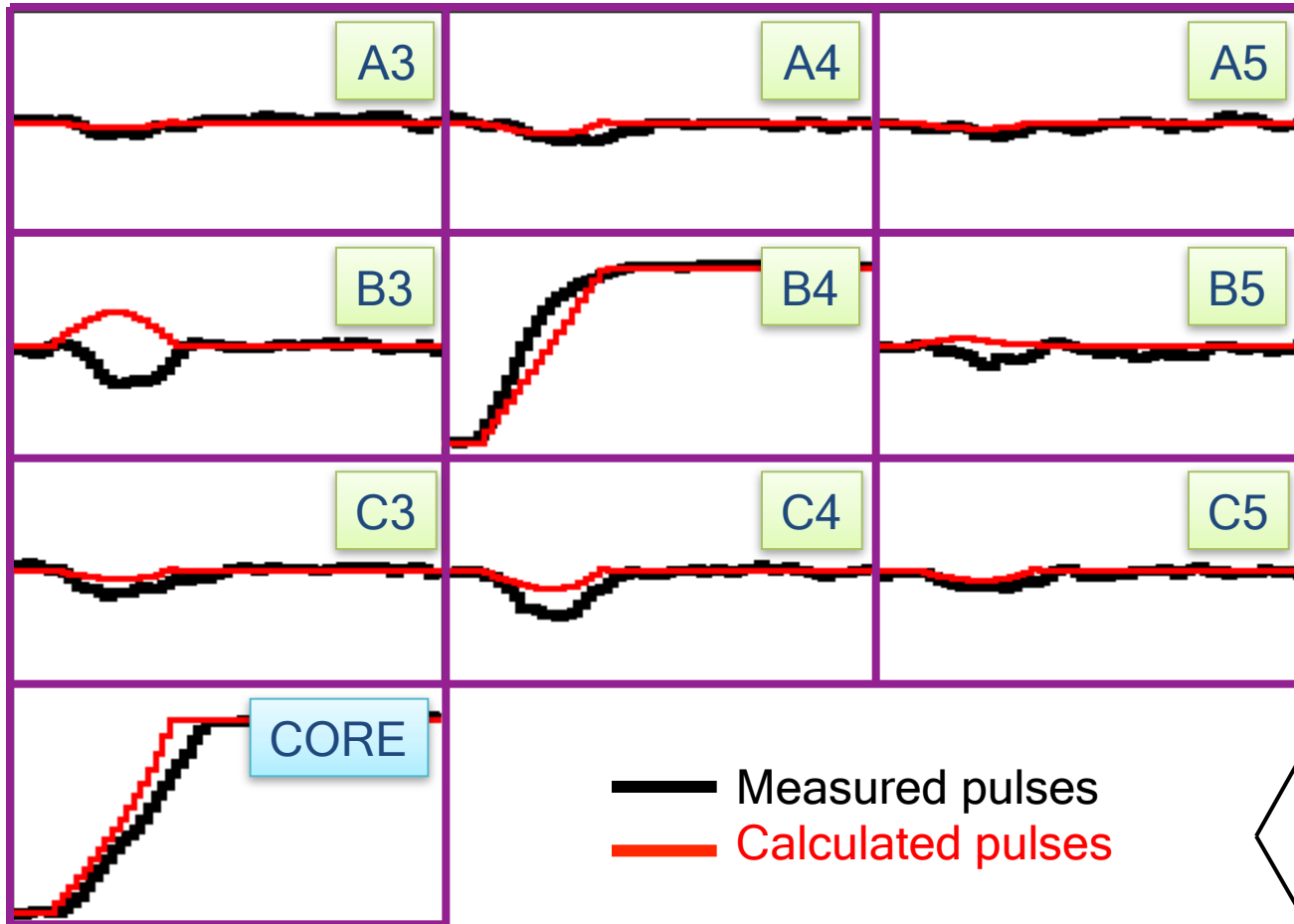


791 keV deposited in segment B4

(10, 15, 46)

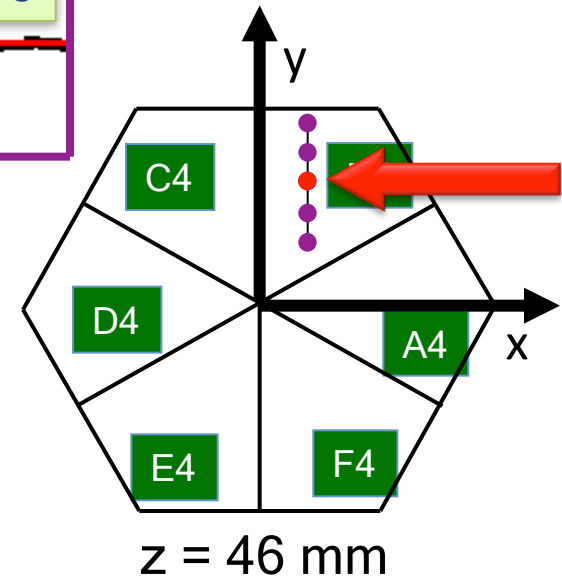


# Pulse Shape Analysis Concept

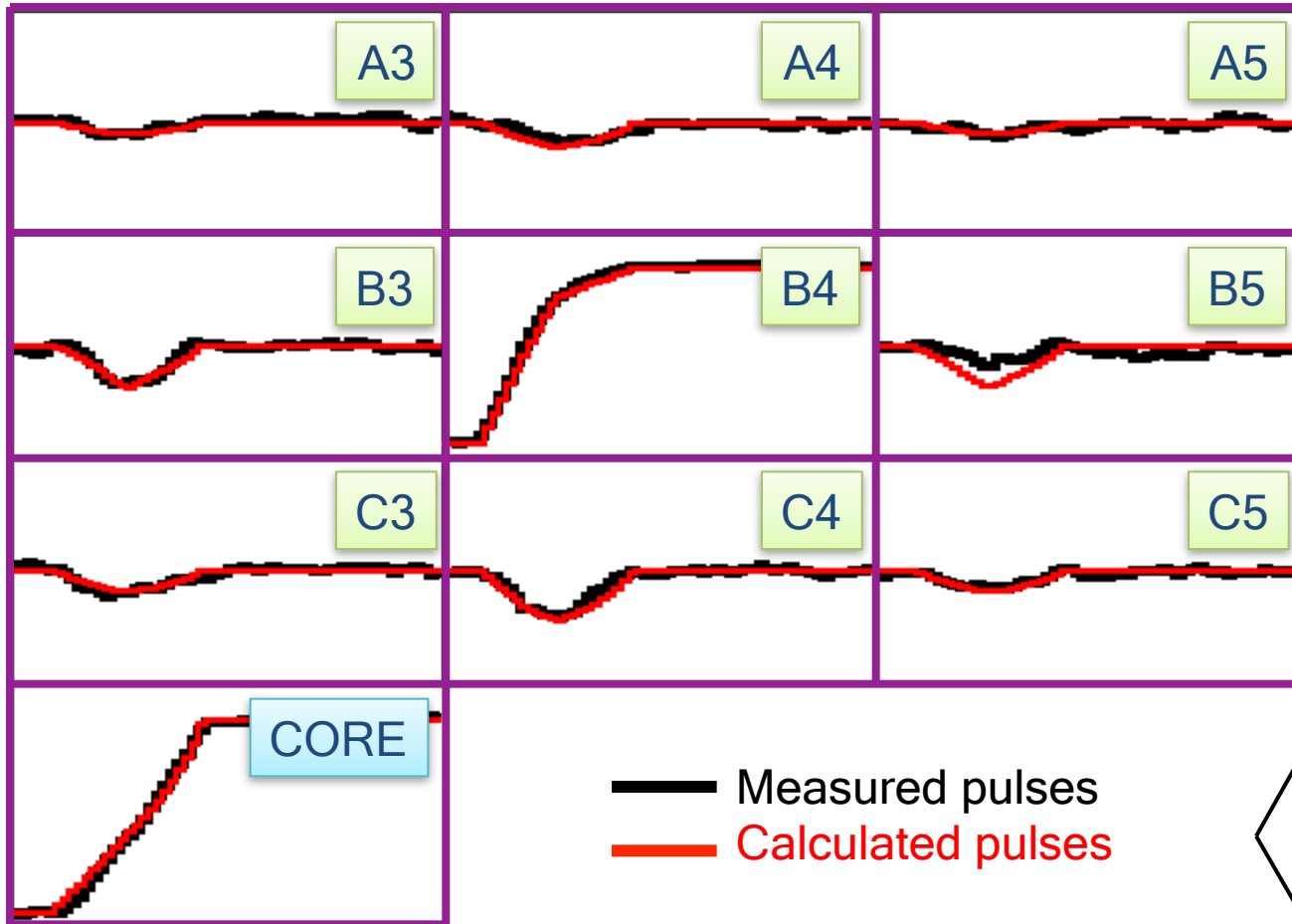


791 keV deposited in segment B4

(10, 20, 46)

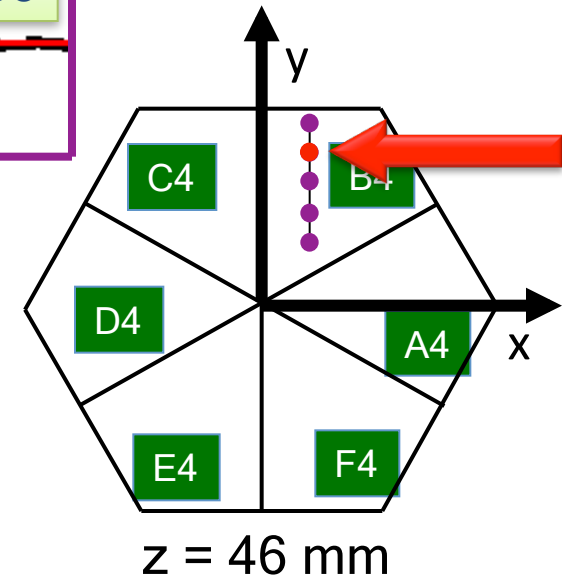


# Pulse Shape Analysis Concept



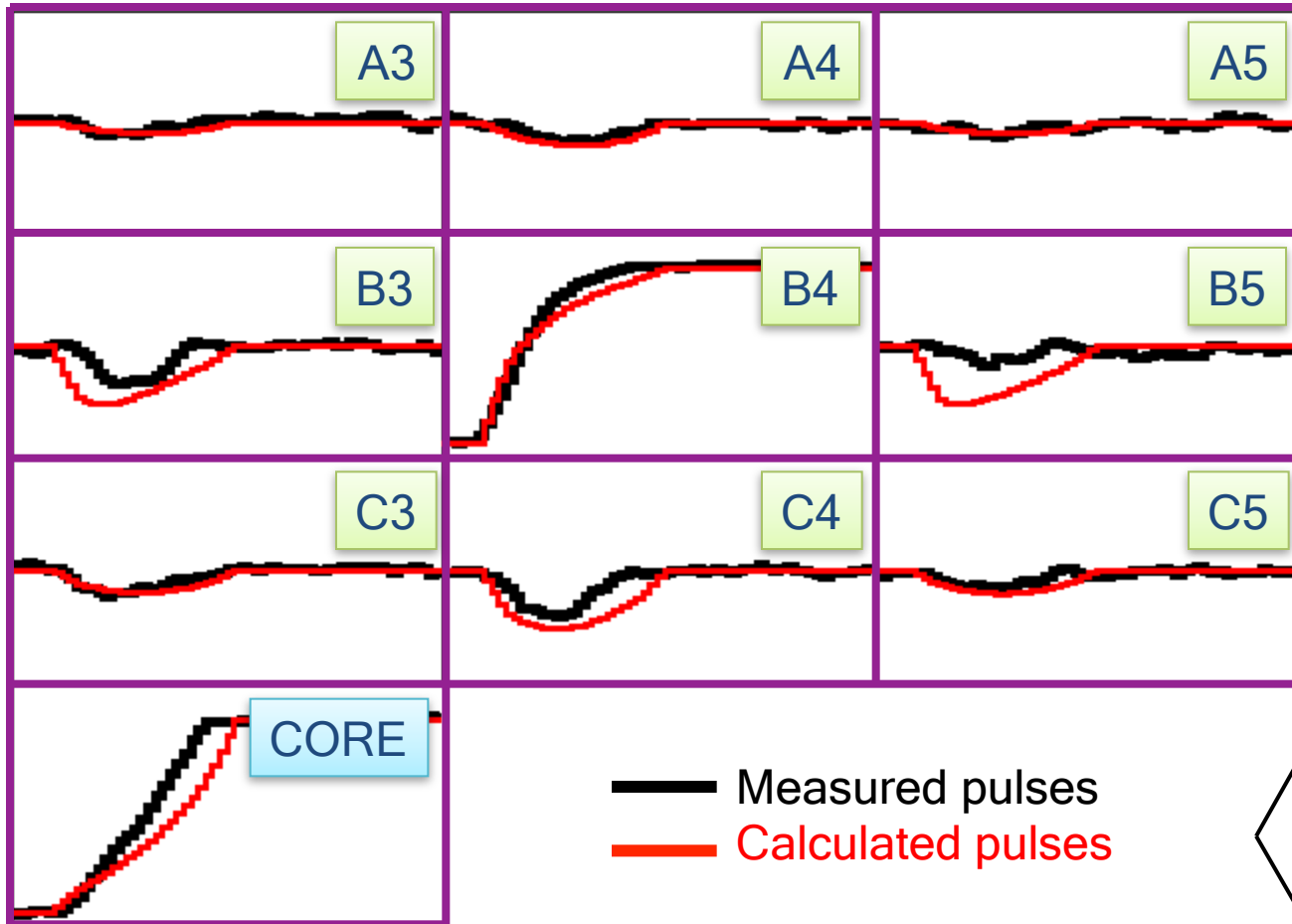
791 keV deposited in segment B4

(10, 25, 46)



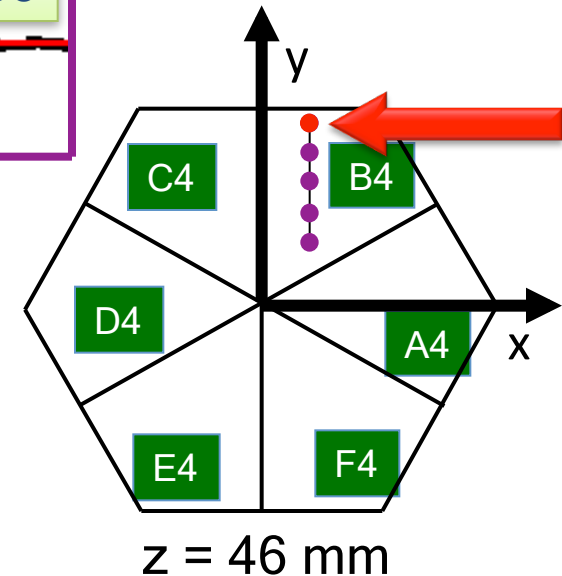


# Pulse Shape Analysis Concept

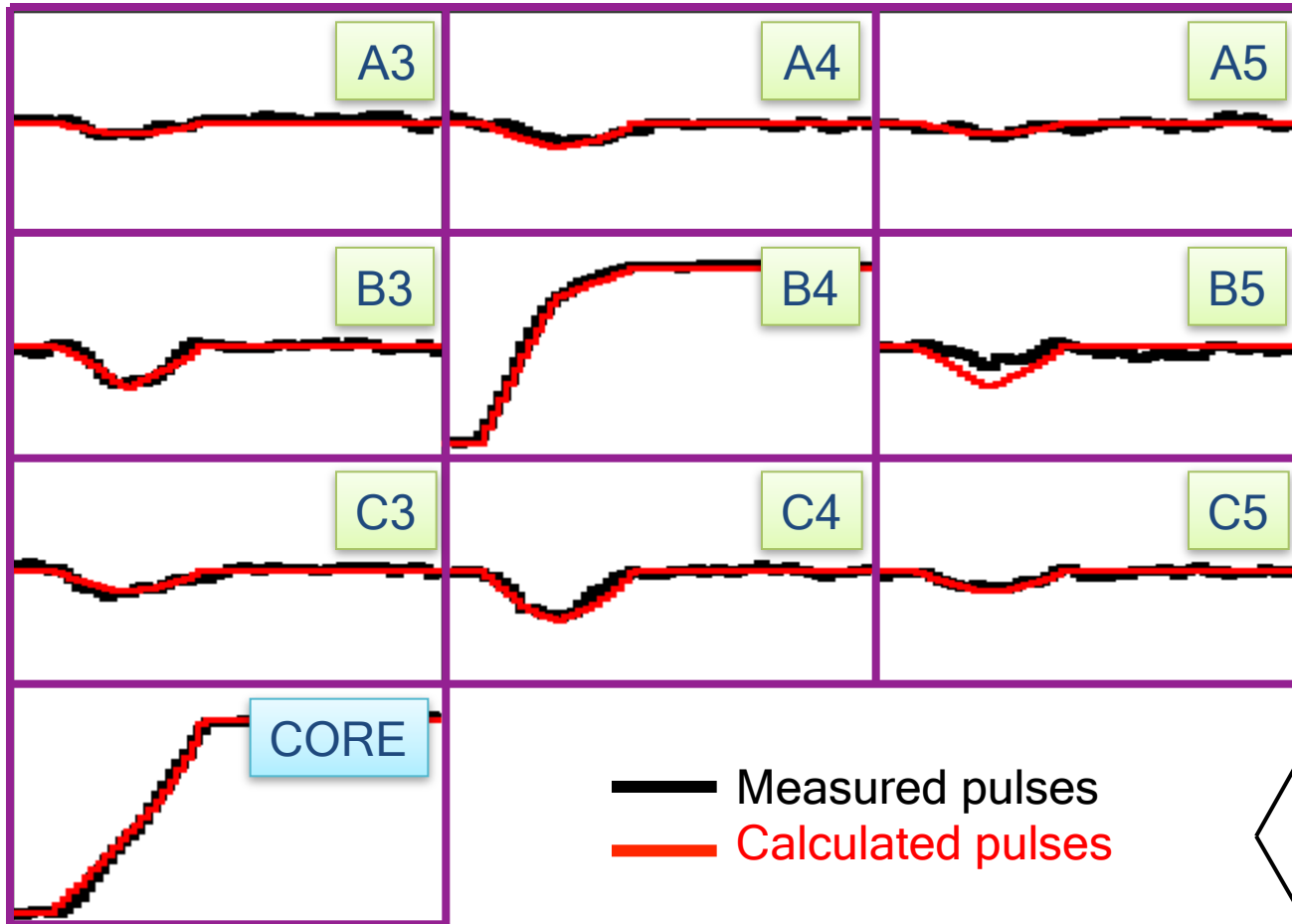


791 keV deposited in segment B4

(10, 30, 46)



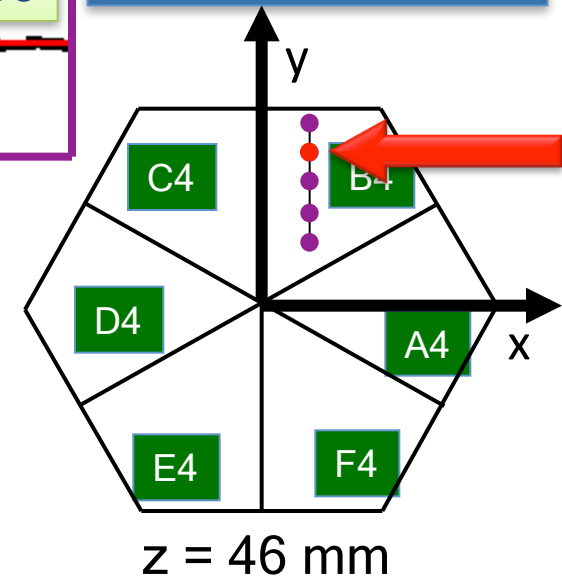
# Pulse Shape Analysis Concept



Result of  
*Grid Search*  
algorithm

*R. Venturelli*

(10, 25, 46)



791 keV deposited in segment B4

Set of Energies +  
Interaction Positions



Tracking

R.Venturelli, D.Bazzacco

# Interaction - Reconstruction Mechanisms

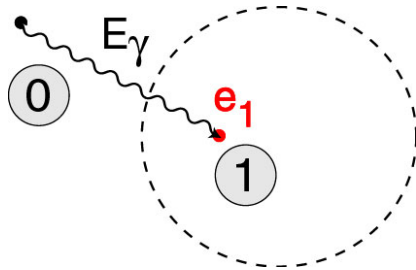
~ 100 keV

~1 MeV

~ 10 MeV

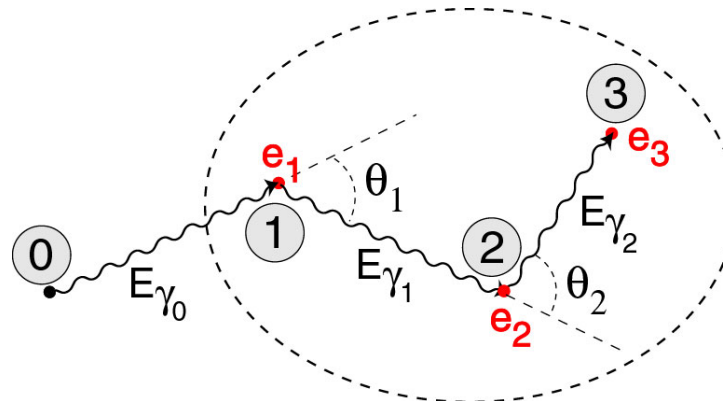
γ-ray energy

## Photoelectric



Isolated hits

## Compton Scattering

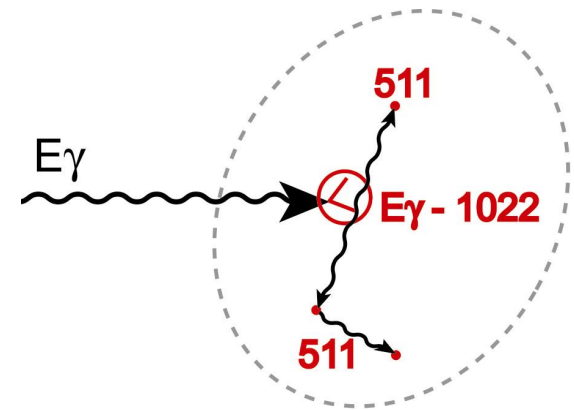


Angle/Energy

$$E_{\gamma'} = \frac{E_\gamma}{1 + \frac{E_\gamma}{m_0 c^2} (1 - \cos\theta)}$$

Probability of  
interaction depth

## Pair Production



Pattern of hits

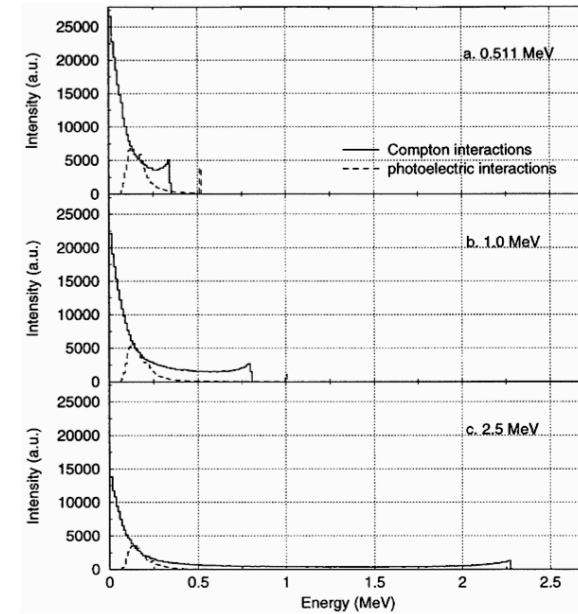
$$E_{1st} = E_\gamma - 2 mc^2$$

Reconstruction efficiencies are limited by :  
Position resolution; Short range scattering; Compton profile.

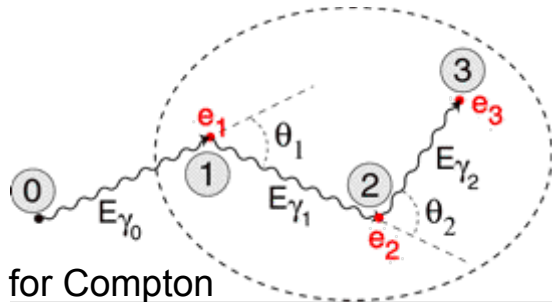
# The tracking Algorithms in AGATA

Two main classes:

- algorithms based on back-tracking
  - J. Van der Marel, B. Cederwall, NIMA 437 (1999) 538.
  - J. Van der Marel, B. Cederwall, NIMA 447 (2002) 391.
  - L. Milechina, B. Cederwall, NIMA 508 (2003) 394.
- algorithms based on clusterisation and forward-tracking
  - G.J. Schmid, et al., NIMA 430 (1999) 69.
  - D. Bazzacco, MGT code developed within the TMR program 'Gamma-ray tracking detectors'
  - I. Piqueras, et al. NIMA 516 (2004) 122

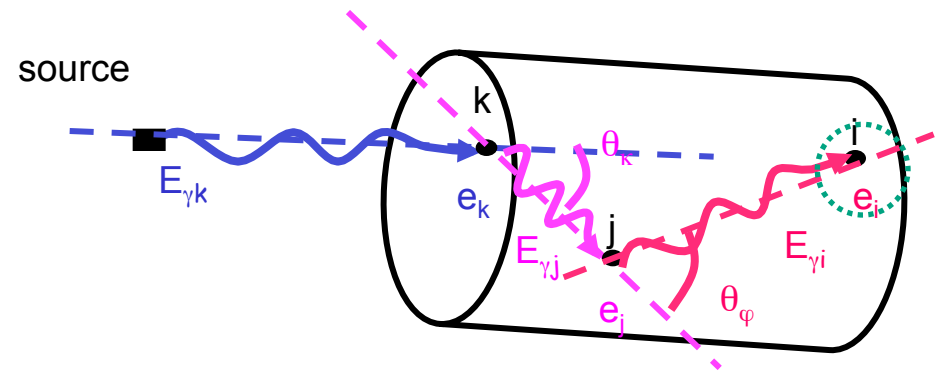


## Forward-tracking



$$E_{s,p} = \frac{E_t}{1 + E_t/m_e c^2 (1 - \cos \theta_p)}$$

## Back-tracking



$$\cos(\theta) = 1 - m_e c^2 (1/E_{sc} - 1/E_{inc})$$

Probability for Compton or photoelectric and for the path in Germanium

$$L = \prod_{n=1}^N P_n \exp \left[ - \left( \frac{E_{\gamma n} - E_{\gamma n, pos}}{\sigma_E} \right)^2 \right]$$

Likelihood

# What can we learn from atomic nuclei with high-resolution $\gamma$ -ray spectroscopy techniques?

Some Examples on:

- Nuclei in the vicinity of  $N=Z$  (equilibrated nuclear matter)
- Neutron-rich nuclei (large isospin values)
- Macroscopic/microscopic behavior of nuclei (collective modes)

# New Trends and Techniques in Nuclear Structure Studies with High-Resolution In-Beam $\gamma$ -Spectroscopy

A.Gadea IFIC-CSIC Valencia

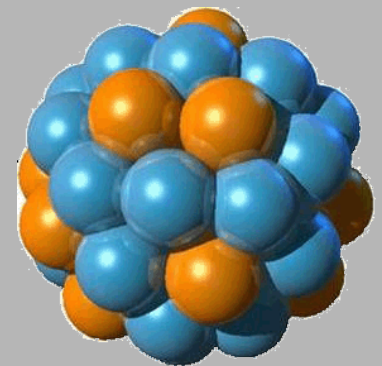
Counts

## 1. High Resolution Spectroscopy techniques

- Introduction
- $\gamma$ -tracking arrays

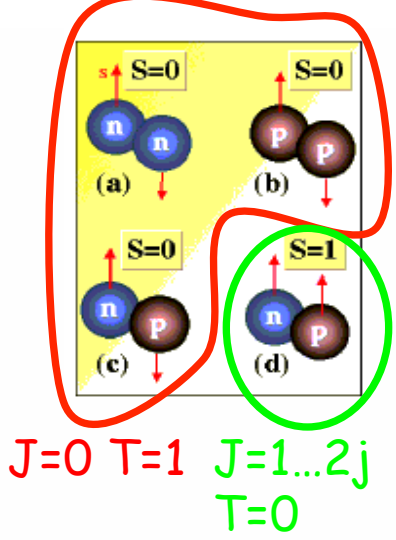
## 2. Nuclear Structure & Complementary instrumentation

- Proton-Rich & N=Z Nuclei
- Neutron-rich  $\rightarrow$  Large Isospin Values
- Collective & Transitional Phenomena



Energy [keV]



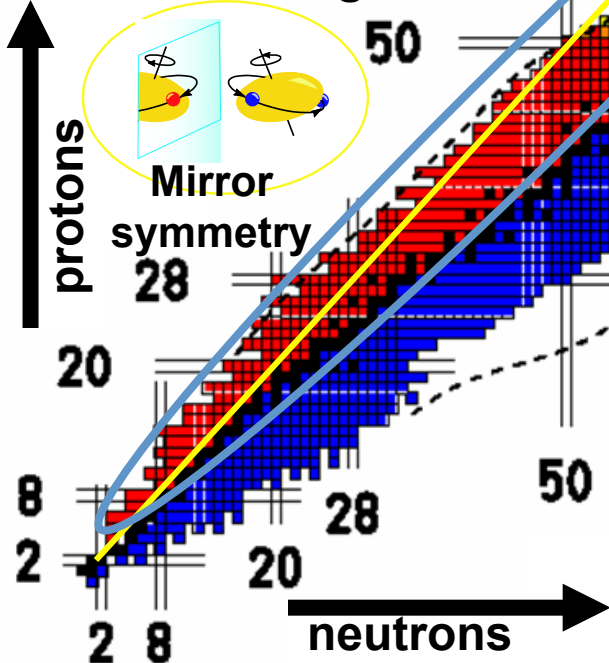
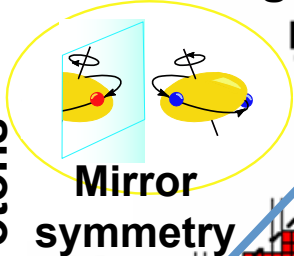


Single-particle and collective states around doubly close shell  $N=Z$  nuclei

The demise of isospin purity: heavier Mirror nuclei are less similar

Isospin  $T=0$   $np$ -pairing

Isospin symmetry breaking



Shape coexistence and collectivity in  $N \sim Z$  nuclei ( $A \sim 70$ )

Exotic structures along the  $N=Z$  line:  $p$ - $n$  enhancement of collective properties

Spectroscopy at large isospin and exotic (particle) decays: multidimensional quantum tunneling

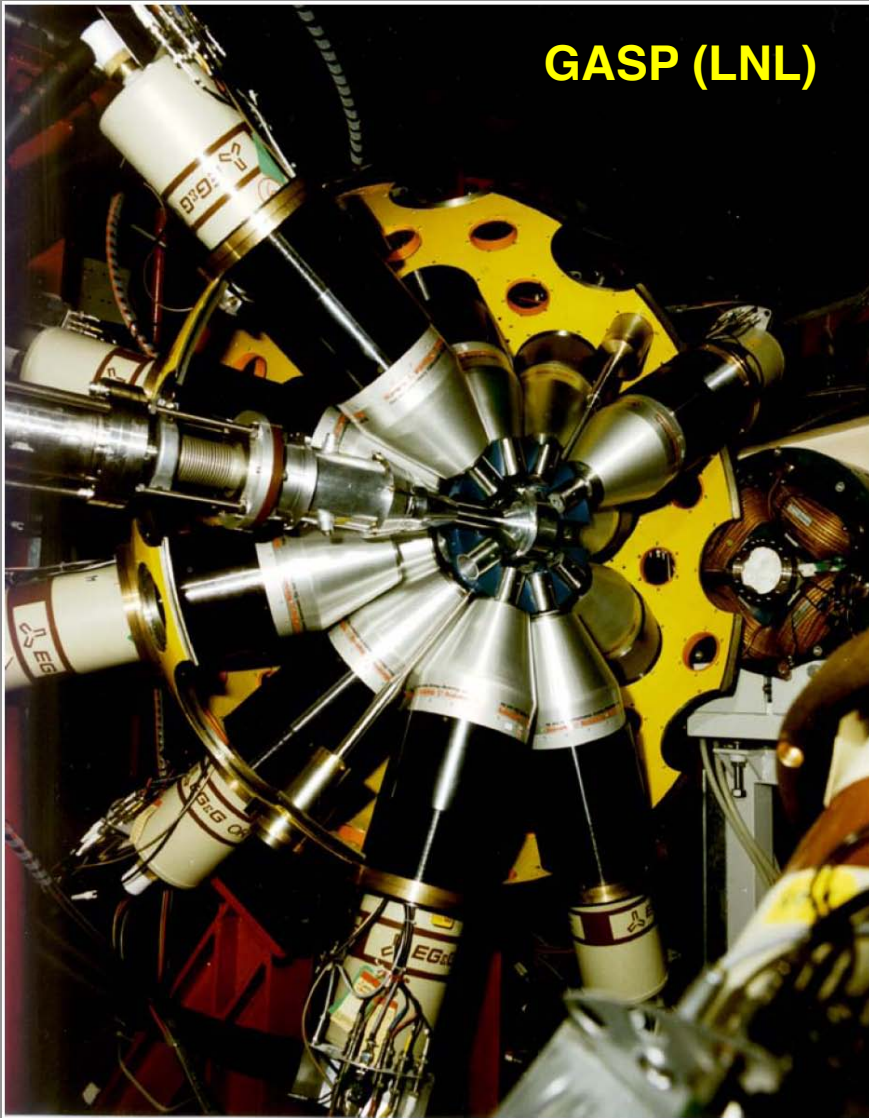
Proton "Islands of Inversion"

Mainly Populated in Fusion-Evaporation reactions

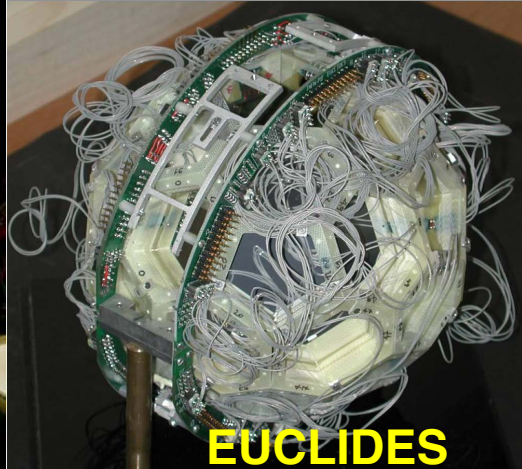
# The GASP array

## Configuration I & II with ancillary detectors

**GASP (LNL)**



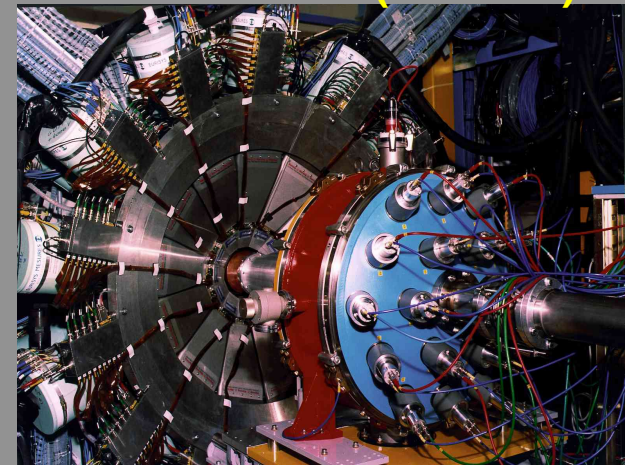
**EUCLIDES**



**Neutron Ring  
BGO inner ball**



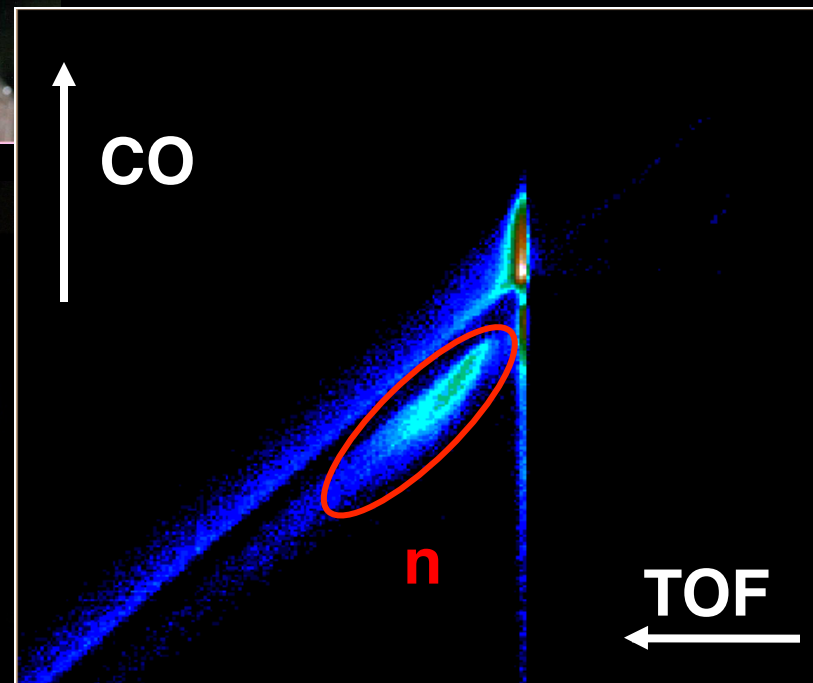
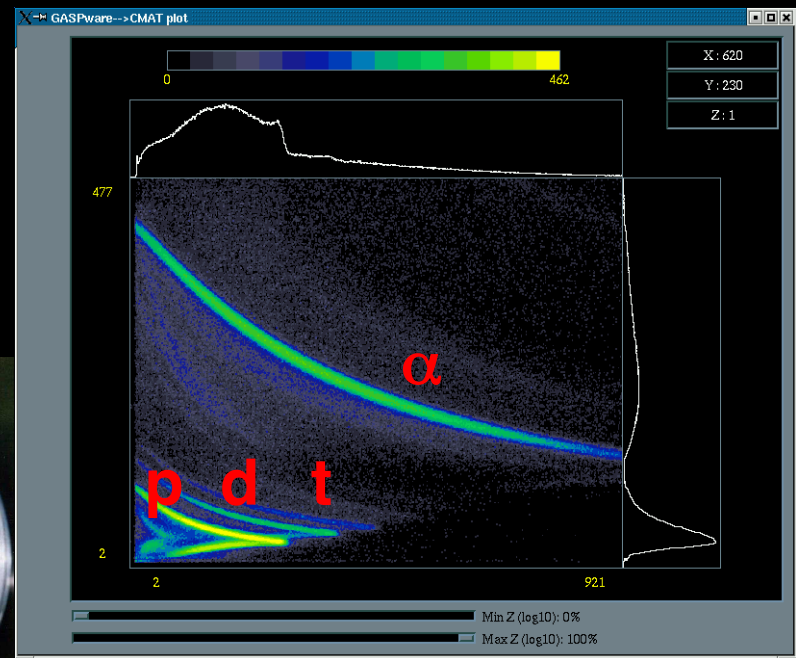
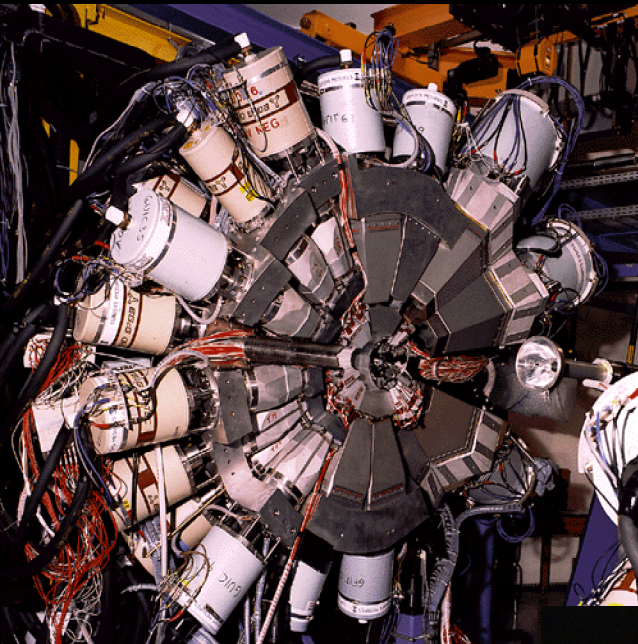
**RFD (Krakow)**



40 Ge+AC  
I  $\epsilon \sim 3\%$   
II  $\epsilon \sim 5\%$   
80 BGO  
 $\Omega \sim 80\%$   
40 DE-E Si  
(EUCLIDES)  
Plunger  
N-detectors  
RFD ...

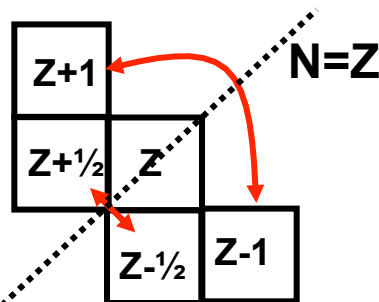
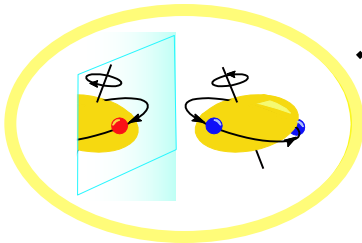
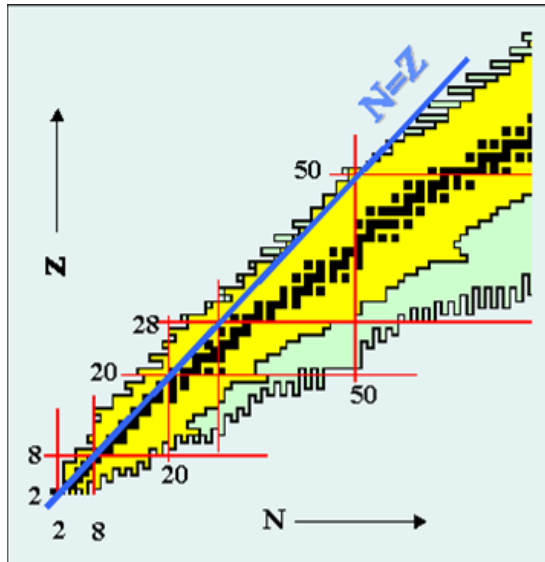


# EUROBALL with Ancillary Detectors

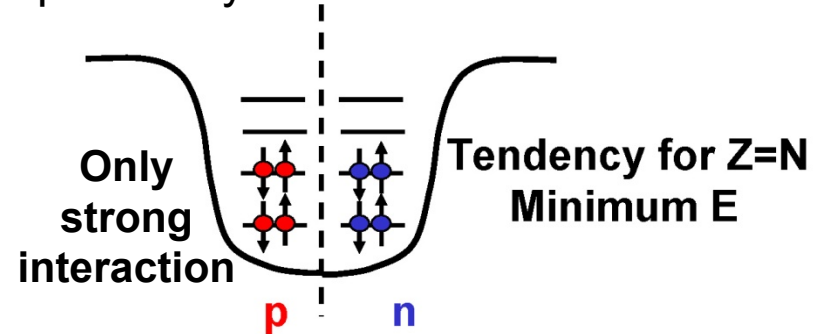


# Mirror Symmetry in nuclei

Isospin symmetry is only approximate in strong interaction

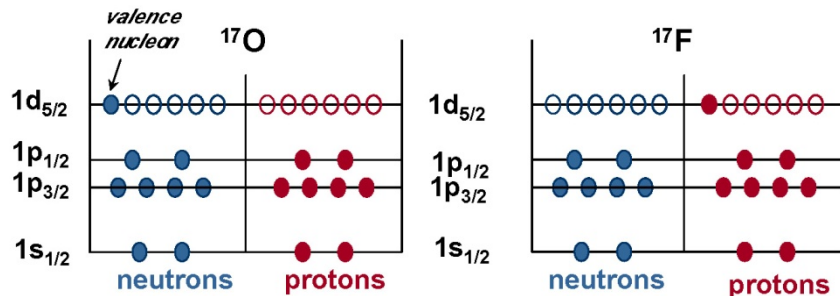
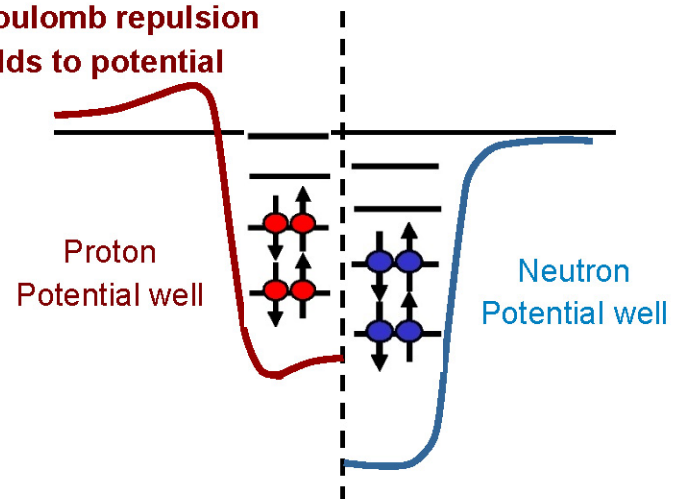


The Pauli principle operates independently for Protons and Neutrons



**In reality**

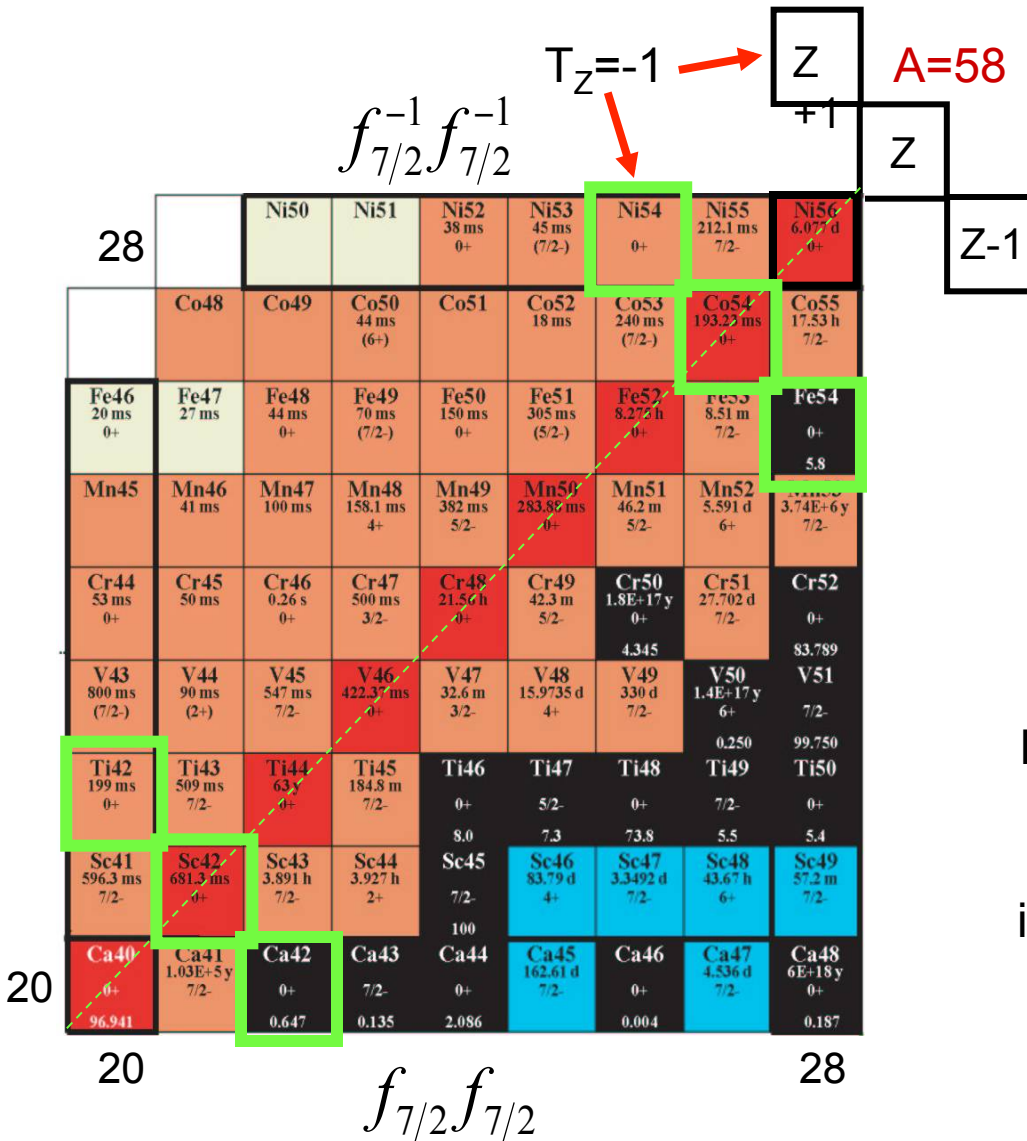
Coulomb repulsion adds to potential



# Mirror energy differences

From odd mirror nuclei is possible to get the isovector energy differences.

From mass triplets is possible to get both isovector and isotensor..



- MDE (Mirror Displacement Energies): binding energy difference between mirror nuclei ( $MDE = BE(Z A_N) - BE(N A_Z)$ ).  
→ from few to tens of MeV.

- MED (Mirror Energy Differences): differences in excitation energies of yrast bands in mirror nuclei

( $MED_J = E_J(Z+2T A_{N-2T}) - E_J(Z-2T A_{N+2T})$ ).  
→ from tens to hundreds of keV.

Due to shell effects coming from the Coulomb and Isospin symmetry breaking potentials.

For a  $T=1$  triplet:

$$MED_J = E_J(Z+1) - E_J(Z-1)$$

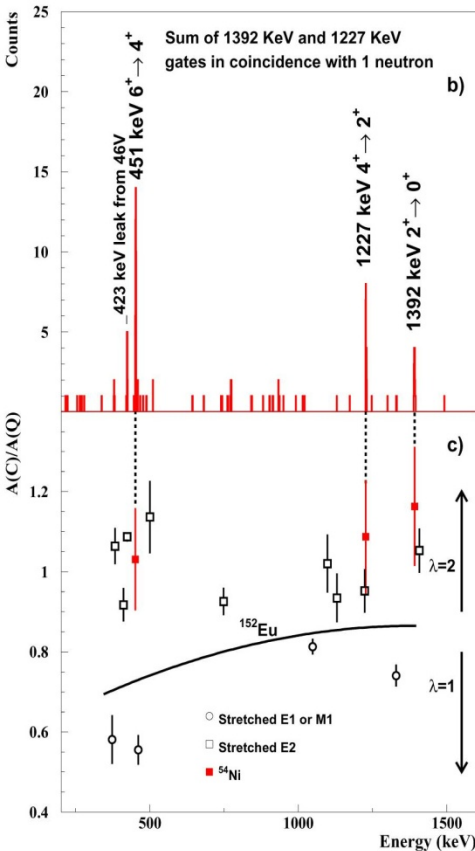
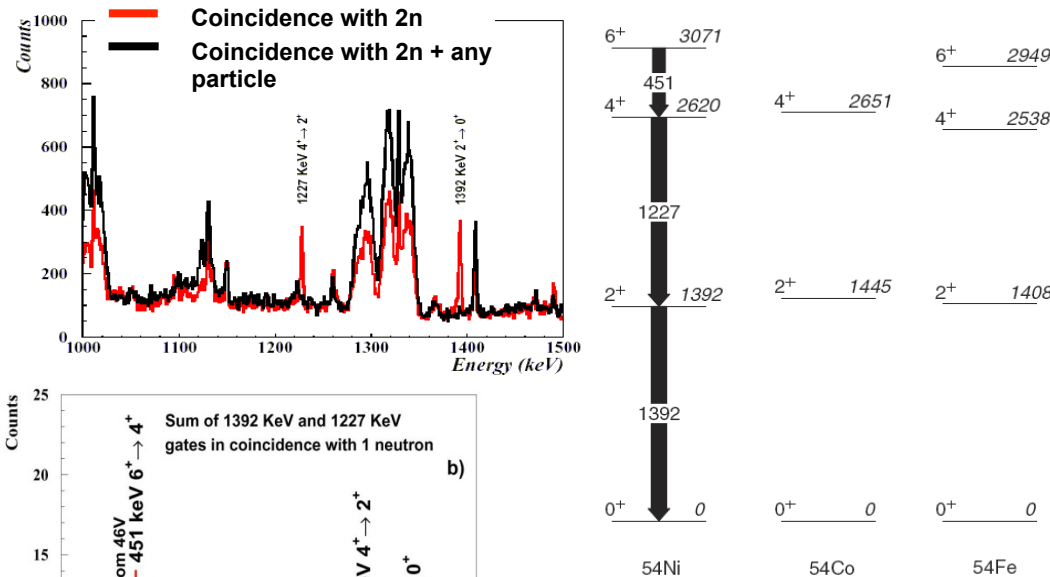
information on CSB terms ( $V^{pp} - V^{nn}$ )

$$TED_J = E_J(Z+1) + E_J(Z-1) - 2E_J(Z)$$

information on CSB & CIB ( $V^{pn}$ ) terms

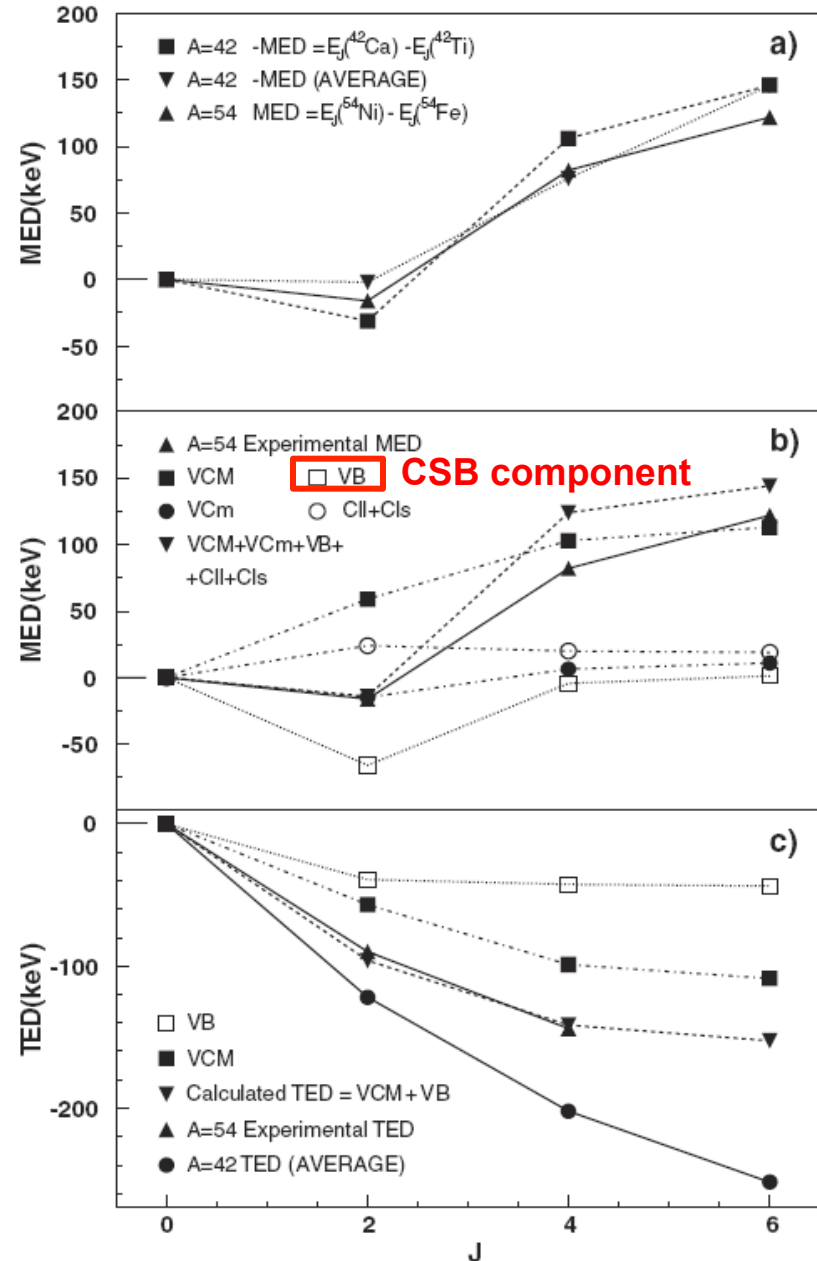


# MED and TED in the A=54 Triplet



## Conclusions:

- Good agreement with the  $A=42 \rightarrow \text{CCS}$  works!!!
- MED trend mainly due to  $V_{\text{CM}}$  and  $V_B$
- The  $2^+$  anomaly present and of the same order for the  $A=42$  and  $A=54$
- **Required CSB component to reproduce**





# Fingerprints of Proton-Neutron Pairing

W.D. Myers, W.J. Swiatecki / *Nuclear Physics A* 612 (1997) 249–261

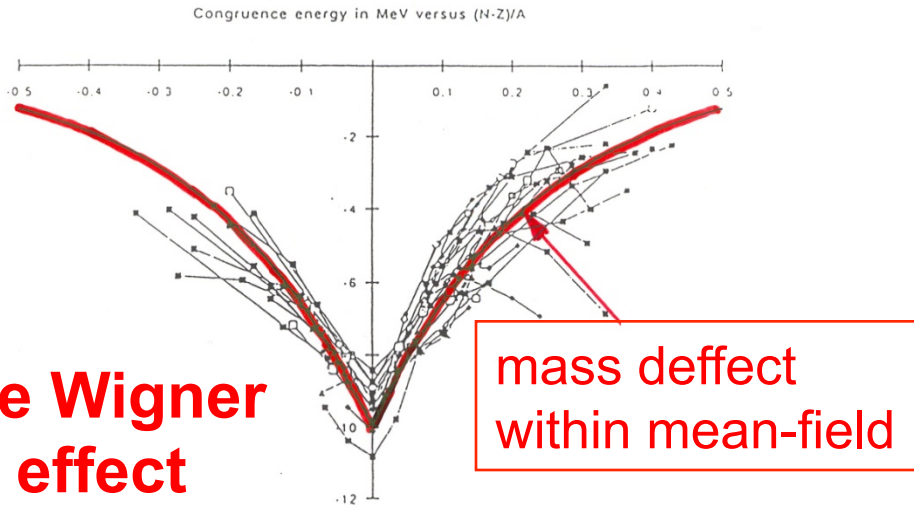
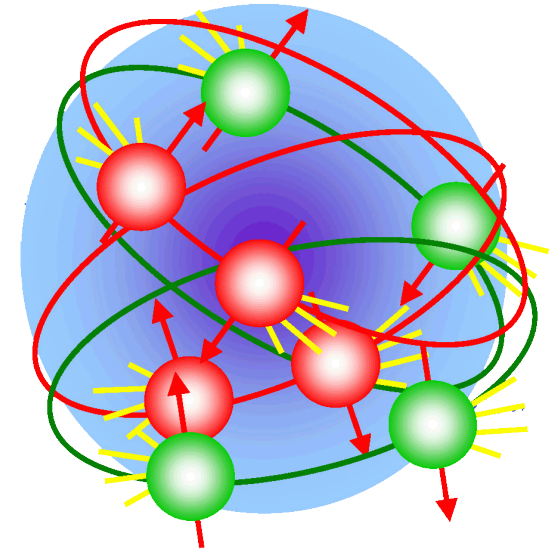
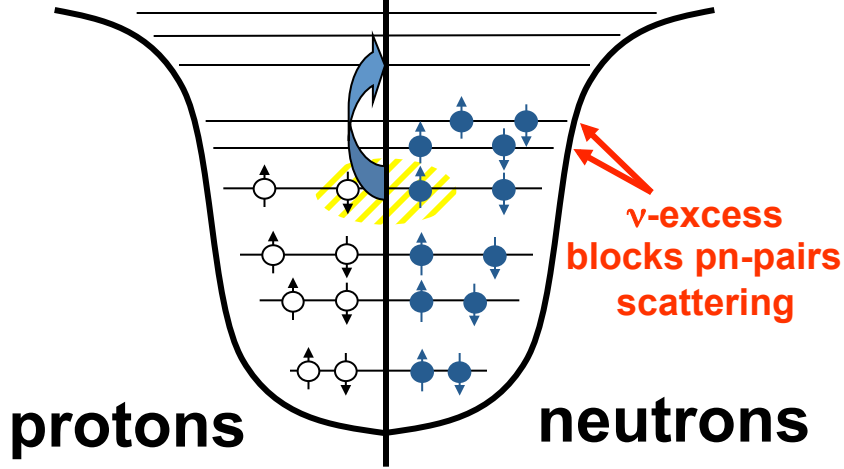
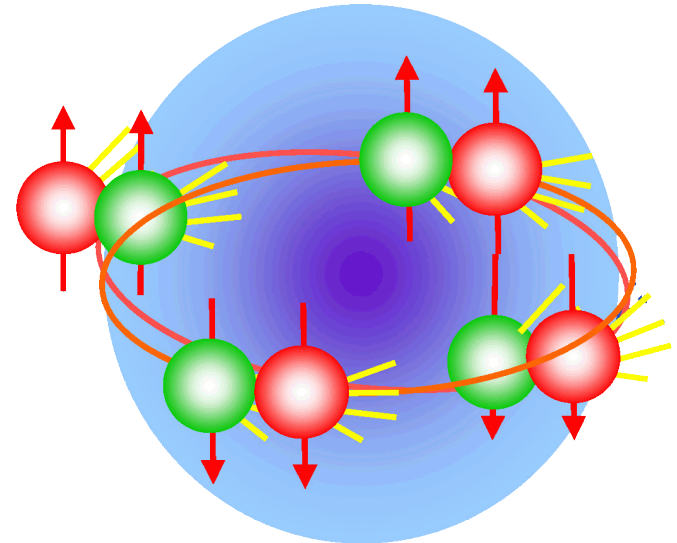


Fig. 1. The difference between measured binding energies and those calculated using the shell- and pairing-corrected Thomas–Fermi model of Ref. [5]. The points (denoted by a variety of symbols) refer to the 28 isobaric chains with  $A = 6, 8, \dots, 60$  that straddle the locus  $N = Z$  in the chart of nuclei. The curve is the semi-empirical fit  $C(I) = \sim 10 \exp[-4.2|I|]/\text{MeV}$ .

**The pn-pairing effects vanish for nuclei  $N \neq Z$**



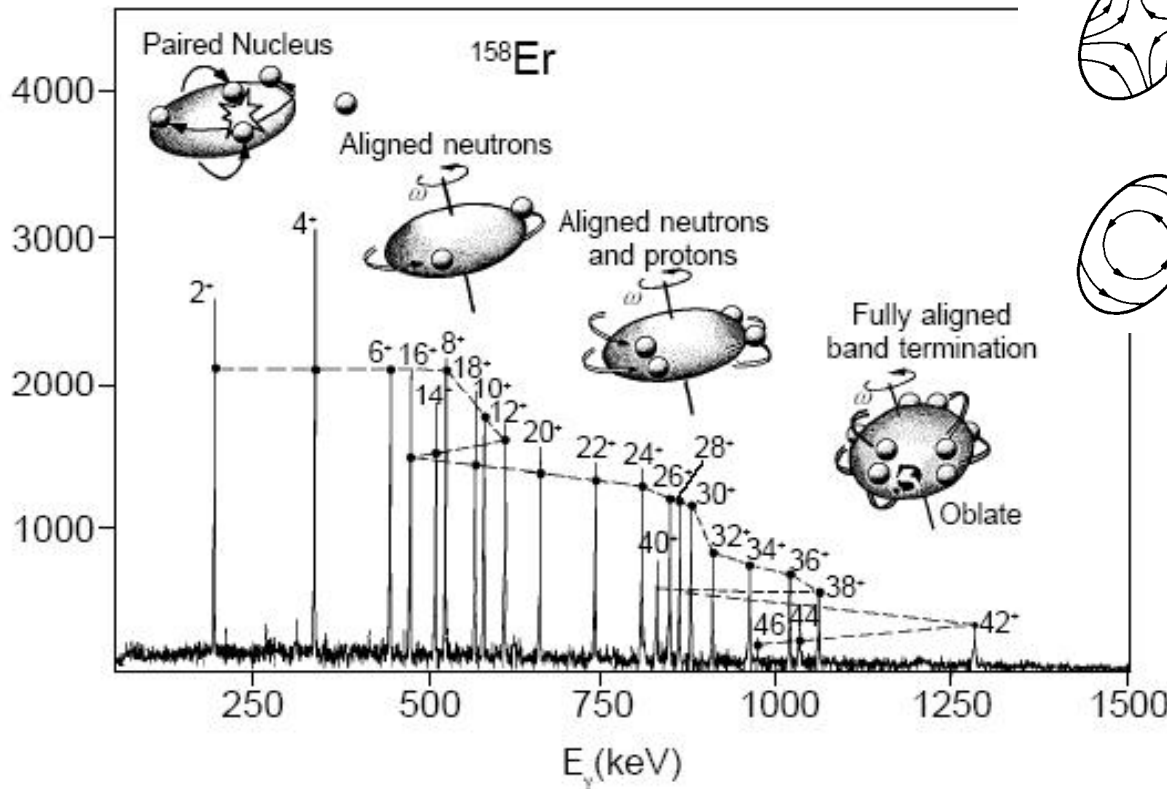
**T=1 J=0 Pairing**



**T=0 J>0 Pairing**

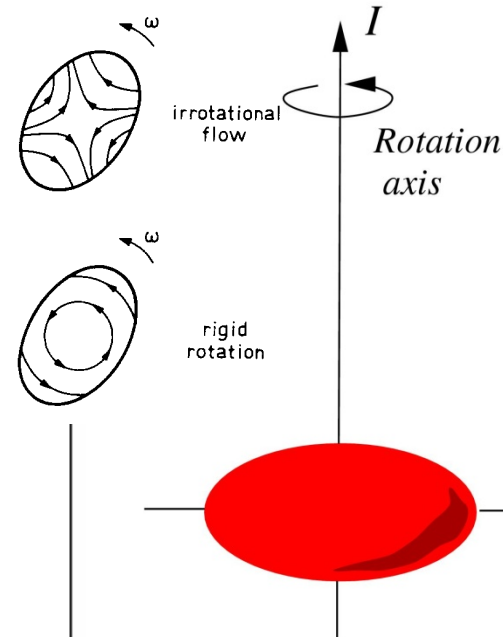
# Deformed Nuclei and Pairing

The “Backbending” phenomena:  
nucleon pairs breaking and alignment



**Proton-Neutron T=0 (J>0)**  
pairs do not need to break to  
produce angular momentum:  
→ Pairing preserved

$$H = H_{DSM} - \omega I_x$$

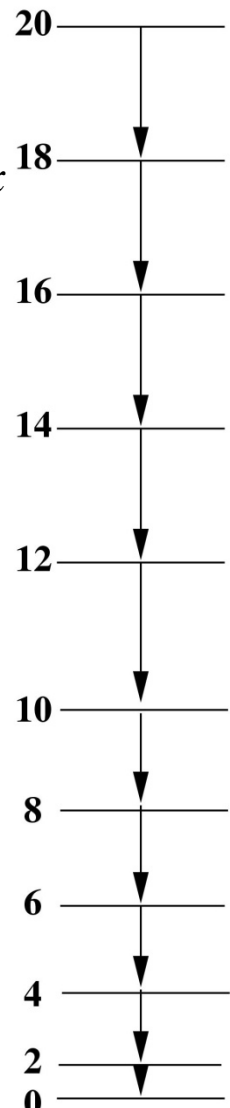


Deformed Nucleus

$$E = E_0 + \frac{\hbar^2}{2\mathfrak{I}} I(I+1)$$

$$\omega = \frac{dE}{dI} \sim \frac{\Delta E}{\Delta I_x} = E_\gamma / 2$$

$$\mathfrak{I} = \frac{dI_x}{d\omega} \sim \frac{\Delta I_x}{\Delta E_\gamma} = \frac{2}{\Delta E_\gamma}$$

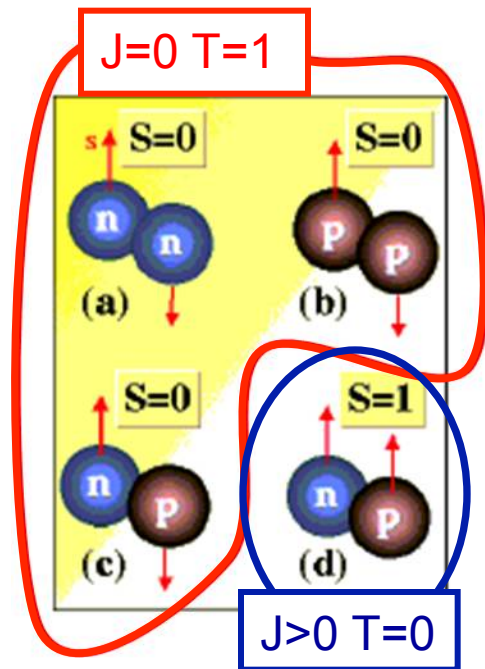
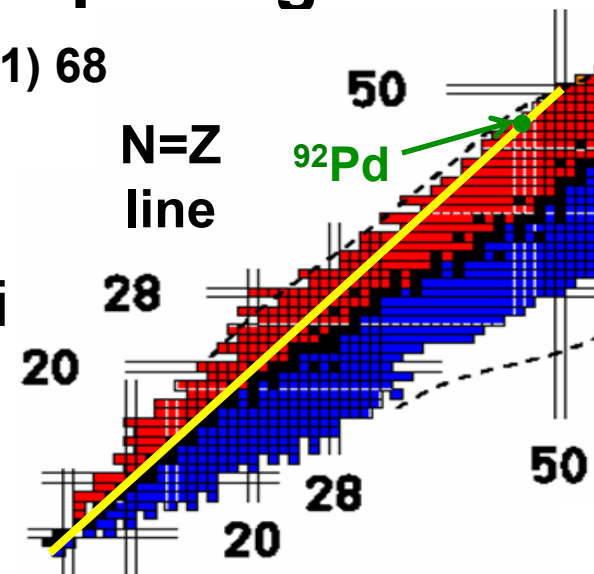


# Isoscalar (T=0) proton-neutron pairing

The Spin-Isospin symmetry family

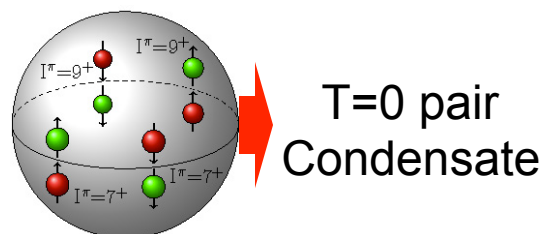
B. Cederwall et al., Nature 469 (2011) 68

Pairing is a fundamental concept in nuclear physics. Since long heavy N=Z nuclei are seen as candidates to study phenomena related with the T=0 pairing.

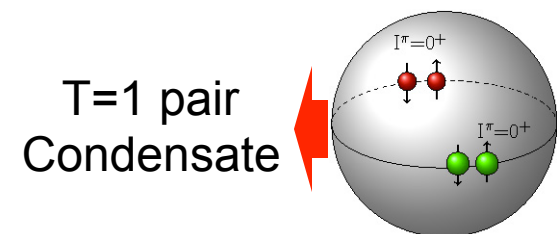


Effects of p-n pairing in Structure: T=0 needed in SM

T=0+T=1					T=1	
8 <sup>+</sup> 3127					8 <sup>+</sup> 2636	8 <sup>+</sup> 2530
(6 <sup>+</sup> ) 2536	6 <sup>+</sup> 2466	8 <sup>+</sup> 2600	6 <sup>+</sup> 2749	6 <sup>+</sup> 2633	6 <sup>+</sup> 2224	6 <sup>+</sup> 2099
		6 <sup>+</sup> 2110	4 <sup>+</sup> 2079	4 <sup>+</sup> 2212		
(4 <sup>+</sup> ) 1786	4 <sup>+</sup> 1708	4 <sup>+</sup> 1518		2 <sup>+</sup> 1417	2 <sup>+</sup> 1460	2 <sup>+</sup> 1415
			2 <sup>+</sup> 1171			
(2 <sup>+</sup> ) 874	2 <sup>+</sup> 878	2 <sup>+</sup> 797				
0 <sup>+</sup> 0	0 <sup>+</sup> 0	0 <sup>+</sup> 0	0 <sup>+</sup> 0	0 <sup>+</sup> 0	0 <sup>+</sup> 0	0 <sup>+</sup> 0
<sup>92</sup> Pd exp	<sup>92</sup> Pd SM	<sup>92</sup> Pd T=0	<sup>92</sup> Pd T=1	<sup>92</sup> Pd no np	<sup>96</sup> Pd SM	<sup>96</sup> Pd exp

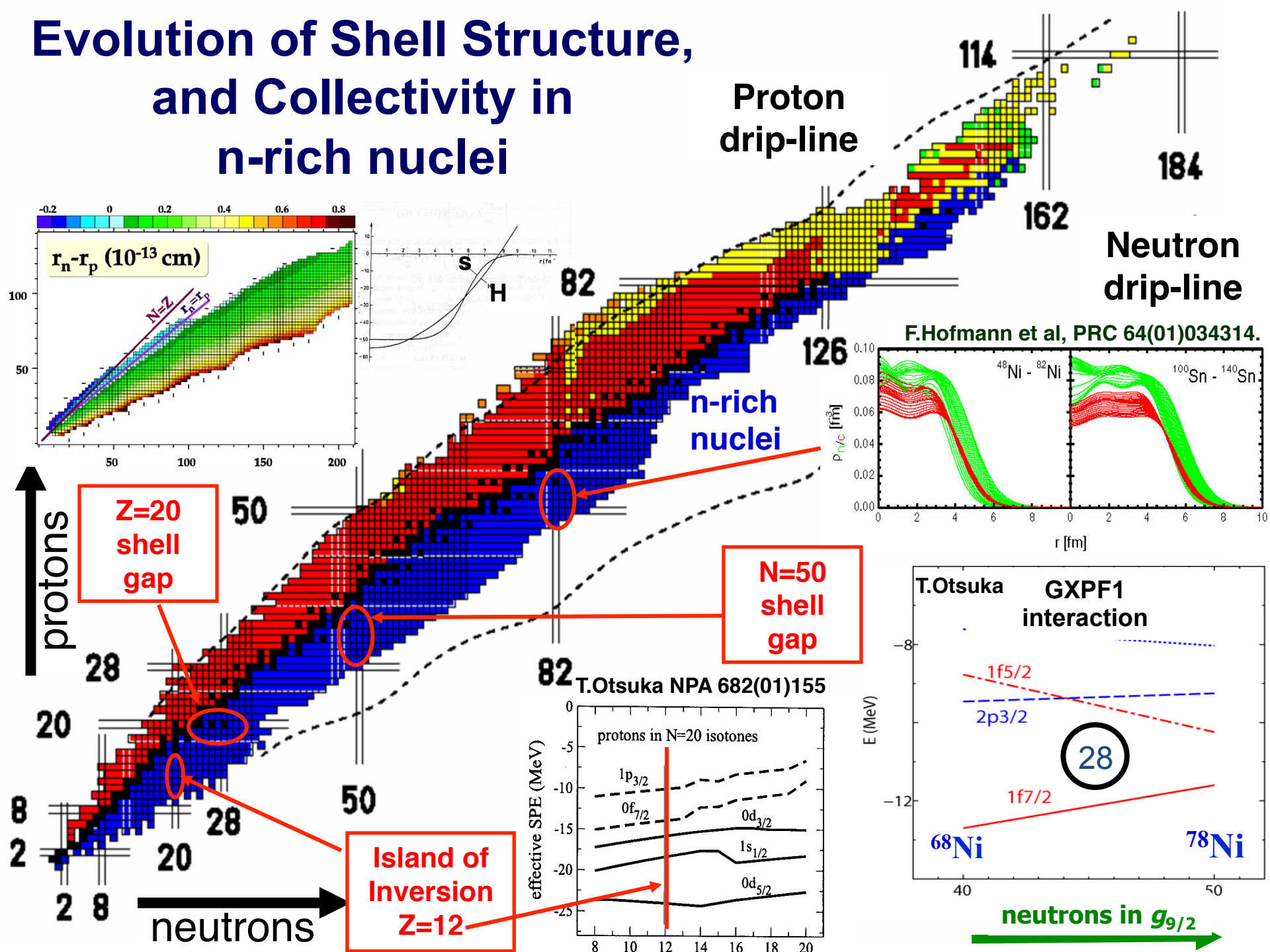


T=0 pair  
Condensate



T=1 pair  
Condensate

# Evolution of Shell Structure, and Collectivity in n-rich nuclei

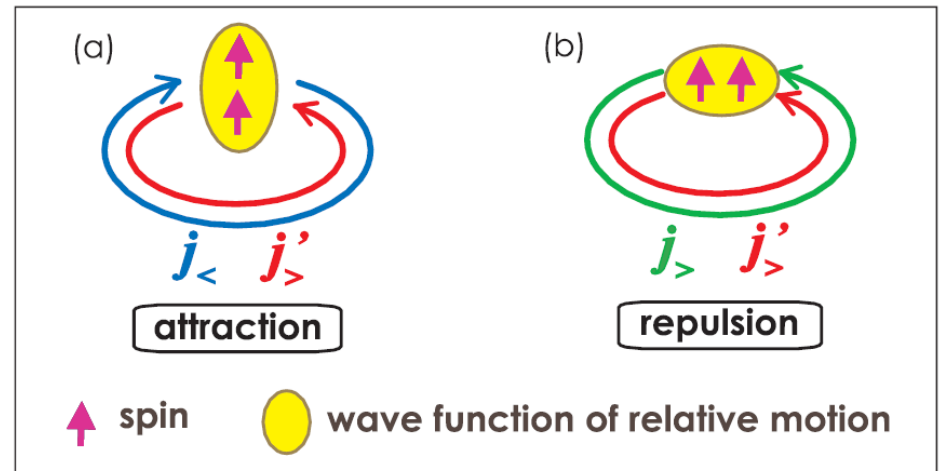
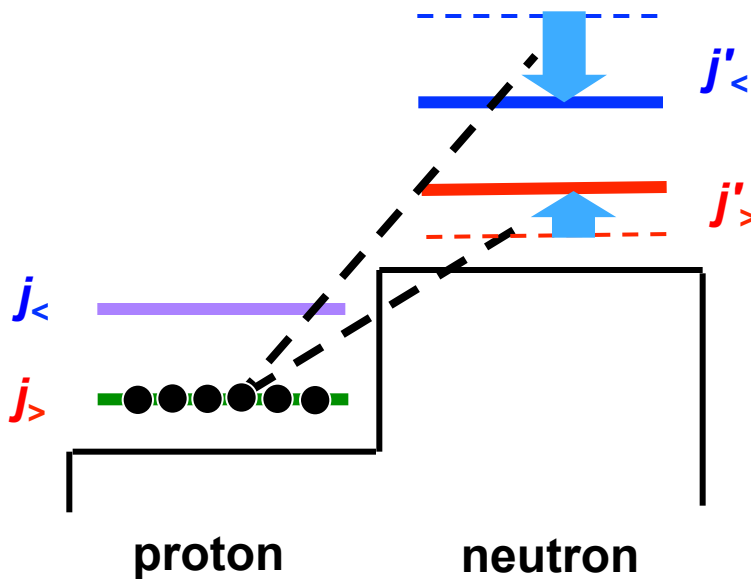


# Monopole interaction

Tensor interaction ( $\pi + \rho$  meson)  
may be responsible for the  
modification of the shell gaps

- Monopole energy of the tensor interaction  $\sigma\tau$

$$V_{j,j'}^T = \frac{\sum_J (2J+1) \langle jj' | V | jj' \rangle_{JT}}{\sum_J (2J+1)}$$



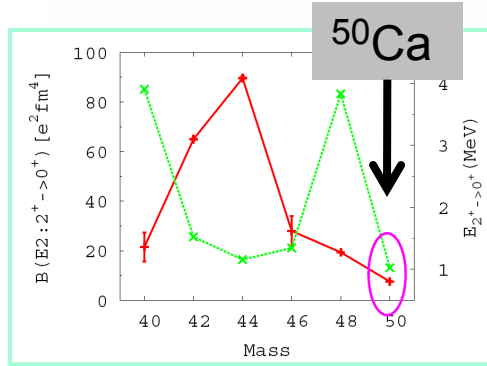
The single-particle orbits may migrate  
leading to a possible change in shell  
structure.

[Otsuka et al., *PRL* **95** (05) 232502]

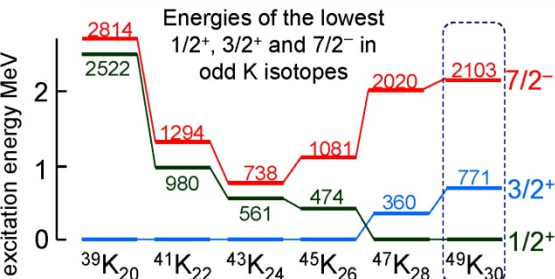
[Otsuka et al., *PRL* **97** (06) 162501]



# Nuclear Structure in n-rich nuclei

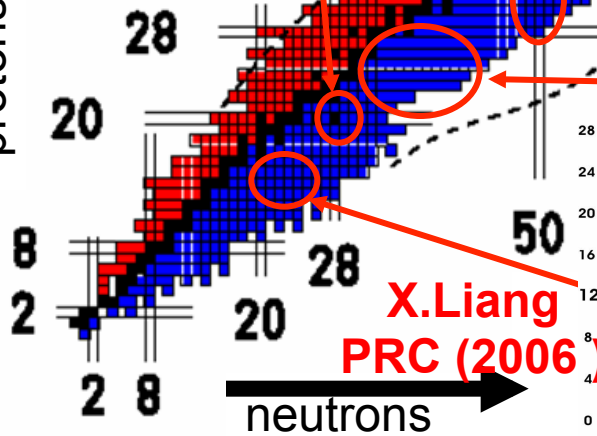


**RDDS Lifetimes  
with the Köln  
Plunger**

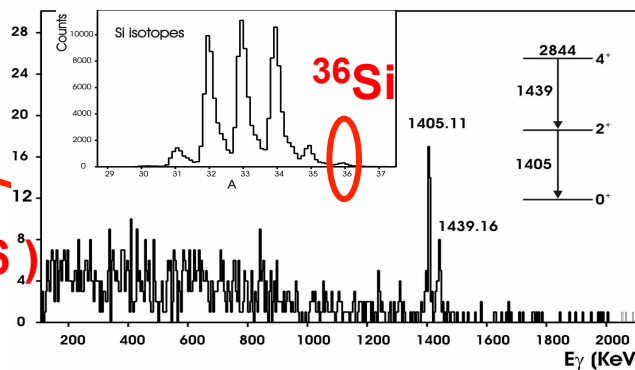


**R.Broda to be  
published**

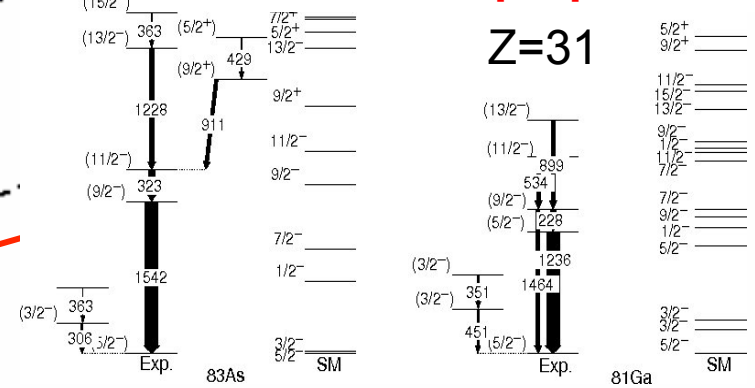
protons



**X.Liang  
PRC (2006)**



**E.Sahin in preparation**



**S.M.Lenzi to be published**

